Politecnico di Milano university

Department of Building and Architectural Engineering Programme

The undersigned hereby certify that they have read and recommend to the School
of Architecture Urban Planning Construction Engineering (AUIC) for acceptance a thesis entitled

OCCUPANT-BASED PARAMETRIC GLARE ANALYSIS FOR OPTIMAL ACTIVE
GLAZING SURFACE IMPLEMENTATION

By

Vladimir Lvov 882538

Ming Xue 883815

In Partial fulfilment of the requirements for the degree of

MASTER OF SCIENCE BUILDING AND ARCHITECTURAL ENGINEERING

Dated: July 25, 2019

_____

Supervisor(s):

_____

Prof. A.G. Mainini

_____

Eng. J.D. Blanco Cadena

**POLITECNICO**
MILANO 1863

# Declaration

We hereby declare that except where specific reference is made to the work of others, the contents of this dissertation are original and have not been submitted in whole or in part for consideration for any other degree or qualification in this, or any other University. This dissertation is the result of our own work and includes nothing which is the outcome of work done in collaboration, except where specifically indicated in the text.

Vladimir Lvov

Ming Xue

July, 25 2019

# Acknowledgements

We would like to express our special gratitude and thanks to our supervisor, Professor A.G. Mainini for imparting his knowledge and experience in this study. His expertise was invaluable in the formulating of the research topic and methodology. Without his help this thesis would not be possible.

We would also like to thank our tutor, J.D. Blanco Cadena for his supporting guidance, critical and helpful recommendations. His advices were always necessary information regarding this research, steering us in the right direction whenever we needed it.

In addition, we would like to thank our colleague Esraa, who's support and assistance helped us in the work on this study.

# Abstract

The occupant-based parametric glare analysis and the analysis of daylight distribution by means of glare metrics (DGP) and illuminance metrics (UDI) was performed to obtain optimal dynamic glazing surface. The method of defining an optimal surface area of dynamic glazing material based on geographical location and occupant's position was proposed and evaluated. The results have shown that the proposed method find its use to find an optimal active glazing surface to control the glare from the sun directly visible in the field of view. The comparison of performance of electrochromic (EC) and suspended particle device (SPD) materials implemented using a proposed method was carried out. Considering the dependence of optical properties of SPD from its thickness the optimal thickness for controlling the glare was suggested. Based on adopted visual comfort parameters and energy consumption analysis it was found that EC is preferable selection for smart window application in comparison to SPD.

# Astratto

L'analisi parametrica dell'abbagliamento degli occupanti e l'analisi della distribuzione della luce diurna attraverso le metriche di valutazione dell' abbagliamento (DGP) e dell'illuminamento (UDI) è stata eseguita per ottenere una superficie ottimizzata di vetro a prestazione dinamica. Il metodo proposto relaziona la porzione di superficie dinamica elettrocromica, con la posizione relativa degli occupanti all'interno dell'ambiente confinato. I risultati hanno dimostrato che il metodo proposto è efficace e può essere utilizzato per trovare una superficie attiva ottimale per controllare l'abbagliamento da radiazione solare presente direttamente nel campo visivo degli utenti. È stato effettuato il confronto delle prestazioni dei materiali per dispositivi elettrocromici (EC) e per dispositivi a particelle sospese (SPD). Considerando la dipendenza delle proprietà ottiche dell'SPD dal suo spessore, è stato suggerito lo spessore ottimale per il controllo dell'abbagliamento in relazione alle proprietà ottiche derivate. Sulla base dei parametri di comfort visivo adottati e dell'analisi del consumo energetico è stato riscontrato che EC è la scelta preferibile per l'applicazione smart window rispetto all'SPD.

# Table of Contents

# List of Figures

# List of Tables

# Nomenclature

| | |
|---|---|
| $EC$ | Electrochromic |
| $SPD$ | Suspended particle device |
| $T_{vis}$ | Visual light transmittance |
| $T_{diff}$ | Diffused transmittance |
| $T_{tot}$ | Total transmittance |
| $T_{dir}$ | Direct transmittance |
| $R_{spec}$ | Specular reflection |
| $R_{diff}$ | Diffused reflectio |
| $R_{tot}$ | Total reflection |
| $DGP$ | Daylight glare probability |
| $UDI$ | Useful daylight illuminance |
| $FOV$ | Field of view |
| $SHGC$ | Solar heat gain coefficient |
| $WWR$ | Window-to-wall ratio |
| $DGI$ | Daylight glare index |
| $UGI$ | Unified glare index |
| $UGR$ | Unified glare rating |
| $CGI$ | CIE glare index |
| $LC$ | Liquid crystal |
| $PCM$ | Phase change material |

# Chapter 1     Introduction

## 1.1    Thesis outline

In Chapter 1 the literature review and the aim of the study are presented.

In Chapter 2 the software adopted for the analysis is presented. A method of occupant-based area definition, adopted metrics for evaluation together with the considered simulation cases are described.

In Chapter 3 the results of glare simulations and horizontal illuminance simulations for considered cases are presented together with the analysis of the obtained simulation results. The summary of results is presented in corresponding sub-chapters. Energy consumption for electrochromic glazing and automated roller blind shading based on developed schedule is calculated.

In Chapter 4 the discussion of the results and conclusions are presented.

## 1.2    Literature Review

### 1.2.1    Daylight as an influence parameter on occupant's comfort

Nowadays the importance and great number of daylighting researches has led to a significant increase of importance of daylight strategies implementation in sustainable design standards and codes (1) (2). An overwhelming amount of them have pointed out that decreased building energy use together with increased well-being of the occupants are the benefits that are brought by the proper access to daylight (3) (4) (5). Daylight studies performed within the built environment have shown that the presence of natural light inside the space and access to a quality view to the outdoors may influence positively productivity, physical and psychological conditions of the occupant (5) (6). Since daylight is generally a free and ecological power source it has great potential to reduce energy use. However, if daylighting designs was not performed properly, the luminous environment may lead to

dissatisfaction and discomfort for occupants from the glare, causing headaches, loss of productivity together with reduction of energy performance of the building.

The benefits of using natural light might be a hard task for a designer since some of the requirements for a sustainable design are in contradicting relationships when considering the effects from the daylight. Proper use of the daylight demands a balance between a number of factors (7). Specifically, a well-designed system should:

     i.     provide sufficient amount of daylight to perform tasks;

     ii.     distribute daylight throughout a space to avoid under-lit areas;

     iii.     provide glare control;

     iv.     ensure that areas receive enough daylight illuminance to modulate electric light levels and achieve energy savings;

     v.     provide occupants with appropriate circadian stimulation;

     vi.     provide quality views of the outside;

     vii.     appropriately limit glazing area;

     viii.     control solar heat gains appropriately.

The fulfilment of these goals is achieved by combination of passive and active control strategies. Passive strategies in the design should be taken into account in the framework of the fundamental design decisions made at various stages of the process. Such decisions are a consideration of many factors: the location of the object and its orientation in space, the type and size of the fenestration system of the building, as well as careful consideration of the properties of the context materials used (e.g. color, reflectance, etc.) (8). Active control strategies include systems that are able to dynamically adjust the amount of daylight entering the room in conjunction with controlling electric light during the day, using manual or automatic mechanisms.

The design of daylight is an optimization task, which at the same time depends on many factors that should be considered together, therefore, in practice such a task is quite complex. At best, such a problem is solved by an integrated design, when designers take into account all the factors at each design stage from the beginning to the end of the design. To help designers maximize the benefits of daylight, researchers have developed metrics (9) (10) that can assess dynamic changes in light levels, which help designers find and better understand the effects of certain design decisions on the final design results, as well as modern technologies that can dynamically respond to changes in luminous environment.

Despite these advances in design, there are many examples of existing buildings and occupied spaces whose users experience visual discomfort with inadequate or excessive levels of natural light. Among of the most common reasons of occupant's discomfort are glare and high internal air temperatures (8). Additional concerns include unfavorable psychological effects and non-uniform illuminance levels, insufficient privacy and lack of view to the outside, as well as decreased productivity and discomfort (11).

Ultimately, no matter how complex the approach to the use of daylight, the quality of design decisions on the use of natural lighting depends on how well they are able to provide user comfort (12).

### 1.2.2  Dynamic lightning and shading strategies

Since quantitatively the level of sunlight exposure fluctuates throughout the day, to create favorable indoor conditions, various strategies are used to disperse, filter and block unwanted solar radiation. Among of the most commonly used strategies to fulfill this purpose are external horizontal or vertical louvers and overhangs, external or internal venetian blinds, shutters, roller shades with different kind of shading fabric, shading elements placed inside the glazing unit, etc.

Different control strategies to operate shading fabrics and blinds were widely studied. These studies can be divided and grouped in a following manner: optimal shade control strategies for venetian blinds (13) (14)  and fabric shades (15) (16) are implemented to optimize building energy use while maintaining visual comfort requirements in terms of illuminance values. The operation of shading mechanism was ruled by external and internal illuminance values and amount of solar radiation received by the sensors. The evaluations range from field studies, to controlled laboratory environments, to simulated. However, it is important to note that none of these studies are aimed at generating forms for shading systems. Previous studies on dynamic shading approaches present comparative performance analysis of multiple shading control models based on predefined occupant's visual comfort criteria and optimal energy consumption loads. While these studies provide shading operation guidelines for improved energy consumption performance and occupants' visual comfort, evaluation of shading control models focus on the application of specific type of shading devices such as venetian blinds or roll-down fabric shades and no form-generating shading design guideline is introduced (17).

Furthermore, allowing direct solar radiation during the under-heated periods (where the sun angles are typically low and sun penetration is deep) contradicts with the visual comfort requirements (i.e. avoiding direct sunlight on task surfaces and occupant's eye). Personal preferences and tolerances of individual occupants to daylight distribution patterns within their field of view leads to the operation of interior shading devices by the occupants, which in most of the cases is ineffective in terms of energy loads management and conflict with the intended by the designer the way of use of a shading devices leading to increase of

loads for heating and cooling systems (17). Static shading might also produce an overshading problem since in most of the cases it is designed for a particular period of time (e.g. summer solstice). The problem is worsened for daylight harvesting, especially on cloudy days, leading to further reduction in daylight levels. Although shading devices impact both visual and thermal comfort, many studies demonstrate that the single best predictor in the operation of shading devices is visual comfort, that is, glare (18) (19).

When analyzing the quality and principles of various shading strategies, it is necessary to take into account the fact that the view to the outside is important among the parameters that provide comfort to the occupant. Daylighting theories commonly intertwine with view preservation theories in ways that can greatly affect building occupants in positive ways, supporting a reduction of stress and potential for increased productivity when exposed to natural views (5). The numerous daylight-managing applications (interior shades or exterior structures) function to obstruct or diffuse direct access visually to the outdoors. Dynamic shading strategies that aid in the preservation of outdoor views, in opposition to those that block them entirely, could be a potentially mediating application that both satisfies the user and the building energy profile. The review of the precedent shading design methods demonstrates that there is a need for a new shading design workflow that would include both the use of new promising emerging technologies, such as "smart windows" to integrate the protection from unwanted visual disturbances preserving the beneficial view to the outside and more integrated occupant-based approach to the design of the shading device itself.

### 1.2.3  Electrochromic materials in window applications

The analysis of researches on the topic of daylight in built environment indicates that new approaches in the design of a shading strategy together with implementation of new emerging technologies in building materials needs to be explored. Qualitative improvement in this area of research can be achieved by using materials that can dynamically change their optical properties. Nowadays, most promising materials that may be used for dynamic modulation of optical properties are electrochromic (EC), gas-chromic, thermochromic, thermotropic, liquid crystal (LC), suspended particle device (SPD) and phase change materials (PCM) (20).

Electrochromic glazing is a dynamic material that is achieving its properties from the phenomenon of electrochromism, when the material automatically and reversibly changes appearance (i.e. colour) and performance (i.e. visual light, solar heat gain coefficient) due to oxidation and reduction reaction when electrical power is applied. The electrochromic stack consists of electron accumulation layer of lithium oxide and an electrode layer sandwiched between two transparent electrical conductors and an ion conductor lying in the middle of two electrodes. When voltage is applied between the transparent electrical conductors,

various lithium ions reversibly move from the accumulation layer through ion conductor to electrode. The effect is that the glazing switches between a clear state to tinted state. Glazing remains the tinted state until the voltage is cut off causing glass turn transparent again (20). **Error! Reference source not found.** presents the operating scheme of electrochromic glass.

Visible transmittance fraction ($T_{vis}$) and solar heat gain coefficient determine the fraction of visible light and total solar radiation that pass through the window unit in each EC state. Visual light transmittance and solar heat gain coefficient are reduced significantly when glass is fully tinted. Visual light transmittance can even reduce to 1% in some EC applications, such as SAGEGLASS® (21).

**Figure 1-2** shows the electrochromic glass control state and how visual light transmittance and solar heat gain coefficents change. Besides, the intermediate state can exist between clear state and fully tinted state which means that the $T_{vis}$ and SHGC can be tuned to obtain an intermediate between two states – fully bleached and fully tinned.
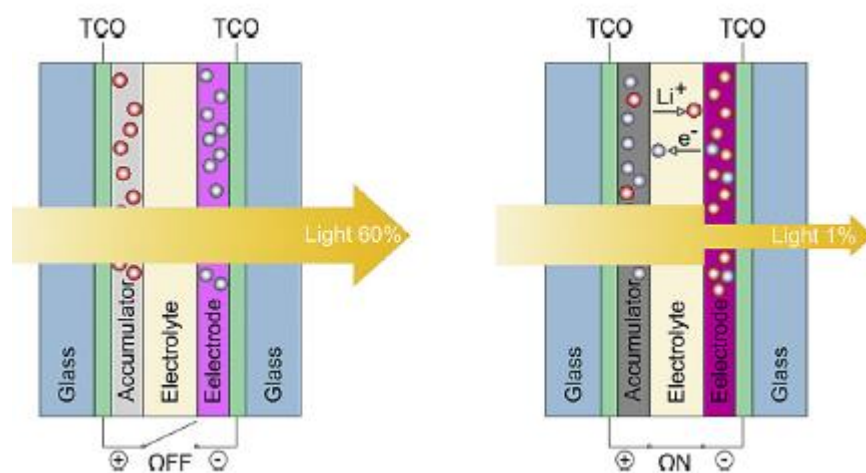


**Figure 1-1**Electrochromic glazing operating scheme (20)
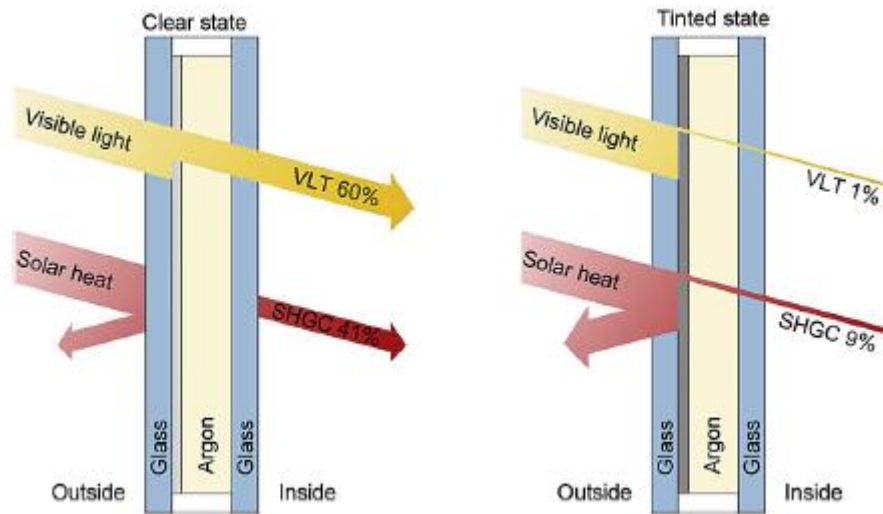
**Figure 1-2** EC control state (20)

Additionally, electrochromic products allow a wide range of glass pane sizes in different shapes and independent modulation of up to 3 control zones on the same pane. SageGlass LightZone® has the ability to create up to three tint zones within a single pane of electrochromic glass, providing combination of clear or tinted zone (22). **Figure 1-3** shows the appearance of SageGlass LightZone ® when three control zones are activated.



**Figure 1-3** Electrochromic dynamic glazing Sage LightZone® (22)

EC glazing of various types have been in development recent years and EC glazing can be classified in terms of controlling the visible light and near infrared (NIR) light transmitted through EC glazing. Three electrochromic glazing windows are classified as follows (23):

*Conventional electrochromic glazing (CEC)*

The characteristic of CEC glazing is blocking transmission of both near infrared (NIR) light and visible light when switching to "dark" state. The benefit is reducing cooling load in the hot climate zone and blocking discomfort light to avoid glare risk.

*NIR-switching electrochromic glazing*

NIR electrochromic glazing (NEC) window reduces transmission of NIR light, without affecting visible light transmission. This feature may give the transparent NIR-switching electrochromic (NEC) glazing an aesthetic advantage over conventional electrochromic glazing in a variety of building applications and climates.

*Dual-band electrochromic glazing (DBEC)*

DBEC glazing combines the properties and switching range of both CEC and NEC glazing. It can modulate transmission of NIR and visible light separately and independently.

**Figure 1-4** and **Figure 1-5** indicate visible transmittance fraction and solar heat gain coefficient of three type of EC glazing.

Switching time from clear state to tinted state also affect the performance of EC glazing. Switching time for coloration and bleaching is defined as the time EC glazing takes to reaching 90% of the its maximum and minimum transmittance level. Generally, the time required for coloration is longer than the requirement for bleaching. Fast switching is desirable for both energy efficiency and visual comfort (24). A medium or large-sized pane of SageGlass transits from clear to tint in 15-20 minutes. The switching speed depends on a number of factors, including the ambient temperature and glass size. The warmer it is outside, the faster the glass transitions. Larger panes take longer than smaller panes to fully transition (22).
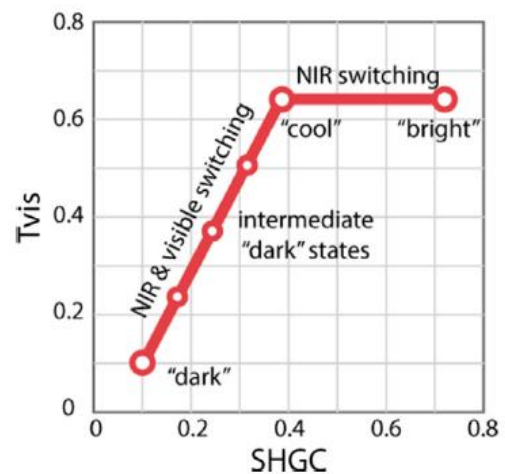


**Figure 1-4** The variation of Tvis and SHGC for three type of EC glazing

(23)
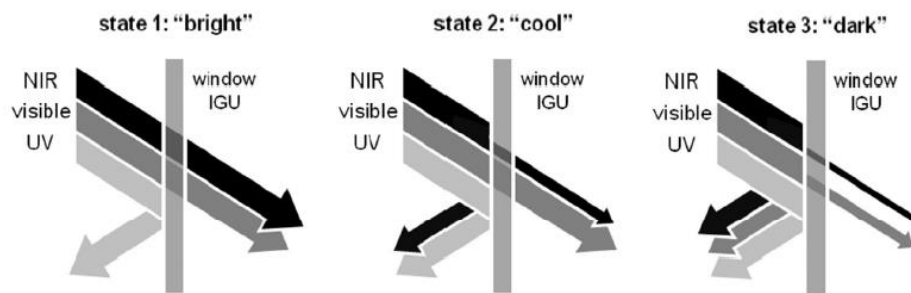
**Figure 1-5** Description of three states for CEC, NEC and DBEC (23)

Currently there are several producers of electrochromic glazings and films (25) (26) (27) (28). To have a better understanding of the performance and operational characteristics the comparison table and a representative graph were created to help the protentional user to select the proper producing according to needs and expectations (**Table 1**, **Figure 1-6**).

Table 1 Comparison of EC products properties

| Property | Halio* | IQ* | Smart Films International® | NanoEC™ SPU™ | Sage Glass® |
|---|---|---|---|---|---|
| Power consumption for state transition, W/m² | 14 | 1 | 2 | 2.5 | 5 |
| Power consumption for maintaining tint, W/m² | 1 | 0.4 | 0.4 | 1 | 0.32 |
| Switching speed, min | 3 | 5 | 20 | 6 | 12 |
| Service life, year | 10 | 5 | 10 | 10 | 10 |
| Minimum visible light transmittance | 0.02 | 0.01 | 0.09 | 0.05 | 0.01 |
| Operating voltage, V | 48 | 100 | 24 | 3 | 5 |
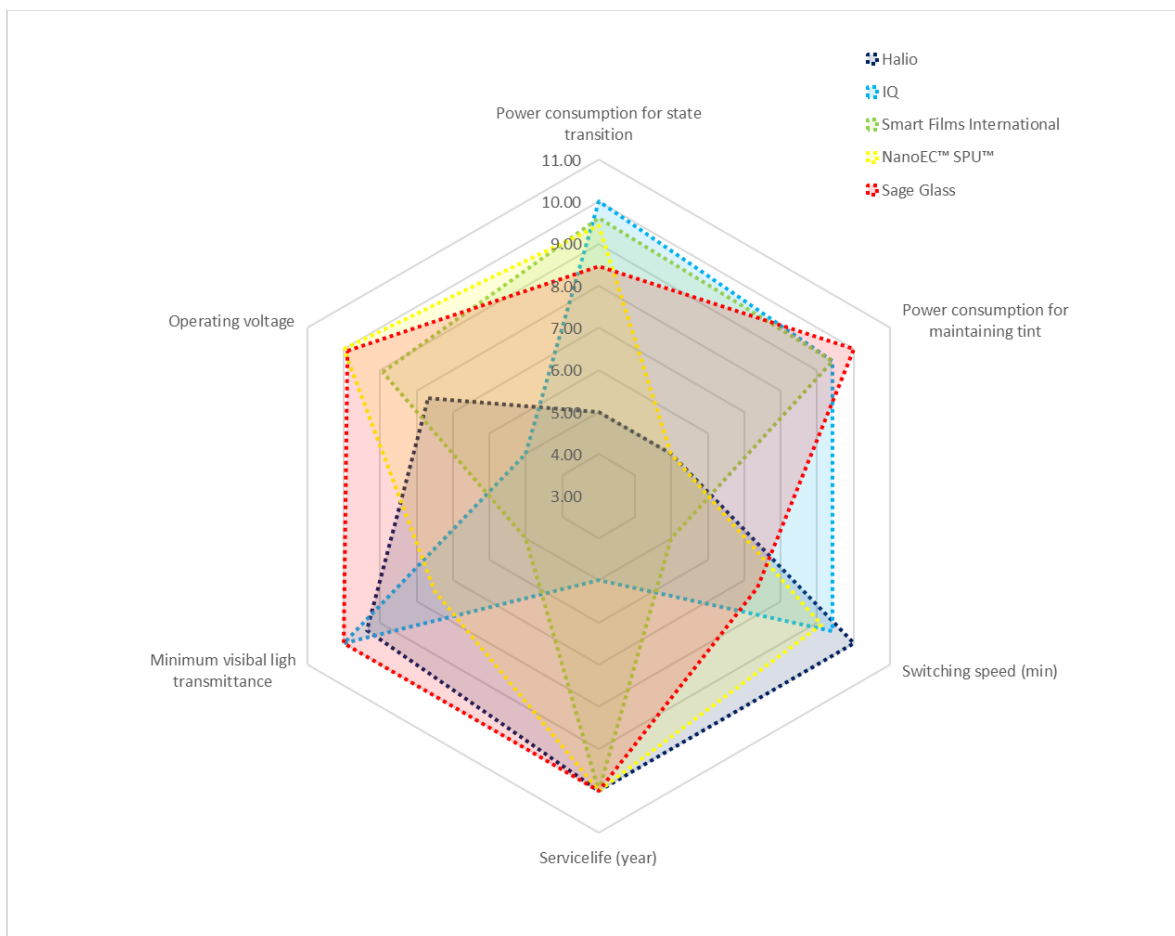


Figure 1-6 Comparison of properties of EC products on a radar chart

Current scientific studies regarding the use of electrochromic materials for window applications are mostly aimed to the investigation of contribution of EC glazing in reducing the energy use of the buildings.

Nicholas DeForest et al. in (29) have used EnergyPlus software to assess possible saving in energy demand for heating and cooling together with lighting savings. Three types of electrochromic windows: conventional EC, that changes its transmittance in a visible state, EC that is changing its transmittance in near infrared wavelength and so-called dual-band EC that is able to operate both in visual and NIR ranges. The simulation was performed considering 16 cities in the US, where each one is representing a climatic zone with its own typical climatic conditions. Three type of spaces were considered: large office with floor space of 46 320 m$^2$, window area of 4636 m$^2$ and WWR of 0.38; medium office with floor area of 4982 m$^2$, window area of 653 m$^2$, WWR of 0.33; residential building with a floor area of 3142 m$^2$, window area of 231 m$^2$ and WWR 0.15. The façade geometry and orientation was not explored in their study. For the control strategy a rule-based algorithm was adopted where the operation and change of state of EC glazing was based on glare index as an initial check. If the glare index was within a predefined boundary, the operation was performed considering whether the zone was in heating or cooling state. The results have shown that for most of the climatic regions dual-band EC windows were outperforming other considered in the study advanced glazings in terms of annual primary energy savings. No considerations about visual comfort in terms of light distribution was considered. Abdelsalam Aldawoud in (30) has compared conventional fixed shading devices with an electrochromic glazing by means of DesignBuilder software. Ten story building with 50% glazed façade area was located in Phoenix, Arizona. Adopted control strategy for operating EC glazing was not reported. The windows shading condition and the glazing type were the only varying parameters. The output data show that electrochromic glazing provides the best performance in reducing solar heat gains compared to other tested shading conditions. Alessandro Cannavale et al. have studied energy savings due to the use of electrochromic glazing (31). The practical implications on the building energy balance were analyzed by means of suitable simulations, carried out in Energy Plus. A reference office building was equipped with different glass technologies on the façade (clear glass, solar control, electrochromic glasses) and located in different cities (Rome, London and Aswan) to also include climatic effects in the analysis. The EC technology outperforms all the others, with overall yearly energy savings as high as 40 kWh/m$^2$yr (referred to window surface) in the hottest climates, assuming the clear glazings as benchmark. Daylighting performances were significantly improved using EC devices, both in terms of Useful Daylight Illuminance (UDI) and Discomfort Glare Index (DGI). In the best case, 82.7% of hours achieved optimal illuminance conditions on an annual basis. The control strategy was based on the internal illuminance sensors.

A sensitivity analysis of different design parameters for office equipped with electrochromic windows was carried out by Jean-Michel Dussault and Louis Gosselin in (32). In this paper, a representative office building zone with an electrochromic glazed facade was simulated in TRNSYS and Radiance/Daysim for a large number of different combinations of

design parameters (i.e. location, facade orientation, etc.). The operation of EC glazing was performed by several rule-based strategies, which were based on incident vertical solar radiation received by the sensor modeled on a building façade, energy flux balance, average temperature inside the room and an illuminance value on a sensor, located 3m away from the glazed façade. The results have shown that the choice of the specific window control strategy is having a limited impact on the energy savings and peak load reductions, the analysis revealed that this parameter has a larger impact on the visual comfort (UDI).

Bernard Paule et al. in (33) have investigated by means of DIAL+ software the performance of glazed façade covered with electrochromic material and divided into three zones that were operated independently. The control strategies to operate EC were based on the amount of the illuminance on a façade in "daylight" mode and the presence of direct sun rays in a predefined area in a "glare" mode. The division of electrochromic façade into separately operable zone has shown a good potential in improving the performance considering visual conditions in comparison with electrochromic glazing being operated as a one single zone.

A little amount of research studies, especially considering a visual comfort of the occupant, has been performed on modern electrochromic products for windows applications available on the market. E.S. Lee et al. in their earlier field-study dedicated to evaluation of performance of real-life examples of applied electrochromic glazing generally point out the fact that while achieving better performance in terms of visual conditions inside the space in comparison with conventional glazing and shading strategies, EC in its darkest state is not able to completely eliminate the glare phenomenon (34). It is important to notice that at lowest visual light transmittance of installed electrochromic glazing was 11%. The producer of electrochromic glazing systems *View Inc.* points out in their research studies that for achieving visual comfort and providing glare-free environment it is necessary to have an electrochromic material that is able to obtain visible light transmittance values of 1% or lower (35). This consideration was also stated by Ahoo Malekafzali Ardakana et. al in their work dedicated to comparison of performance of electrochromic glass vs. fritted glass (36). Nevertheless, in (37) authors have performed an evaluation of end user impacts of EC windows in a retrofit application and besides stating that total energy savings obtained were 39-48% and peak electric demand was reduced for 22-35%, they also conclude that discomfort glare appeared to be adequately controlled by the tint level of the EC windows and in general users did not tend to override the automated control system.

### 1.2.4  Suspended particle device

Besides electrochromic materials, suspended particle devices (SPD) found their use in the field of dynamic glazing materials. In comparison to EC materials, where the modulation of optical properties is obtained by chemical reaction, SPD technology, uses the alignment of optically absorbing particles suspended in a cross-linked polymer matrix. Light transmission is

controlled by the application of an AC voltage of high amplitude. An SPD consists of 3–5 layers with a schematic construction according to **Figure 1-7**.

SPD is able to achieve lower visual light transmittance value in comparison to EC (20) which might be beneficial in controlling the glare from the direct sun. Another difference that distinguishes SPD from EC is the fact that due to the nature of the materials used, SPD has a bigger value of haze which causes the light transmission in a diffused manner, especially in its "off" state. In the "off" state, the suspended particles are randomly oriented and absorb and scatter visible light. The SPD then shows a bluish-black dark color, since most of the light is absorbed by the SPD layer. The scattering effect is mainly due to the particles and is most prominent at short wavelengths. In the "on" state, when the electric field is applied, the particles line up perpendicularly to the substrates and then more light is allowed to pass so that the transmission is increased (38).
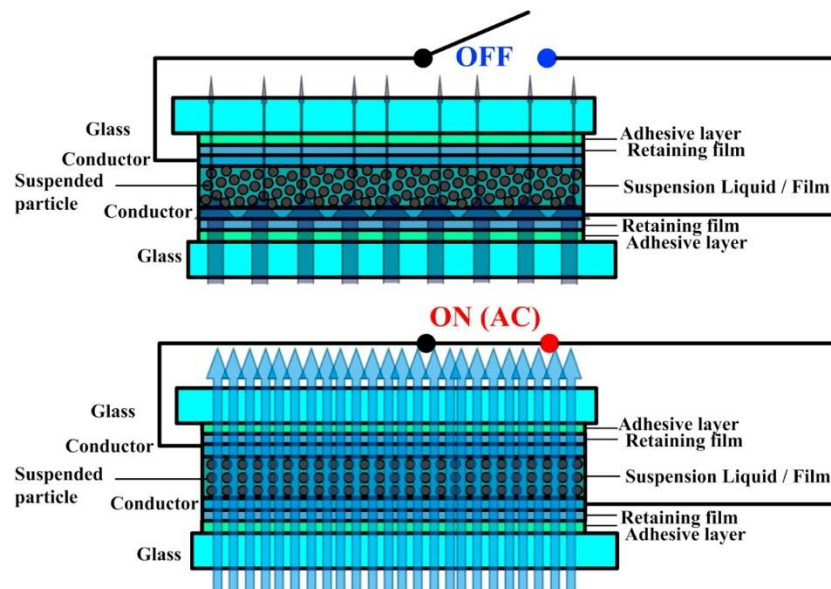


Figure 1-7 Schematic multilayer structure of a SPD in "off" and "on" states (38).

The literature review of state-of-the art of SPD devices dedicated to their daylight performance has shown that very limited number of researches were produced in this area. Aritra Gosh et al. (39) have analyzed the daylight performance of SPD switchable glazing using a test cell oriented south. With a glazing to wall ratio 1:8 and transparency of SPD between 5% and 55% was found to control the glare. Most of the research articles regarding SPD material are aimed at the analysis of its physical and optical properties (38) (40) (41).

To comprehensively understand the active glazing material used in our study, we compare the property of electrochromic glass and the one of suspended particle device. The information is present in **Table 2** Comparison of main properties between EC glazing and SPD. (20).

Table 2 Comparison of main properties between EC glazing and SPD.

| Properties | EC | SPD |
|---|---|---|
| Technology | Electrochromic | Polarized particles |
| Clear state - Dark state | Off-On | On-Off |
| Visible Light Transmission (Clear-Dark) | 60%-1% | 65%-0.5% |
| Solar Heat Gain Coefficient (Clear-Dark) | 0.46-0.06 | 0.57-0.06 |
| UV transmission (Clear-Dark) | 0.4%-0% | 0.1%-0.1% |
| Number of light control levels from clear to dark | Typically, 4 states | Unlimited |
| Continuous states between dark and clear | Yes | Yes |
| Operating voltage | 12 V DC | 65-110 V AC |
| Power requirement for state transition | 2.5 $W/m^2$ | 5 $W/m^2$ |
| Power requirement for state maintenance | 0.4 $W/m^2$ | 0.55 $W/m^2$ |
| Switching speed | Typically, 5-12 min | Typically, 1-3 s |
| Colors | Typically, Blue or Green | Typically, Blue |
| Maximum size | 1550*4400 mm | 1524 mm*any length |
| Shapes | Rectangle, square, trapezoid, triangle | Any shape, curved, including holes anywhere |
| Operating temperature | from -20 to 70℃ | from -40 to 120℃ |
| Control | Wall switch, Remote control, Movement sensor, Light and temperature sensor, Timer | |
| Cost | Medium | High |
| Durability | > 30 years | > 20 years |

Comparing with EC glazing, SPD material instantly tints windows to select the amount of daylight that user want to let in, from clear to dark or any shade in-between. SPD material is fast because it is field-effect device. It relies on an electric-field effect, responding in 1-3 seconds and even faster response time is possible. Another reason is that SPD has no memory. It means the device will go to dark state if user turn off the applied voltage. Besides, larger range of visible light transmittance and unlimited intermediate control levels provide more daylight options.

AC voltage is the operating supply for SPD material which can be directly connected to the main power supply whereas EC glazing needs inverter to power directly with main supply, since DC is the voltage supply for EC. However, SPD energy consumption is more than EC

glazing, consequently from energy consumption point of view they are preferable for places in which windows remain opaque for most of the time.

## 1.3   Aim of the study and Research question

The review of the current literature on a topic of visual comfort and the strategies that are aiming to provide it has shown that this objective can be fulfilled when considering several parameters such as providing sufficient amount of daylight inside the room, guarantee its distribution in a way that unlit spaces are reduced as low as possible, controlling the glare, providing the view to the outside and at the same time making sure that the heat gains through the glazing are balanced to reduce as low as possible the energy consumption of the building. This task is containing the goals that are achievable but at the same time the achievement of one can lead to inability of reaching the other. The review of currently present strategies to fulfill mentioned design goals is showing that new methods in the design of control strategies to provide visual comfort should be investigated. Recent progress in the field of smart materials that are able to dynamically control the daylight provides an opportunity to make a break-through in daylight control strategies. In this study we are trying to answer following research questions:

(a) Can the glare from the sun directly visible in the field of view of the occupant be controlled by using materials with dynamically adjustable optical properties?

(b) What is the optimal area of the dynamic material that would guarantee a glare probability within acceptable range and how it can be found parametrically, based on the geographical location and a position of the occupant?

(c) What type of dynamic material is the most suitable for providing comfortable visual conditions in terms of glare evaluations and interior daylight distribution?

# Chapter 2    Research methodology

The review of the existing literature has led us to the development and testing of an occupant-based algorithm that utilizes glare as a visual comfort metric for establishing an area of the glazing that should be covered with a smart window film (electrochromic or suspended particles device)  to control the glare from the directly visible sun in the field of view of the occupant.

## 2.1    Software

Rhinoceros, a 3D computer graphics and computer-aided design (CAD) application software based on the NURBS mathematical model, and Grasshopper (42), a graphical algorithm editor integrated with Rhino's 3-D modeling tools are used for the development of simulation model. For performing daylighting simulations DIVA-for-Rhino software (43) was used. DIVA-for-Rhino allows users to carry out a series of environmental performance evaluations of individual buildings and urban landscapes including Radiation Maps, Photorealistic Renderings, Climate-Based Daylighting Metrics, Annual and Individual Time Step Glare Analysis, and others (43). The image-based simulations were performed using Ladybug and Honeybee plug-ins (44) for Grasshopper.

## 2.2    Simulation Model Definition

### 2.2.1    Geometry

To evaluate the performance of smart glazing we have created a digital model of a test room. The geometry of this test room was based on ASHRAE Standard 140-2001 case 600 model (45). The basic test room is a rectangular single zone (8 m wide x 6 m long x 2.7 m high) with no interior partitions and 12 m$^2$ of windows on the south exposure (WWR 55,6%). Each window is 3 m wide and 2 m high. The transmittance of the window was set to 65% T$_{vis}$ representing the generic double pane low-e window. The test room is also equipped with a table and standard monitor in front of an occupant. Every table is 1.83 m wide, 0.91 m long, and 0.86 m high **Figure 2-1**.

In this study we were interested in evaluation and comparison of different advanced smart materials and strategies in their capabilities of providing visual comfort considering the glare from the presence of a direct sun in a field of view and illuminance distribution inside the test room. Such properties as thickness of structural elements, size and material properties of a window frame can affect the results. For this reason, to reduce the number of factors that can play a role in obtained data from the daylight simulations, the thickness of walls and a presence of window frames were not considered.
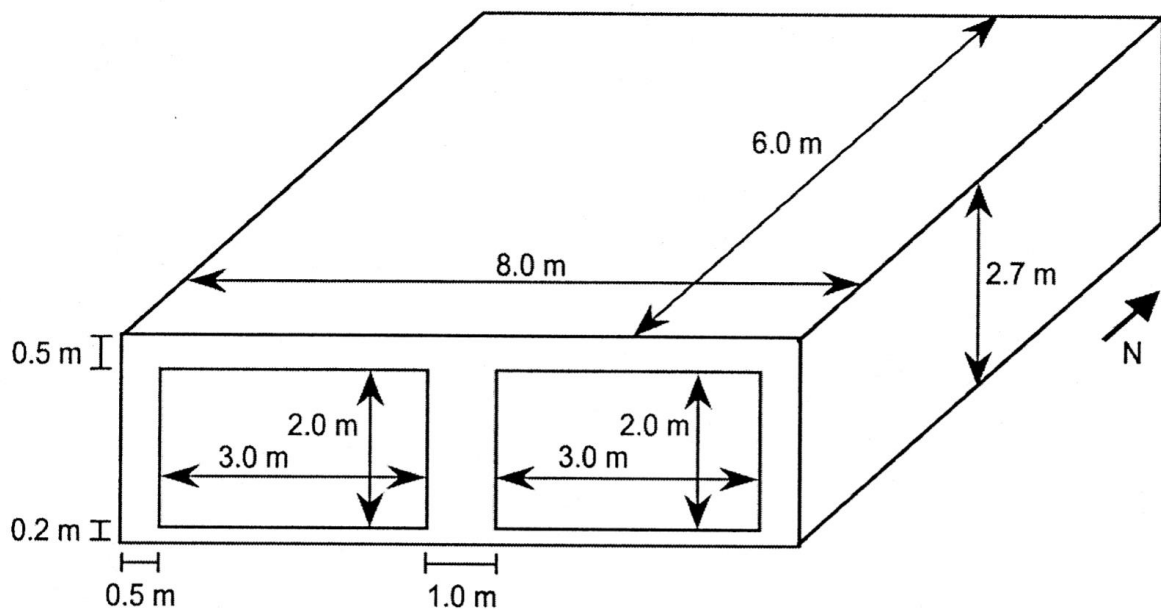


**Figure 2-1** ASHRAE-model dimensions (45)

## 2.2.2  Radiance material definition

To run a daylight simulation using Radiance engine all geometry has had to be assigned with a special definition.  The definition of all materials used for simulation was done by using Honeybee_createHBSrfc component. This component allows to assign Radiance material properties to a geometry built in Rhino. To do that, a text definition in a format that is recognized by Radiance engine must be provided as a text input.  Using this component, each type of material, represented by a reference geometry in Rhino, was assigned its own Radiance material. In our work we have used several types of Radiance materials: *plastic* (used for opaque materials), *glass*, *trans* (used for modeling SPD) and glow (used for monitor's screen) (46).

*Plastic*

Plastic is a material with uncoloured highlights. It is defined by a red green and blue reflectance value, a specularity value and by a roughness value (46). The example of opaque material assignment is illustrated on a **Figure 2-2.** Optical properties of opaque materials used for simulation are specified in **Table 2-1**.
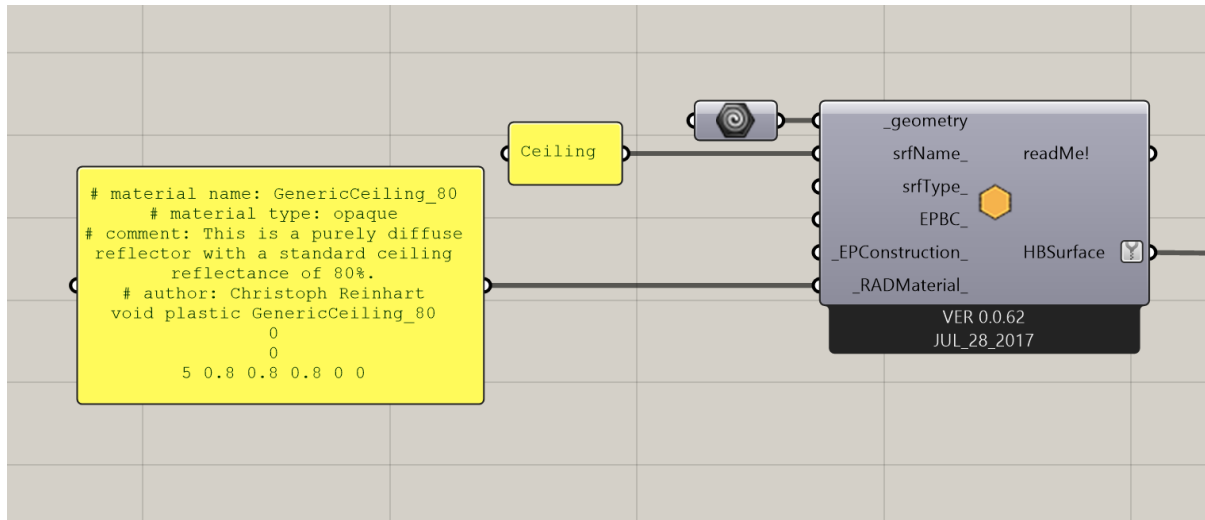


Figure 2-2 An assignment of Radiance properties of opaque material in Grasshopper to a reference geometry in Rhino

Table 2-1 Reflectance of opaque materials used in simulation

| Opaque material | Reflectance, % |
|---|---|
| Outside ground | 20 |
| Interior walls | 50 |
| Floor | 20 |
| Table | 50 |
| Monitor | 50 |
| Ceiling | 80 |

*Glass*

The glass type primitive is a specially modified dielectric. The material has been optimised to only produce one reflected ray and one transmitted ray through a single thin surface. In this way internal reflections are avoided. The glass type has a standard refractive index of 1.52 and all that is needed to be defined is the transmission at normal incidence (46). Electrochromic material was also modelled in the same way but with different transmittance – to evaluate the optical performance of EC in its darkest state, red green and blue transmittances were set to 1%.  **Figure 2-3** shows an example of glass material assignment.
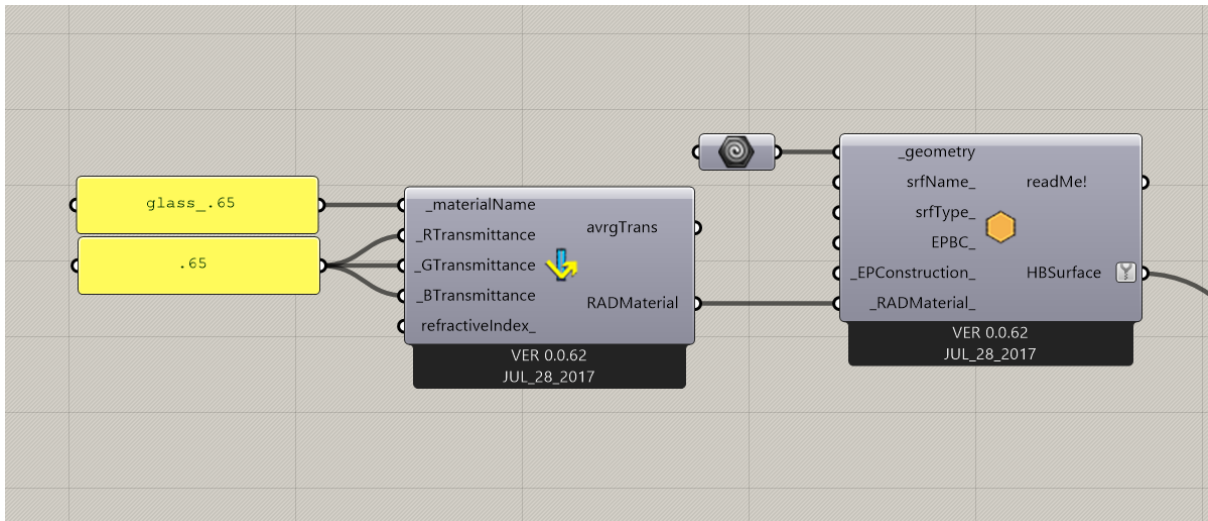
**Figure 2-3** An assignment of Radiance properties of glass material in Grasshopper to a reference geometry in Rhino

*Trans*

Trans material was used to simulate optical properties of SPD material. SPD material in comparison with EC or conventional glass is characterized not just by specular or direct transmittance and reflectance, but also by a diffused component of total transmittance and reflectance. To consider these properties of SPD, we have used a Honeybee Radiance Trans material component where RGB diffused reflectance, specular reflectance, direct and diffused transmittances had to be set **Figure 2-4**.
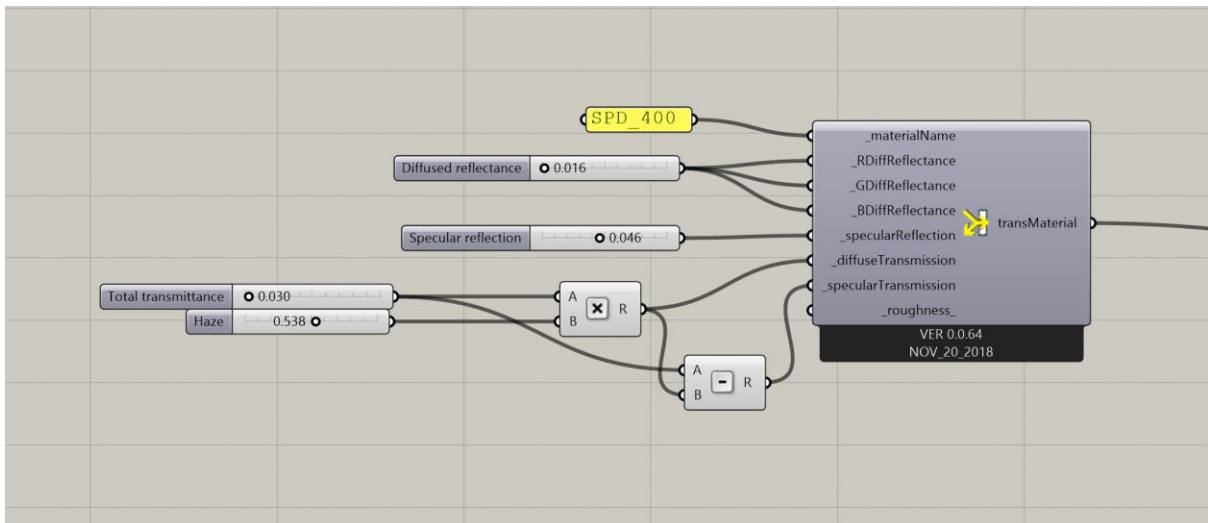


**Figure 2-4** An assignment of Radiance properties of translucent material in Grasshopper to a reference geometry in Rhino

## 2.3   Occupant-based form finding method

A glazing unit partially covered with electrochromic material is capable of reducing the glare from sun directly visible in a field of view of the occupant (36). If the position of the occupant inside the room is known, the area of the glazing through which the rays from the direct sun will be visible can be found. A sun path diagram was built for the test room using a Ladybug_SunPath component in Grasshopper. This component allows to obtain a sun position at a given instance and/or period of time. The most uncomfortable visual conditions in terms of glare will occur under clear sky and with the sun within the field of view of the occupant and to ensure that, the 21st of December, with the lowest sun position throughout the year, was selected to do an analysis. This date was used as an input date for sun path component in Ladybug. The time period considered for building the solar envelope was from 8 a.m. to 6 p.m. The occupant inside the office is represented as a mannequin in a seated position. The geometry of a mannequin was obtained using a Ladybug_ComfortMannequin component. Connecting each sun position at a specified date and a point, representing the eye-level of the occupant, allows us to obtain a loft surface, see Figure 2-5.
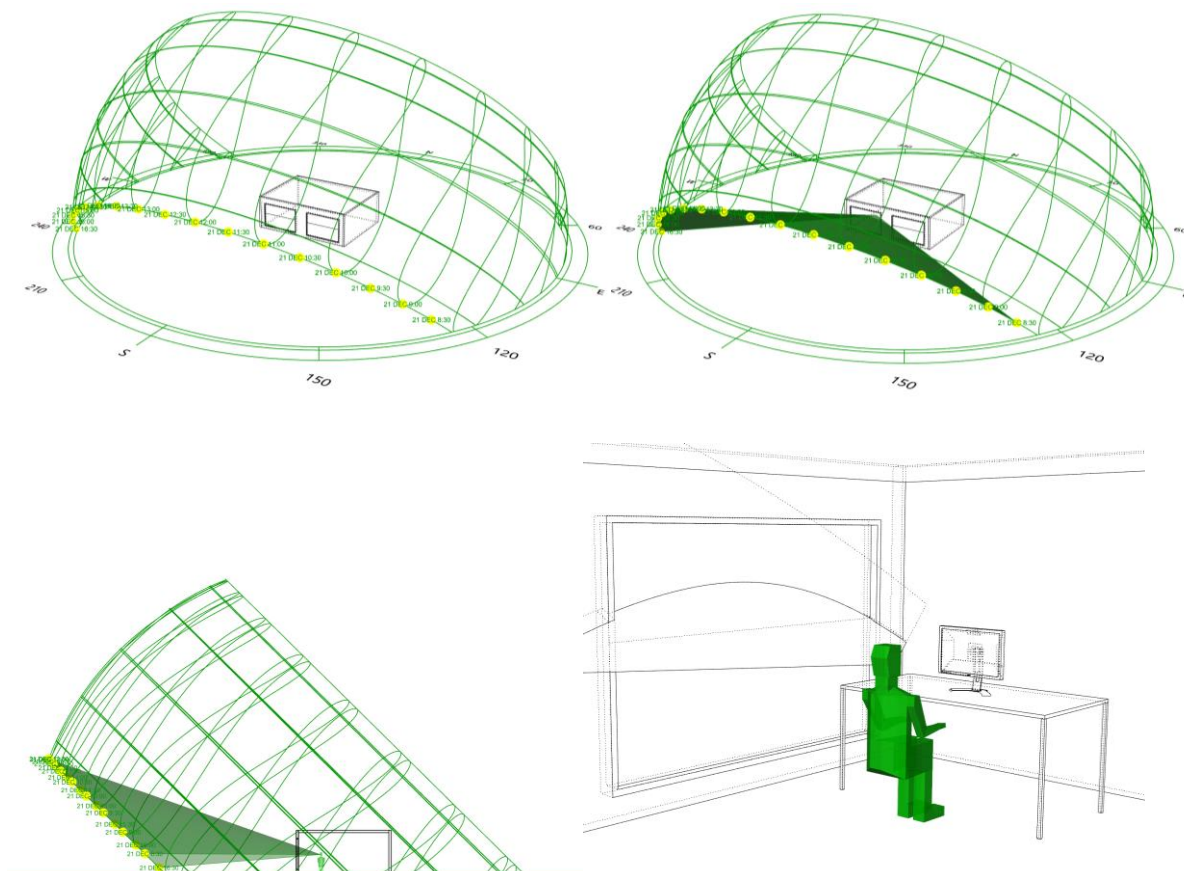


Figure 2-5 Form finding algorithm

By intersecting the loft surface and a surface of the glazing we have obtained a curve on the glazing, the end points of which were used as constraints to outline the area on the glazing. Obtained rectangular area from the top of the glazing to the end point of the curve of intersection was then assigned a smart film material. The conditions where the upper zone is an electrochromic glazing and a lower zone is a conventional glazing were used as a starting condition for further evaluations **Figure 2-6**.
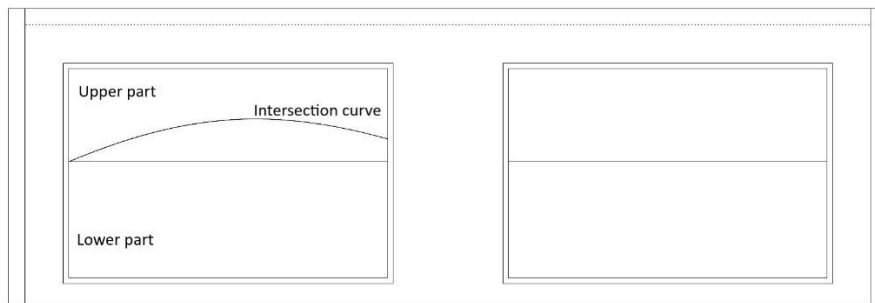


**Figure 2-6** Division into upper and lower parts by an intersection curve

The assumption is that the obtained geometrical configuration of the glazing with a portion of the glazing that would be assigned a dynamic material would provide a glare-free field of view for the occupant, with the sun being shaded by the dynamic portion of the glazing. As one of the inputs that is required for this method is the position of the occupant closest to the glazing. Relatively to the position of the closest to the fenestration system occupant, the rest of the users of the space would obtain the situation where the sun is present in their FOV for a shorter period of time, and furthermore the relative position of the sun to the occupant in the depth of the space would assure that the sun would be shaded by the upper part. (**Figure 2-7**).
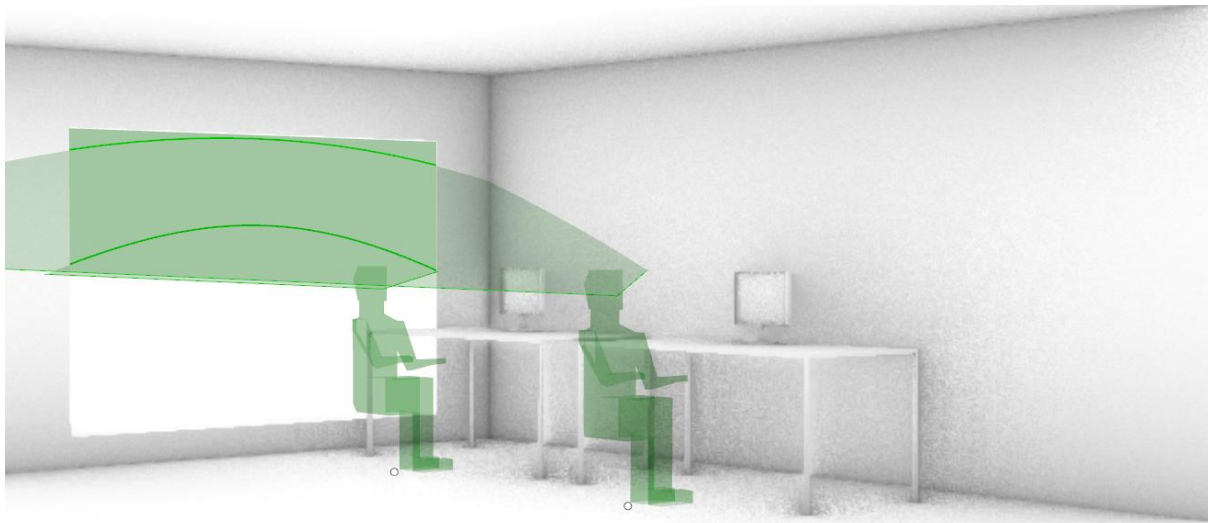
Figure 2-7 Positions of the occupants and according sun path envelope

The height of the upper is dependent on the relative position of the occupant to the fenestration system and a sun's altitudes and azimuths. Last two variables are changing according to the geographical location. Generally, the closer the location to the equator, the higher the sun's position in the winter solstice, thus the smaller would be the portion of the glazing that is dedicated to blocking the rays from the sun directly visible in the field of view when the user's position is fixed. An example of the area of the upper part of the glazing found by using adopted method is shown on **Figure 2-8** . Here, the position of the occupant is also fixed at 1.5 m. away from the glazing and the chosen locations are London and Athens. These locations were also chosen for evaluation in **Chapter 3.3**.
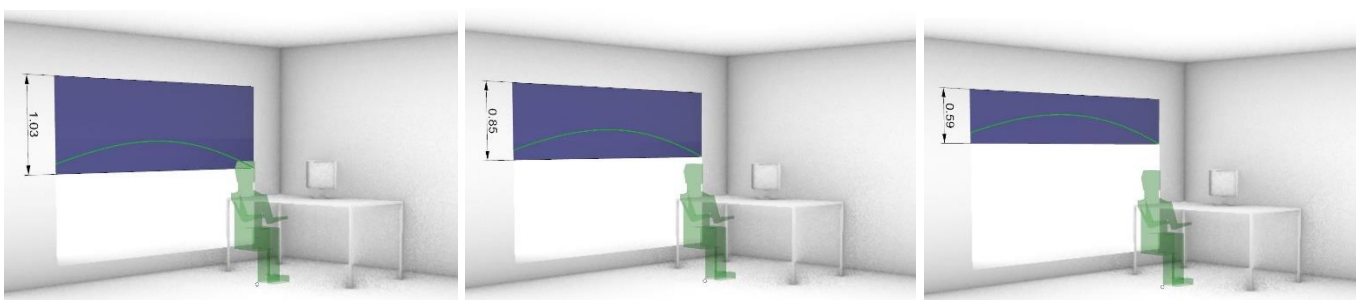


Figure 2-8 The height of the upper part in dependence from location (from left to right: London, Milano, Athens)

Taking into account the fact that the curve of the sun path was built for 21$^{st}$ of December, we had to make sure that all surface of the upper part should be consistent and with no need of further division. **Figure 2-9** represents the sun paths in relation to the position of occupant's eye level for Milano on the dates of 21.12, 15.11, 1.11 and 20.10. Based on this, we may make a conclusion that for any location during the time period when the sun is in the FOV of the occupant, the sun position may be found in any point during the year considering upward direction from its lowest possible positions on December 21$^{st}$.
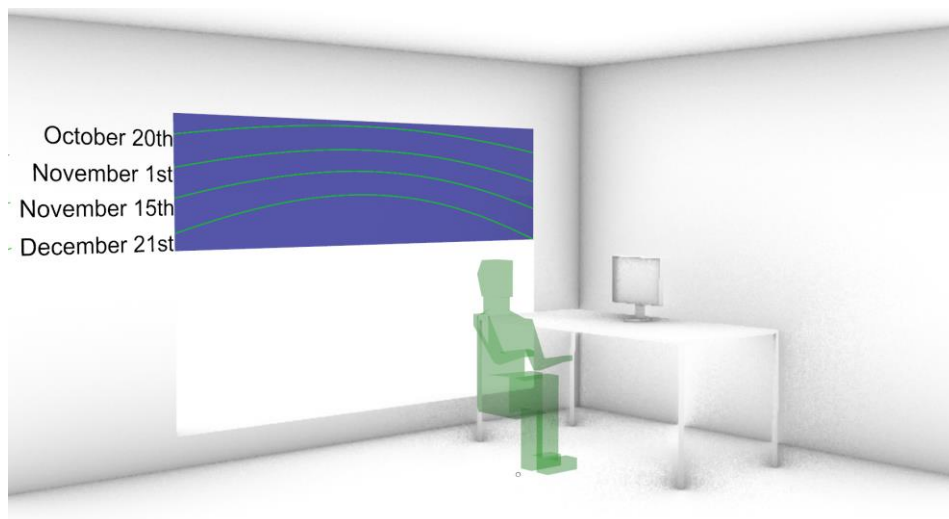


**Figure 2-9** Sun path curves for Milano for 21st of December, 15th of November, 1st of November and 20th of October relatively to occupant's eye-level

Considering the change of orientation of the glazed façade to be analyzed, the height of the upper part is observed not to be changing. Analyzing relative to the occupant's eye level position of the point where the sun is (21.12, 6 p.m., Milano, **Figure 2-10**) with the rotation of the façade (rotation of direction North) the point representing the lowest sun position is moving in a horizontal plane while the height of the upper part remains the same. Considering the fact that during the year the sun path is moving in a way that the relative point of the sun position at, for example, 21$^{st}$ of September at 4 p.m. would be shifted sideways and upwards (considering from a point of view of a human standing on the ground), it might be suggested that using this method, the height, obtained considering the sun path on 21$^{st}$ of December , would be suitable for any orientation. For the same reason mentioned previously, it might make sense not to restrict the zone where the dynamic glazing should be applied as it is shown on **Figure 2-10**.

Summarizing the approach, when a position of the user and a corresponding eye level must be used as an input, together with the location. When location is known, a sun path diagram may be found for 21.12, since on this period the altitudes of the sun are the lowest, thus making sure that by assuring the coverage of the sun in, perhaps, the worst conditions, the rest of the times would be covered as well. When inputting a desired time period of the

day (e.g. 8 a.m. – 6 p.m.) the sun positions for that period are obtained. Connecting the points representing the sun position and the point that represents the eye-level of the occupant, an intersection curve on the glazing may be found.  By moving the location of the occupant without changing his distance from the façade or by changing the orientation of the façade, the height of the intersection curve itself would not be changing with respect to a horizontal plane (floor). The parameters affecting the height of the upper part are mainly the distance from the glazing of the occupant and a site location, together with geometry of the space and WWR.

Since the use of dynamic glazing may find more use in applications on South façade, this case was considered in our research.
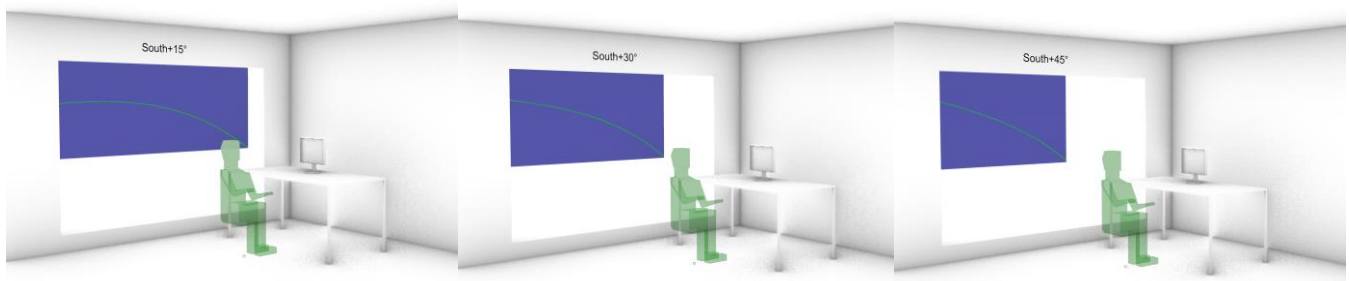


**Figure 2-10** Sun path intersection curve in relation to different orientations of the exposed facade: left to right South +15°, South +30°, South +45°

## 2.4   Glare evaluation

The ability of adopted approach to provide visual comfort was analyzed by means of glare metrics. DIVA-for-Rhino, Ladybug and Honeybee plug-ins are capable of preforming point-in-time glare simulations using Radiance. As an input information it requires a date and time, the camera setting as a perspective view in Rhino viewport, type of the camera, sky conditions and Radiance parameters for the simulation. As an output it provides a picture in a tif. and hdr. format together with a txt. file containing information about DGP, DGI, UGR, CGI. DGP is a commonly adopted index for evaluation of glare probability in the scene and it is proven to be the most reliable and developed metric since it has been developed based on experiments with real human subjects (47) (48) (49) (50).

The DGP is calculated according to the following equation:

$$DGP = 5.87 \cdot 10^{-5}E_v + 9.18 \cdot 10^{-2}\log\left(\left(1 + \sum_i \frac{L_{s,i}^2 \omega_{s,i}}{E_v^{1.87}P_i^2}\right)\right) + 0.16 \qquad (1)$$

where $E_v$ is the vertical illuminance at eye level [lx]; $L_s$ is the light source luminance [cd/m$^2$],$\omega_s$ is the light source solid angle [sr]; $P$ is the position index [-], which expresses the variation in glare sensation experienced relative to the angular displacement of the light source from the observer's line of sight. This equation consists of two terms: the first one considers the vertical eye illuminance, while the second accounts for the contrast between the scene background luminance and the luminance of the light sources within occupant's visual field.

The DGP value range is sub-divided into four sub-ranges: *Imperceptible glare, Perceptible glare, Disturbing glare and Intolerable glare.* This subdivision was purposed by Jan Wienold (9). The values of DGP corresponding to each comfort range are presented in the table **Table 2-2**

Table 2-2 Daylight glare comfort classes and relative DGP values

| Daylight glare class | DGP threshold |
|---|---|
| Imperceptible glare | < 35% |
| Perceptible glare | 35% ≤ DGP < 40% |
| Disturbing glare | 40% ≤ DGP < 45% |
| Intolerable glare | DGP ≥ 45% |

The Radiance parameters used to execute the simulations are presented in Table 2-3. The camera type chosen was fisheye lens. The sky conditions were set to be CIE Clear Sky.

Table 2-3 Radiance simulation parameters and assigned values

| Radiance parameter | Description | Value |
|---|---|---|
| -ps | Pixel sampling rate | 2 |
| -pt | Sampling threshold | 0.05 |
| -pj | Anti-aliasing jitter | 0.9 |
| -dj | Source jitter | 0.7 |
| -ds | Source substructuring | 0.05 |
| -dt | Direct thresholding | 0.15 |
| -dc | Direct certainty | 0.75 |
| -dr | Direct relays | 3 |
| -dp | Direct pretest density | 512 |
| -st | Specular threshold | 0.15 |
| -ab | Ambient bounces | 6 |

| -aa | Ambient accuracy | 0.1 |
|---|---|---|
| -ar | Ambient resolution | 128 |
| -ad | Ambient divisions | 4096 |
| -as | Ambient super-samples | 4096 |
| -lr | Limit reflection | 8 |
| -lw | Limit weight | 0.005 |

## 2.5    Horizontal illuminance evaluation

In order to analyze the interior daylight distribution, horizontal illuminance evaluation is implemented in terms of daylight point in time and climate-based metrics, horizontal illuminance, useful daylight illuminance (UDI). Considering each of them is grid-based calculation, sensor node grid is set up on the work plane level inside of the test room. The size of the grid is 0.4 m and the distance from the ground floor is 0.9 m. The test grid is present in Figure 2-11. Ladybug and Honeybee plug-ins are adapted to perform these series of simulations.

Point-in-time illuminance measures interior daylight level at a specific date and time, under a specific sky condition. Milano Linate EPW. Weather file obtained from EnergyPlus is input to gather the climate data. 21$^{st}$ on December is selected as the date to evaluate the point-in-time illuminance and the simulating time is from 8 a.m. to 6 p.m. with one-hour interval.

The real  daylight illuminances across the work plane exhibit large variations both spatially and temporally. For example, daylight illuminance typically diminish rapidly with larger distance from windows. Equally, daylight illuminance at a point can vary greatly from one moment to the next due to changing sun position or sky conditions. If the daylight illuminance is too small (i.e. below a minimum), it may not contribute in any useful manner to either the perception of the visual environment or in the carrying out of visual tasks. Conversely, if the daylight illuminance is too great (i.e., above a maximum), it may generate visual discomfort.

Hence, it is proposed by *Mardaljevic and Nabil in 2005* that the daylight illuminance at the calculated points fall within the range 100 lux to 2000 lux should be considered as useful (10). In more detail, daylight illuminances in the range 100 lux to 500 lux are considered effective and daylight illuminances in the range 500 lux to 2000 lux are often perceived either as desirable or at least tolerable. Daylight illuminances less than 100 lux are generally considered insufficient and Daylight illuminances higher than 2000 lux are likely to produce visual discomfort (10).
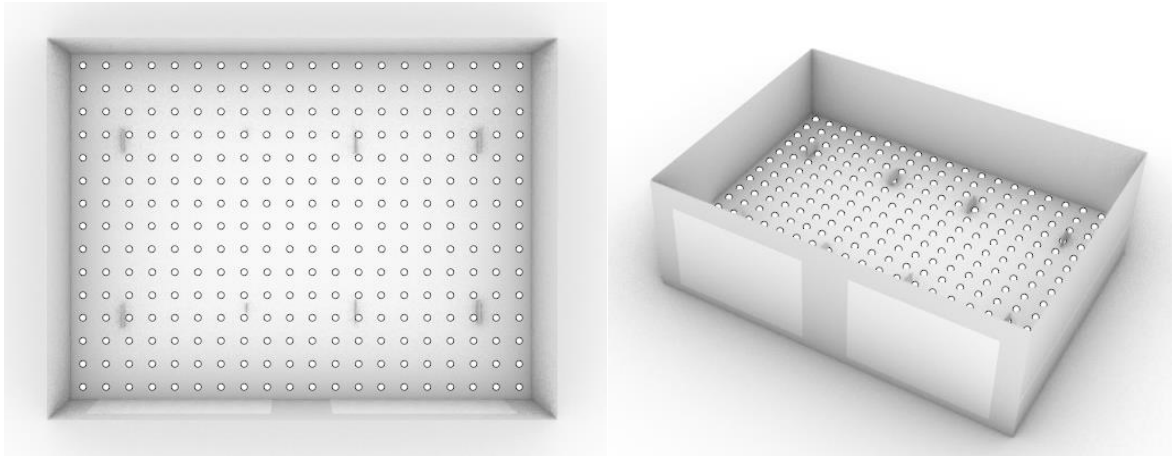
Figure **2-11** Test grid for horizontal illuminance

## 2.6   Simulation cases

To analyze the occupant-based form finding algorithm described in section 2.3 in terms of its efficiency in providing glare control from the sun directly visible in the field of view we have considered 14 simulation cases.

All 14 cases are essentially representing 7 design options and each design option is then further analyzed considering two orientations of the occupant – East and West **Figure 2-12**. This consideration is representing quite particular, but yet possible condition in a standard office room where the desk position and orientation is chosen in a way that the window is located on the side from the occupant (19) (48) (35). The cases where occupant is facing South exposed window and North wall were not considered in this study, since it is not a common practice to locate a work station in an office room right in front of the south facing window and a case when an occupant is facing the North wall gives no opportunity to evaluate the capabilities of smart dynamic window films in controlling the glare.
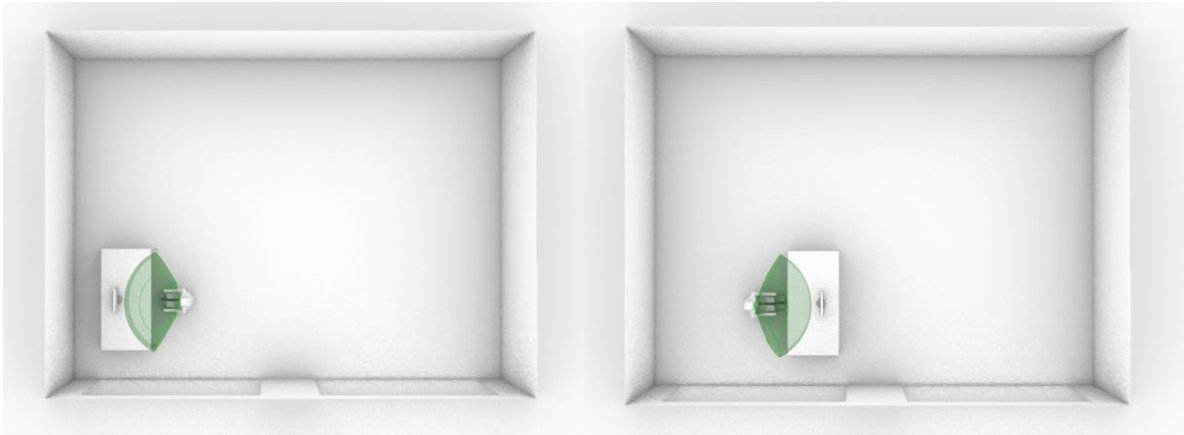
**Figure 2-12** West oriented occupant (left) and East oriented occupant (right)

Each design option in analyzed simulations was chosen to evaluate different influence that those options create in terms of visual conditions.

The reference cases, where no shading strategies were used, were performed to have an initial understanding and a starting point to compare different design solutions.

EC base case is representing the evaluation of performance of electrochromic film being applied on the upper part of the glazing and the height of the electrochromic part was found using the method described in secion 2.3.

EC increased size case was performed to investigate the influence of a larger portion of the electrochromic film being used to asses the influence of such desigion on the second term of the DGP equation (1) that is considering contrast level. Besides the contrast, increased height of the upper portion of the glass might have a positive effect in blocking the high luminus flux from the sun corona (51). Here, the heigh of the upper part was increased to 1.275 m. in comparison with 0.85 m. for the base case.

The SPD cases are performed to see the influence of the fact that considerable portion of transmitted light is diffused. This might affect both terms of the equation (1). The number in the name of the case is representing the thickness of the SPD material: SPD base case 200 is a case where the height of the covered part is the same as in EC base case and the optical properties used  are respectively equal to the ones that can be found for an SPD material with a thickness of 200 µm.

All considered cases are presented in the **Table 2-4**

**Table 2-4** Simulation cases

| Simulation case № | Simulation case | Distance from the glazing, m. | Orientation of the occupant | Upper part height, m. | Transmittance of the upper part, % | Haze of the upper part, % | Transmittance of the lower part, % |
|---|---|---|---|---|---|---|---|
| 1 | Reference case West | 1.5 | West | 0 | 65 | 0 | 65 |
| 2 | Reference case East | 1.5 | East | 0 | 65 | 0 | 65 |
| 3 | EC base case West | 1.5 | West | 0.85 | 1 | 0 | 65 |
| 4 | EC base case East | 1.5 | East | 0.85 | 1 | 0 | 65 |
| 5 | EC increased size West | 1.5 | West | 1.275 | 1 | 0 | 65 |
| 6 | EC increased size East | 1.5 | East | 1.275 | 1 | 0 | 65 |
| 7 | SPD 200 base case West | 1.5 | West | 0.85 | 15 | 17.5 | 65 |
| 8 | SPD 200 base case East | 1.5 | East | 0.85 | 15 | 17.5 | 65 |
| 9 | SPD 400 base case West | 1.5 | West | 0.85 | 3 | 53.8 | 65 |
| 10 | SPD 400 base case East | 1.5 | East | 0.85 | 3 | 53.8 | 65 |
| 11 | SPD 500 base case West | 1.5 | West | 0.85 | 1.7 | 65.5 | 65 |
| 12 | SPD 500 base case East | 1.5 | East | 0.85 | 1.7 | 65.5 | 65 |
| 13 | SPD 550 base case West | 1.5 | West | 0.85 | 1.2 | 70.3 | 65 |
| 14 | SPD 550 base case East | 1.5 | East | 0.85 | 1.2 | 70.3 | 65 |

### 2.6.1   Reference case

The reference case configuration was used as a benchmark for comparing the results with any other configuration. In this way the influence of applying dynamic film on the upper part of the glazing with different modifications to its size and material used can be quantified. The geometry remained the same. The location was chosen to be Milano Linate. The test room glazed façade is oriented facing South and glazing being fully composed by a conventional double pane low-e glazing with 65% visual transmittance. The occupant position was set to be 1.5 m away from the center of the West sided glazing unit **Figure 3-3**. The considered orientations of an occupant are West and East. No interior lightning is considered in this and following simulation cases.

### 2.6.2   EC base case

To develop a base case configuration, we have used a method described in section **2.3** to find dimensions and area of the upper part of the glazing. Similarly to a reference case, the position of the occupant was 1.5 m. from the glazing. The eye-level of the sat occupant represented by Ladybug comfort mannequin is 1.17 m. Using these parameters, the obtained height of the upper part was 0.85 m. (**Figure 2-13**) The transmittance of the EC glazing portion 1% $T_{vis}$ corresponding to the lowest visual transmittance that can be obtained with the current

state of electrochromic glass producers' technologies (21). The lower part was considered to be 65% $T_{vis}$, similarly to the reference case.
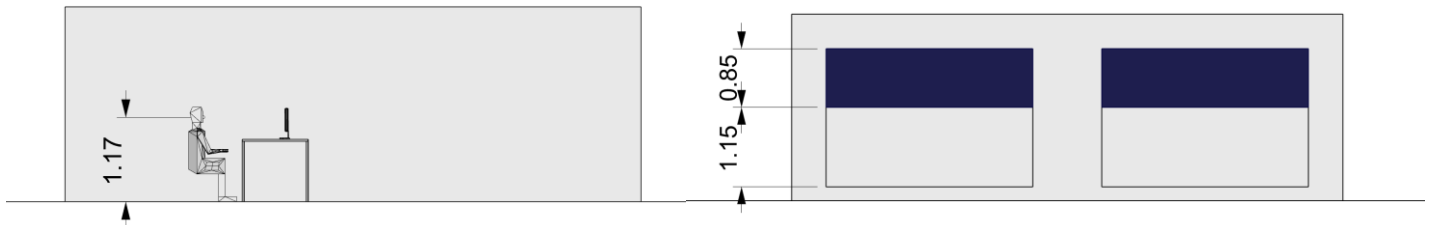


**Figure 2-13** Mannequin eye-level height (left) and base case upper- and lower-part heights (right)

To build a sun path diagram, a center point of the diagram must be set. The center point of a test room's floor was found and chosen to be as a point, around which the sun path diagram was built. For this reason, the trajectory of the sun is symmetrical with respect to the central axis of the test room. Since all cases were done considering an occupant's position in front of one of two windows, symmetry in this case legitimizes the results for whole test room.

### 2.6.3 EC increased size

The first consideration was to evaluate the performance of upper EC part being increased from 0.85 m. to 1.275 m. (**Figure 2-14**). The adopted approach of finding EC-covered area only takes into account the sun positions, thus, even if the direct sun rays would be covered by the electrochromic part, there is a risk that the presence of the sun corona would cause uncomfortable visual conditions due to the fact that sun's corona luminance values can increase the DGP term (51).  The size reduction was not considered as an option since this would cause the conditions when the sun would be directly in a field of view and without any shading strategy or obstruction applied which would cause undesirable uncomfortable visual conditions. The further increase in size was not considered because this would result in glazing unit being mostly covered with electrochromics, which, when being turned into its darkest state to control the glare from a direct sun, would cause insufficient amount of daylight inside the test room reducing  IEQ parameters related to amount of light and psychological conditions. This would not only cause increase of energy use for lightning but also create unfavorable psychological conditions for users inside the space turning it into too gloomy (37).
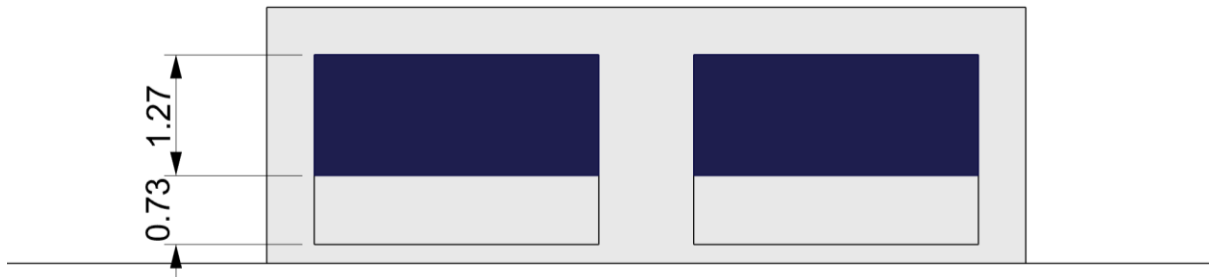
**Figure 2-14** Upper- and lower-part heights for EC increased size case.

### 2.6.4  SPD base case

The suspended particle devices are currently considered as one of the possible options to dynamically control the daylight inside the space. Their optical properties are mainly similar to the optical properties that can be found in electrochromic devices, but due to a different coloration mechanism, SPD is characterized by a considerable amount of sunlight being transferred through in a diffused manner. To obtain numerical characteristics of optical properties of this material we have used data obtained by David Barrios et al. in their research article dedicated to simulation of the thickness dependence of the optical properties of suspended particle devices (38). In their research it was found that the values of diffused reflectance, specular reflectance, direct and diffused transmittances are dependent on a thickness of SPD. Their data was obtained based on using two-flux and four-flux model calculations and findings from their previous works with a real SPD sample (41). The considered state of the SPD was the "off"

In our work we have considered several possible thicknesses of SPD: 200 µm, 400 µm, 500 µm and 550 µm. Each of considered thicknesses have different optical properties that are reported in table **Table 2-5**

**Table 2-5** Optical properties of SPD

| Thickness | Specular reflectance, % | Diffused reflectance, % | Total transmittance, % | Haze, % |
|---|---|---|---|---|
| 200 µm | 4.6 | 2.3 | 15 | 17.5 |
| 400 µm | 4.6 | 1.8 | 3 | 53.8 |
| 500 µm | 4.6 | 1.6 | 1.7 | 65.5 |
| 550 µm | 4.6 | 1.6 | 1.2 | 74.4 |

The values in Table 2-5 were obtained by interpolation of data from (38) . Considered state of the SPD was "off", since it is the darkest state of the material (**Figure 2-15**, **Figure 2-16**).
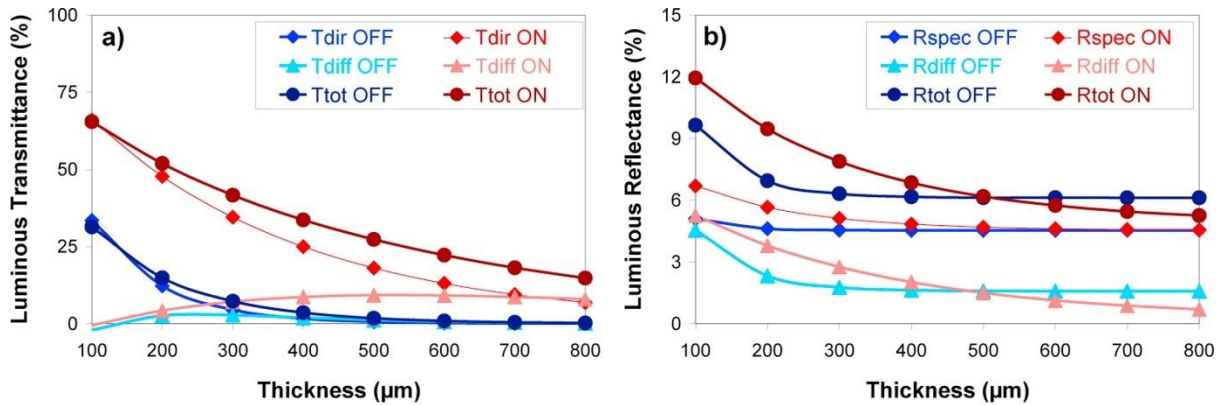


**Figure 2-15** Thickness dependence of transmittance T and reflectance R of SPDs in dark ("off") and clear ("on") states, given in percent units. (38)
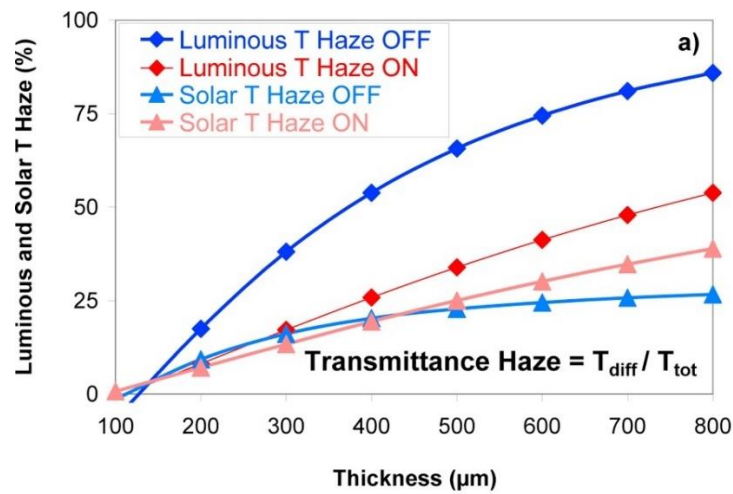


**Figure 2-16** Thickness dependence of luminous and solar transmittance haze (38)

# Chapter 3    Simulation results

## 3.1    Glare analysis results

### 3.1.1    Reference case

The series of point-in-time glare simulations were performed for the reference case, where the transmittance of the glazing of the test room was set to 65% $T_{vis}$ . The considered location of the occupant was set to 1.5 m. away from the center of the glazing unit and was maintained for all following simulation cases. Field of view of the occupant oriented East and West is presented on **Figure 3-1**.
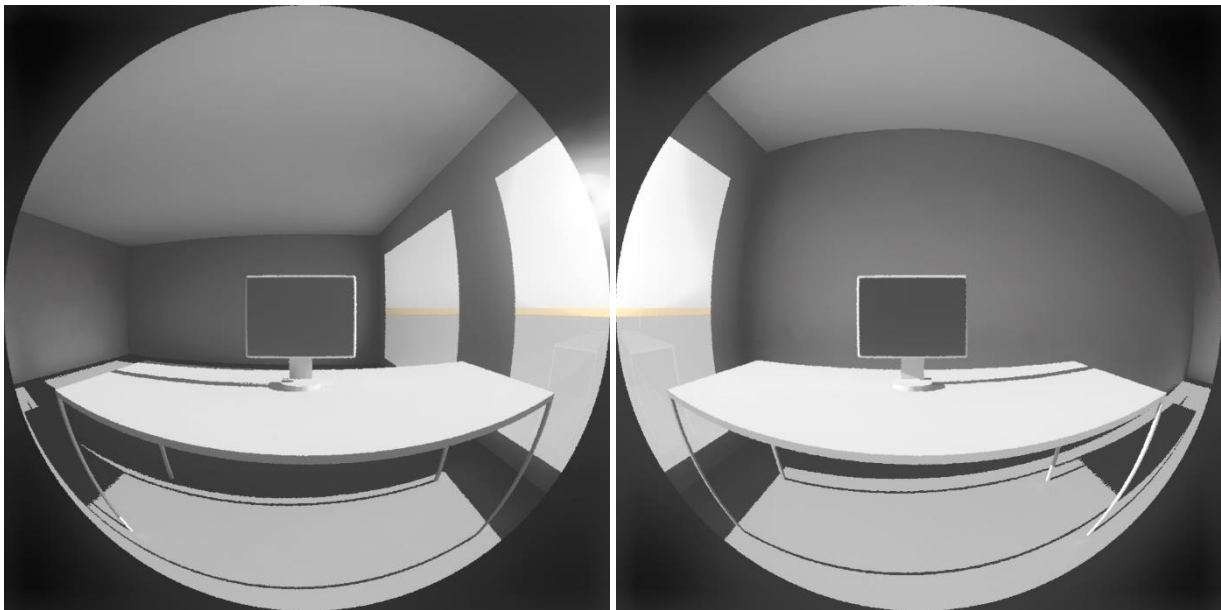


**Figure 3-1** Occupant location and orientation to East (left) and West (right) at midday

The results of point-in-time glare simulations are presented on a **Figure 3-2**. The chosen timestep between simulation was set to half an hour and was maintained for all following simulation cases. The results are showing that without any shading strategy applied, for chosen position and occupant orientations the DGP values are reaching its maximum values (100%) for the periods of time, when the sun is in a field of view of the occupant. The blue line

is representing the DGP values during the day for the occupant oriented East and the orange line is representing the same, but for West orientation of the occupant. It is noticeable that for East orientation the sun first appears in the field of view after 8:00 a.m. and leaving after 12:30 p.m. For West oriented occupant the sun is visible after 12:00 a.m. and is leaving the field of view at 4:00 p.m. We can observe from the graph that when the sun is not in the field of view (behind the occupant's back), the DGP value does not exceed the perceptible threshold of 35%.
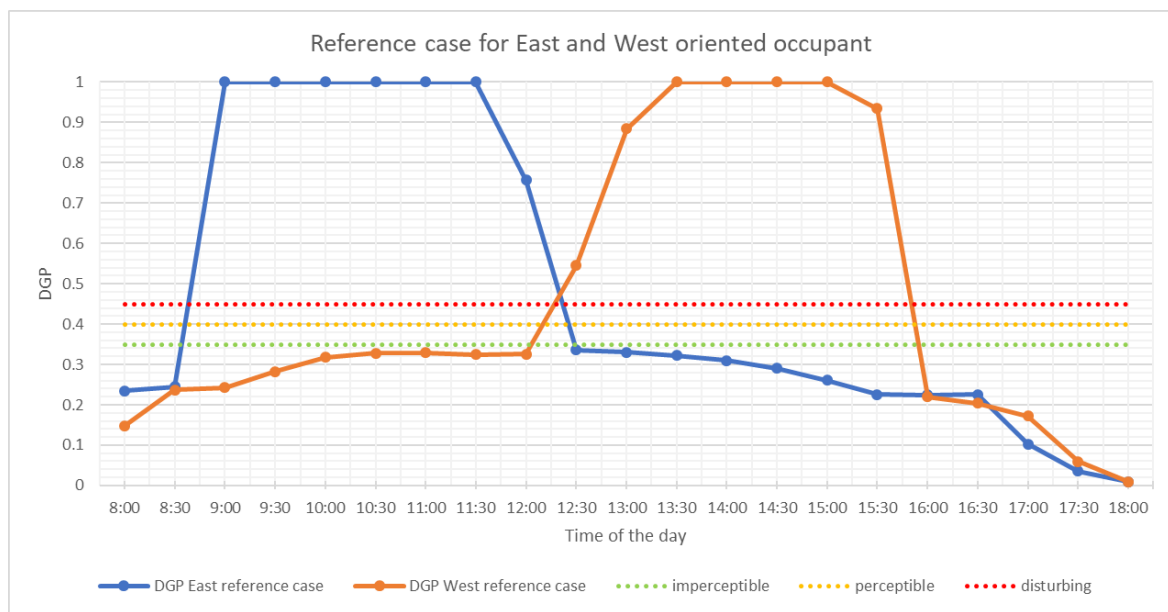


**Figure 3-2** DGP values during 21st of December for East and West oriented occupant. Reference case

The next step of our research was to evaluate the applicability of the occupant-based approach described in section 2.3.

### 3.1.2  EC base case West

In the EC base case West occupant is oriented West and the height of the upper, electrochromic part is 0.85 m. (**Figure 3-3**). The results of point-in-time glare simulations are presented in the **Figure 3-5**. For the West orientation from 8 a.m. to 12:30 p.m. the sun is not visible in the field of view, so the visible conditions and the amount of luminance are provided just by the diffused sunlight from the surrounding environment. The DGP value is within comfortable range and reaches its maximum value at 12:30 p.m. with a value of 25.2%. The brake in line is noticeable at 12:30 p.m. and at this time the sun is becoming directly visible. Being on the far-left side of the field of view its influence is not critical up to around 1:45 p.m. The closest measured DGP value when the glare conditions are characterized as imperceptible is at 1:30 p.m. and the value is 32.7%.



Figure 3-3 EC base case West. West-oriented occupant at midday

During the time interval from 2 p.m. to 3:30 p.m. the glare is becoming perceptible with the maximum value of 39.3% at 3 p.m. After 3:30 p.m. the sun is leaving the view field of the occupant and DGP value is rapidly decreasing approaching zero at 6 p.m. Such fast decrease of DGP value is explained by the fact that the sun is no longer providing direct daylight to the human eye, furthermore, the tined state of 1% $T_{vis}$ is remaining throughout the whole day in the simulation. As a result, in a base case simulation and West orientation of the occupant perceptible glare conditions are occurring for about 1:45 hours during the day of 21st December, which is 15% of the analyzed time period 8 a.m. − 6 p.m. It could be assumed that for given test room geometry, view orientation, clear sky conditions and visual properties of the materials in this simulation observed glare risk values are perhaps the worst condition during the year.

### 3.1.3 EC base case East

The field of view for the East oriented occupant is presented on **Figure 3-4**. For the East orientation the DGP value reaches 36% at 9:00 a.m., directly when the sun first starts to be visible in the field of view. From 9:00 a.m. to 9:30 a.m. the DGP rises by 2.5 % reaching value of 38.5 % with its maximum value of 38.6% at 10:00 a.m. and continues to be in perceptible comfort class up to 11:00 a.m. After 11:00 a.m. the DGP falls into imperceptible range with the sun still being in the field of view until 12:00 p.m. Starting from midday, East oriented occupant only sees diffused daylight and the DGP remains in imperceptible comfort class. As a result, for chosen configuration and model settings, the glare results to be in only perceptible range for approximately 1:45 hours, from 9:00 a.m. to around 10:45 a.m. (**Figure 3-6**).
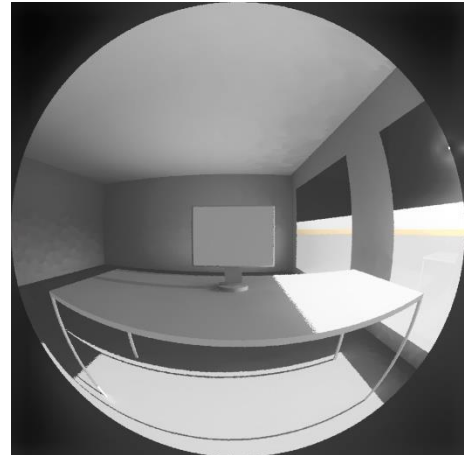


**Figure 3-4** EC base case East. East-oriented occupant at midday
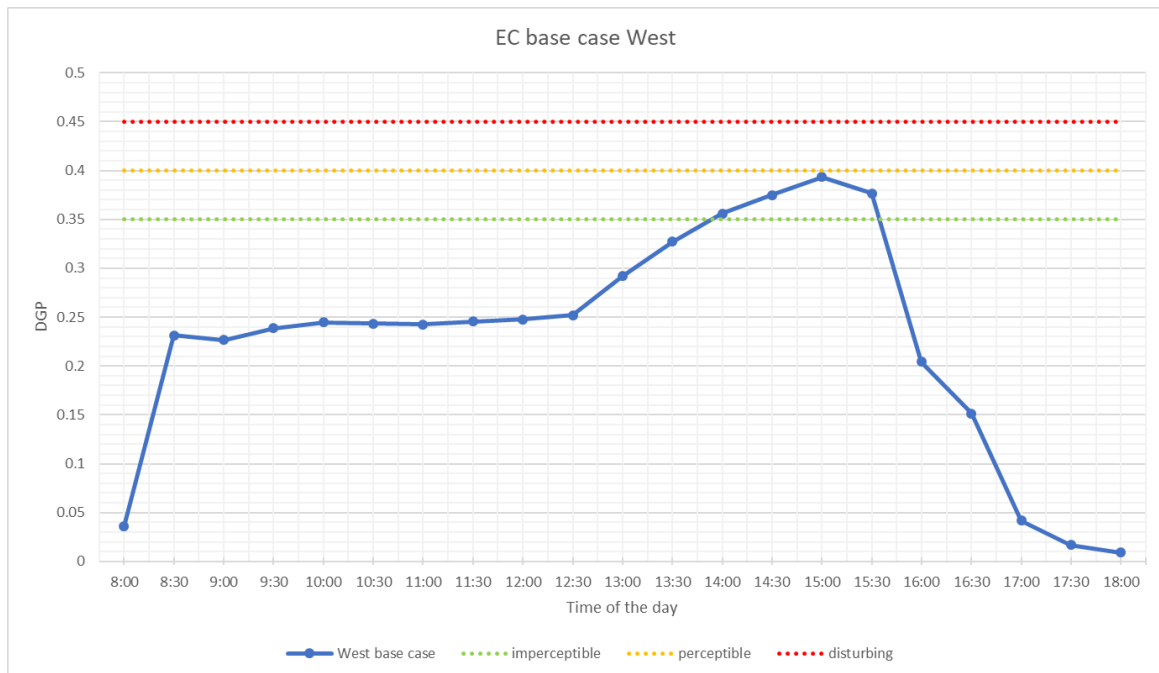


**Figure 3-5** DGP values for 21st December for EC base case West
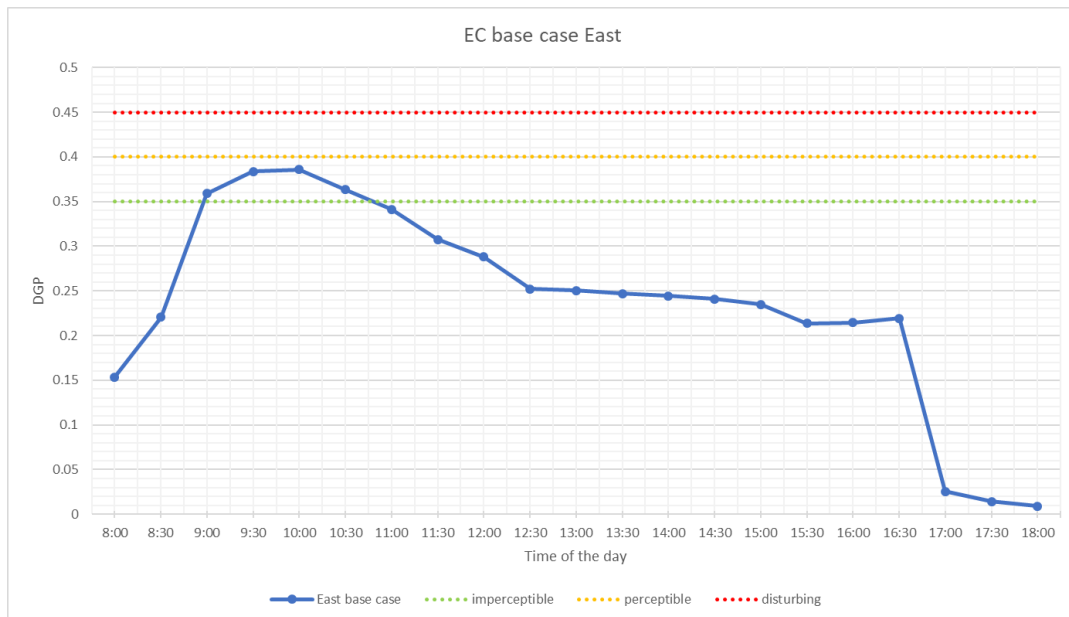
**Figure 3-6** DGP values for 21st December for EC base case East

### 3.1.4    EC increased size West

In this case the height of the upper electrochromic part is 1.275 m to investigate if enlarged dimensions of fully tinned electrochromic glazing would be beneficial in reducing possible negative effect of extreme values of the sun's corona luminance that is causing glare. The user's orientation and field of view are presented in the **Figure 3-7** and the results of point-in-time glare simulations are presented in the **Figure 3-10**. Analyzing the graph, we can note that in the first part of the day, when the sun is not directly visible, the DGP value of the increased case is 5% - 10% smaller than for the base case. This could be explained by the fact that when measuring the value of DGP only diffused and reflected light is reaching the eyes of the occupant. Within this condition, the enlarged height of the upper part is only reducing the amount of luminance values in the field of view, which is accordingly followed by reduction of DGP values. Nevertheless, this changes as soon as the sun appears in the field of view. At 1:00 p.m. the value of DGP is 29% and it is smaller only by 0.1% with respect to the base case in the same conditions. Further in time the increased size case performs worse: the daylight glare probability increases with
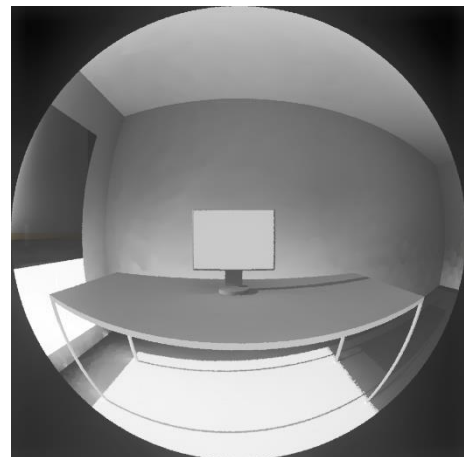


**Figure 3-7** EC increased size. West oriented occupant at midday

respect to the base case. At 2:30 p.m. this difference becomes 2.4% and is 39.9 % for the increased size case, on the border between perceptible and disturbing glare comfort class. At 3:00 p.m. The DGP rises to the value of 41.7% and becomes disturbing. After 3:00 p.m. the glare probability starts decreasing very rapidly in comparison with the base case and at 3:30 p.m. becomes imperceptible with the value of DGP being 25.1%, when for the base case at this point in time the DGP is still in perceptible comfort range (**Figure 3-10**). As a result, for the increased size case, the amount of time when the glare is in perceptible and disturbing comfort class is 1:30 hours, which is around 12% of the analyzed period of time. This is slightly fewer than for the base case, but in the modified case the DGP becomes disturbing for around half an hour.

The fact that daylight glare probability value is greater for the modified case, where electrochromic part is bigger at first seems counterintuitive. To find a possible explanation for this we have analyzed HDR output files from EvalGlare software, which is built in Radiance, by means of wxFalsecolor (52) that was used to display Radiance RGBE images and read luminance/illuminance values (**Figure 3-8**).
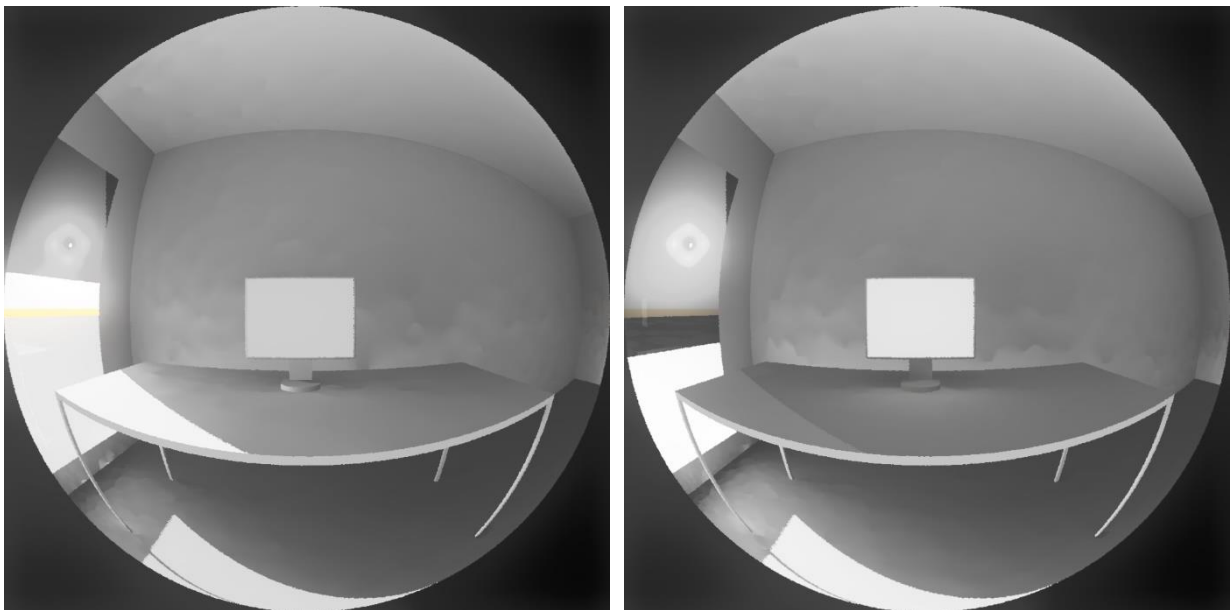


**Figure 3-8** EC Base case West at 3 p.m. DGP = 39.3% (left); EC increased case West at 3 p.m. DGP = 41.7% (right)
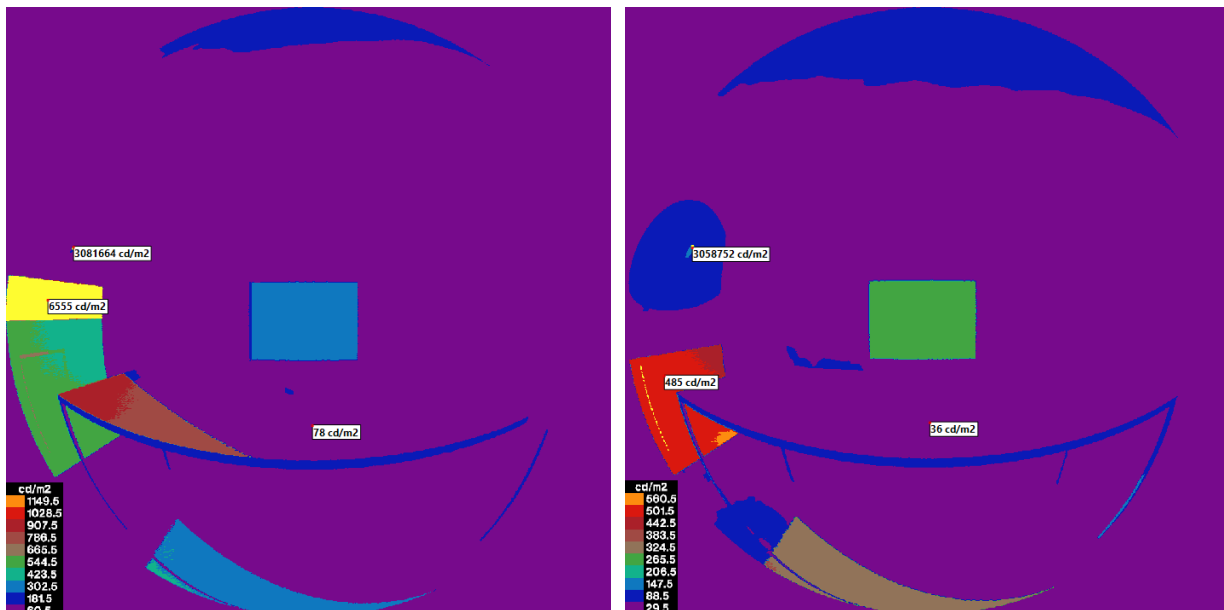
**Figure 3-9** Falsecolour image with luminance bands for EC Base case West at 3 p.m. (left); EC increased case West at 3 p.m. (right)

The equation which is used by EvalGlare to calculate DGP (Equation 1) is consisting of two main terms: first term considers vertical illuminance value and the second considers the luminance from the glare sources in the scene. The luminance source is determined by calculating the luminance pixel by pixel and comparing its value with the average luminance value in the scene. By default, if the luminance of the pixel is 5 times larger than the average luminance value, it is considered as a glare source. The influence of each term in the equation is not linear.

For the base case1 the average luminance value which we have obtained from EvalGlare detailed output is 241.7 cd/m$^2$. This means that every light source with a luminance value above 1 208.5 cd/m$^2$ is considered as a glare source. To display on a falsecolour picture (**Figure 3-9**) glare sources we have set a scale with a maximum value of 1 210 cd/m$^2$. As a result, areas, coloured in yellow are the glare sources. We can see three main glare sources: the small yellow point which is the sun visible through the tinned EC part on the left side of the figure which is split by the software as two sources and the portion of the sky visible between the upper part of the glazing and the ground level. The size of the first and the second glare source from the sun is 6 and 21 pixels respectively. The light source luminance from the visible sky is 4 966.6 cd/m$^2$ and the calculated by EvalGlare luminance from the sun is 18 377.7 cd/m$^2$ and 1 591 249 cd/m$^2$ for the first and the second source respectively. The E$_v$ is equal to 697 lux and the contribution from the glare sources to this value is 354 lux. Altogether the luminance from the glare sources, the quantity, position and the size of the glare sources in these conditions result in a perceptible DGP value of 39.3%.

The falsecolour image of increased size case is presented on **Figure 3-9**. The average luminance in the scene is 116.9 cd/m$^2$ which results in areas in the scene with the luminance larger than 585 cd/m$^2$ being identified as a glare source. The colour legend is set in a way that yellow zones in the picture are defining the glare sources. In this case, it is also the sun which is visible through the upper, electrochromic part of the glazing and a thin vertical line on the lower part of the glazing. The illuminance on the eye-level is 338.7 lux with a contribution of 134.1 lux from the glare sources. The sun in this case was also identified as two glare sources with the size of 5 pixels and 22 pixels and the luminance of 19 179.9 cd/m$^2$ and 1 514 967.7 cd/m$^2$ respectively. The third glare source has a size of 159 pixels and luminance of 653.3 cd/m$^2$. The size and luminance intensity of the glare sources is smaller for the increased size case but because of the lower average luminance and the E$_v$ the DGP calculated is larger by 2.4%.

Since the vertical illuminance value E$_v$ is smaller for modified case, the difference in DGP most probably is brought by the second term of the Equation 1. Indeed, average luminance is smaller with increased height of the electrochromic part, while the sun luminance values are still extremely high. Combination of these factors lead to an increased contrast ratio between bright and dark objects in the scene and which is considered by the second term of the DGP equation. This drives us to a conclusion that for West orientation enlarged height of the electrochromic part is not beneficial: it is reducing illuminance values that can further possibly lead to higher needs in energy demand for artificial lightning together with reducing visual comfort in terms of glare conditions and contrast ratio. For this reason in our further analysis (chapters 3.1.6-3.1.8) considers the use of SPD which is a more diffusive material and presumably might have a better performance in controlling glare.
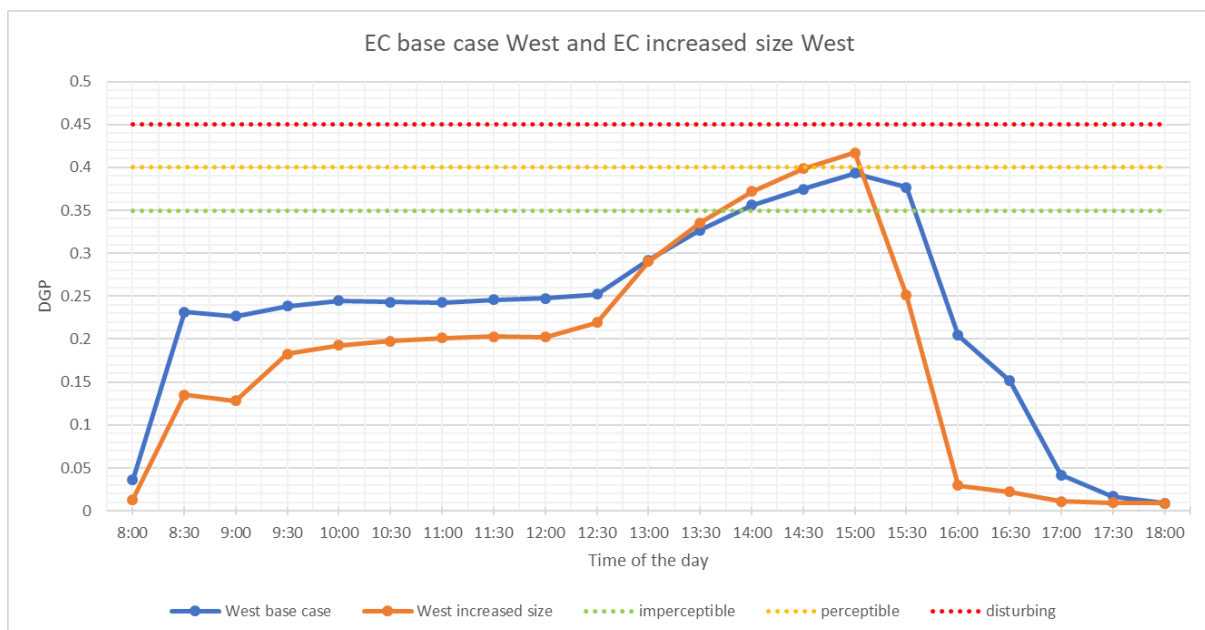


**Figure 3-10** DGP values for 21st December for EC base case West and EC increased size West

### 3.1.5    **EC increased size East**

In this simulation case the occupant is oriented to the East. The height of the upper part is 1.275 m. (**Figure 3-11**). On the **Figure 3-12** the DGP distribution during the day is shown with a blue line. During the first hour from 8 a.m. to 9 a.m. the daylight glare probability is remaining very low because the sun is not yet in the field of view and the illuminance in the test room remains low. From 9 a.m. the sun starts to be visible and the DGP value instantly rises to higher levels in comparison with the EC base case East. The rise continues to 10 a.m. where DGP is reaching its maximum value of 40.4% (disturbing glare) which is 1.8% greater than in the base case 2 at the same instance of time. After 10 a.m. DGP starts to decrease and falls below lower threshold of perceptible glare at 11 a.m. As a result, in a modified case 1.2 perceptible glare occurs



**Figure 3-11** Modified case 1.2 at 10 a.m.

for around 13% of the time and disturbing glare occurs for 4% of the time on December 21$^{st}$ .

As for the EC increased size West, we have plotted falsecolour images with luminance counter bands to analyze more in detail daylight conditions in the scene comparing the base case and increased size case.

To properly find the glare sources that were considered, as previously mentioned, we have to multiply by 5 the average luminance values in the scene and whichever light source has a higher luminance value would be considered as a glare source. For the EC base case East the average luminance value obtained from evalglare detailed output is 378.5 cd/m$^2$ which means that in this case considering the users adaptation the threshold luminance for the glare would be 1 892.5 cd/m$^2$. On the **Figure 3-14** (left) the falsecolour image with luminance bands is presented. The upper value is set to 1 900 cd/m$^2$ and subdivided into 10 steps, in this way the yellow zones are representing the glare sources. Five glare sources are defined for the base case: two of them are produced by the presence of the sun, with areas of 6 and 22 pixels and luminance values of 23 926.6 cd/m$^2$ and 1 936 417.4 cd/m$^2$ respectively, third and fourth are produced by the portion of the sky which is visible between the upper electrochromic part and the ground with sizes of 9836 and 1909 pixels and luminance values of 5 320.7 cd/m$^2$ and 2 459.4 cd/m$^2$ respectively and fifth zone which is coming from the light reflected from far-left table leg, the size of it is 163 pixels and luminance value is 3 494.6  cd/m$^2$. E$_v$ is 1 103 lux and the contribution from the glare sources to this value is 401.7 lux.
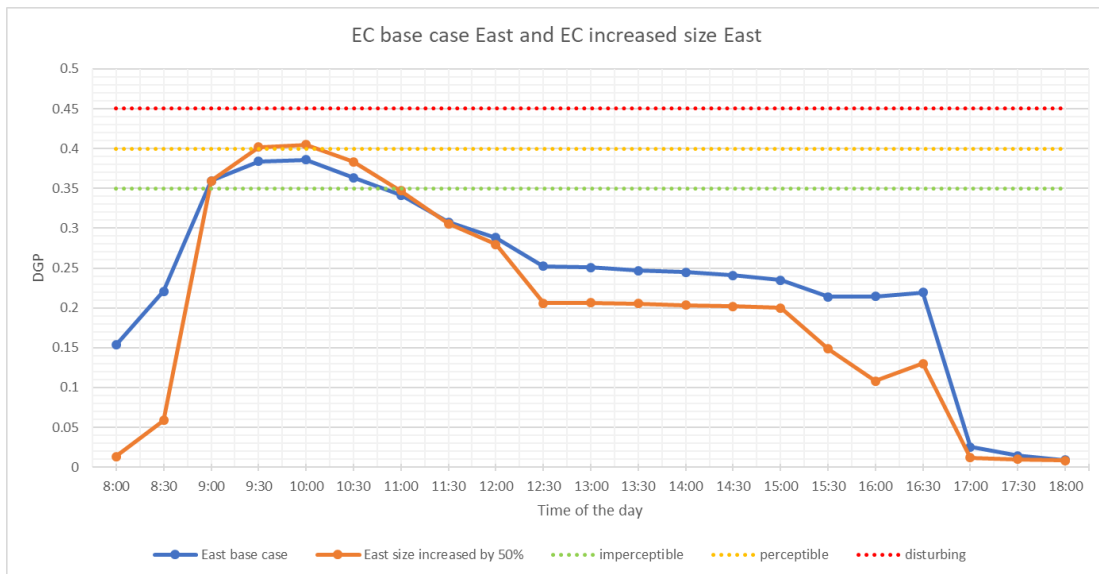
Figure 3-12 DGP values for 21st December for EC base case East and EC increased size East

**Figure 3-14** (right) is showing the falsecolour image of the EC increased size East. The average luminance is 195.5 cd/m$^2$, making a threshold for glare source to be 977.5 cd/m$^2$. There are three glare sources: two from the sun with the size of 4 pixels and 20 pixels and luminance of 25 060.8 cd/m$^2$ and 1 940 286.7 cd/m$^2$ respectively, and the third being on the surface of far-left table leg, as in the base case. The size of the third glare source is 113 pixels and luminance is 3 037.5 cd/m$^2$. Vertical illuminance at the eye-level is 559.3 lux and the contribution to this value from the glare sources is calculated to be 157 lux.

Described visual conditions are found to be similar to the conditions in the EC base case West and EC increased size West: enlarged fully tinned electrochromic part worsens visual conditions in terms of glare and the amount of light, thus making it not useful to increase size of the upper part.
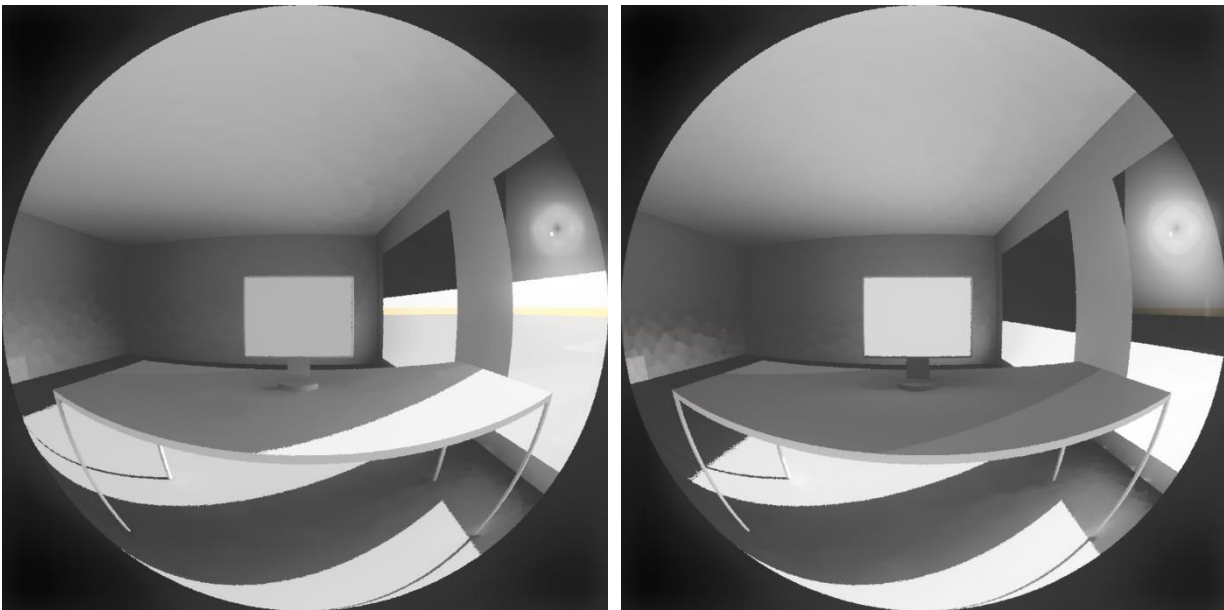
**Figure 3-13** EC base case East at 10 a.m. DGP = 38.6% (left); EC increased 1.2 at 10 a.m. DGP = 40.4% (right)
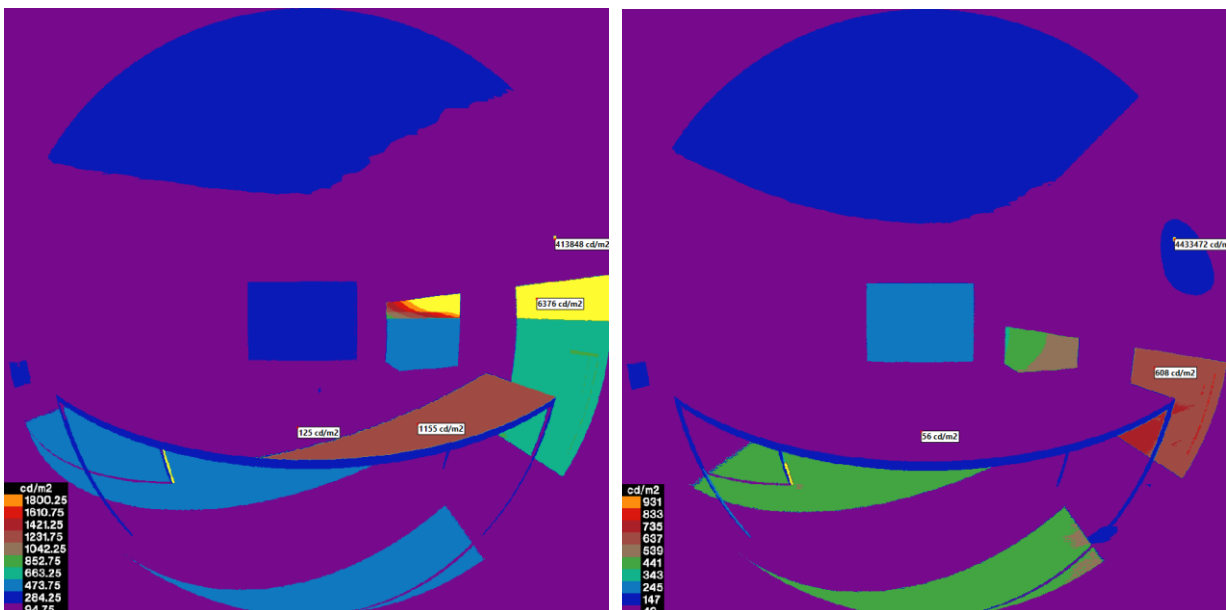


**Figure 3-14** Falsecolour image with luminance bands for EC base case East at 10 a.m. (left); EC increased size

East at 10 a.m. (right)

### 3.1.6 SPD 200 base case West and East

The analysis of the performance of electrochromic smart film in previous cases has shown that with given test room geometry and material optical properties in its darkest state (1% $T_{vis}$) it is capable of reducing the DGP value to acceptable levels (< 40%). The results have shown that the area of the glazing found by using an adopted occupant-based approach is optimal in a sense that when being increased, the DGP values are also increasing due to the rise of contrast levels. In order to try to reduce the contrast we have analyzed the SPD materials with different thickness assuming that having a portion of transmitted light being diffused, we would be able to increase the total light transmittance of the upper part thus reducing the contrast and increasing the overall amount of daylight in the room. The size of the upper zone was kept the same as in EC base case.



**Figure 3-15** SPD 200 base case West at midday

We have started our analysis by adopting SPD material with a thickness of 200 μm. SPD with such thickness would have in its "off" state a total transmittance of 15% and haze value 17.5% meaning that 17.5% from total transmitted light would be transmitted in a diffused manner.

Occupant's position and his field of view for the West case is presented on a **Figure 3-15.** Here, starting from 8 a.m. the DGP values have the same trend as they do in a corresponding EC base case. From 8 a.m. to 12 p.m. the sun is not in the field of view and DGP is remaining in an imperceptible



**Figure 3-16** SPD 200 base case East at midday

range. Nevertheless, looking at the Figure we observe that the DGP is around 2-3% higher for SPD 200 in comparison with EC material which is an indirect sign of higher illuminance levels in a test room. The situation is radically changing after 12 p.m. At this time the sun starts to be visible and we note rapid increase in DGP value from 26.3% at midday to 37.9 % at 12:30 p.m. The DGP is continuing to increase reaching its maximum value of 66.7 % at 2:30 p.m. The glare probability remains in intolerable range up until 4:00 p.m. when the sun is no longer in the field of view. In general, from 1 p.m. to 4 p.m. the glare is intolerable.

When considering East orientation, the situation is similar. The position of the occupant and his orientation is presented on a **Figure 3-16.** The results of point-in-time glare simulations are presented on a figure. From the obtained results we can see that in the first half of the day the daylight glare probability is reaching intolerable levels with a maximum value of 68.1% at 9:30 a.m. Again, the visual conditions in terms of glare are returning to an acceptable range only after the sun disk is leaving the field of view of the occupant.

This means that SPD material with a thickness of 200 is uncapable of providing glare-free environment when used to control the light from directly visible sun due to overly high visual transmittance value and more thick SPD material with lower visual transmittance have to be evaluated.



**Figure 3-17** DGP values on 21st of December for EC base case West and SPD 200 base case West

**Figure 3-18** DGP values on 21st of December for EC base case East and SPD 200 base case East

### 3.1.7 SPD 400 base case West and East

The results obtained from the analysis of performance of SPD with a thickness of 200 µm suggested us to further increase the thickness of the SPD. Considered in this part of research SPD with thickness of 400 µm has total visual transmittance of 3% and a haze of 53.8%. Significant reduction in total visual transmittance (by 12% in comparison with SPD 200) and increase of haze level was presumed to produce visual conditions close to the ones that were obtained from EC material.

The results of DGP simulations are presented on **Figure 3-20** and **Figure 3-21**. As we can note from these figures, in comparison with previously analyzed SPD 200 case, the DGP values are reduced. The significant decrease is observable during the time when the sun is in a field of view of the occupant. After 12:30 p.m. and before 12:30 p.m. for East and West orientations respectively, the DGP values are the same as the values for corresponding time for EC cases. This is indirect sign of the fact that illuminance levels and light distribution inside the room are relatively similar for SPD 400 case and EC case. As a general conclusion, analyzing values of DGP during the 21st of December we can note that the performance of SPD material with a thickness of 400 µm is similar to electrochromic material, for East orientation the DGP values are increasing proportionally to the increasing proximity of the sun to the center of the view direction: for East orientation the difference in DGP between SPD 400 and EC at 11:30 a.m. is 3.2%, while at 10:00 a.m. the difference is 6.1%. This might be explained by the fact that the sun disk, which is still visible through the SPD and EC materials has higher luminous intensity

for the case with SPD. To investigate this assumption, we have analyzed evalglare output files together with a falsecolour picture **Figure 3-19**.
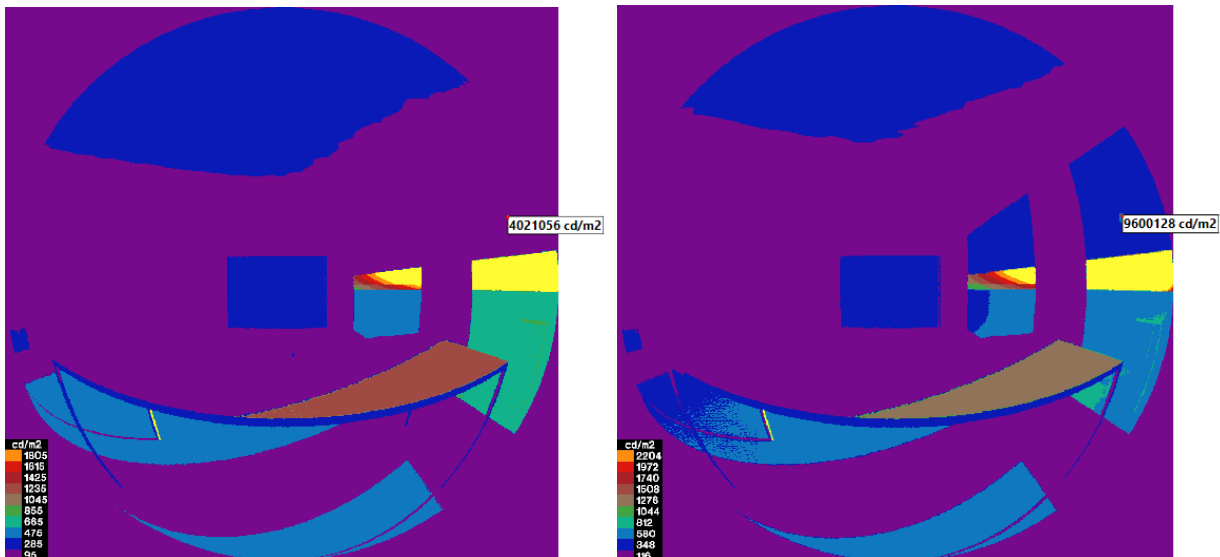


**Figure 3-19** Falsecolour image with luminance bands for EC base case East at 10 a.m. (left); SPD 400 base case East at 10 a.m. (right)

At 10:00 a.m. for the SPD 400 East the average luminance is 464 cd/m$^2$, making a threshold for identifying a glare source in the scene being 2320 cd/m$^2$. The colour legend is set in a way that all glare sources considered by evalglare are highlighted in yellow.

The number of glare sources, their position, size and luminous intensity is relatively similar for both cases except for the sun disk. In EC case the luminous intensity of the sun is almost two times smaller than in the case of SPD 400. Obtained data correlates with the fact that SPD 400 having a direct transmission value of around 1.4% and combined together with the fraction of diffusely transmitted light might produce observed difference of luminous value from the sun disk in two considered cases.

Our particular interest was drawn to the fact that for SPD 400 West the value of DGP at 3:00 p.m. was smaller than at 2:30 p.m. and 3:30 p.m.. The possible explanation for this inconsistency can be found analyzing detailed output from the evalglare software. For all previously done point-in-time glare simulations we have observed that usually, the sun disk is recognized as two glare sources with sizes of 5-7 pixels and 20-24 pixels. Particularly, at 2:30 p.m. and 3:30 p.m. for the SPD 400 West case the sun is recognized as a glare source with a size of 24 pixels and 21 pixels respectively. The luminous intensity of those glare sources are 3 138 636 cd/m$^2$ at 2:30 p.m. and 1 716 327 at 3:30 p.m. On the other hand, at 3:00 p.m. the size of a glare source recognized as a sun disk is 12 pixels and luminous value is 2 618 360 cd/m$^2$. The fact that the sun at 3:00 p.m. is considered by the software to be two times smaller with respect to adjacent cases, might be the explanation. From those

considerations we had proceed to evaluate more thick SPD material with lower transmittance value.
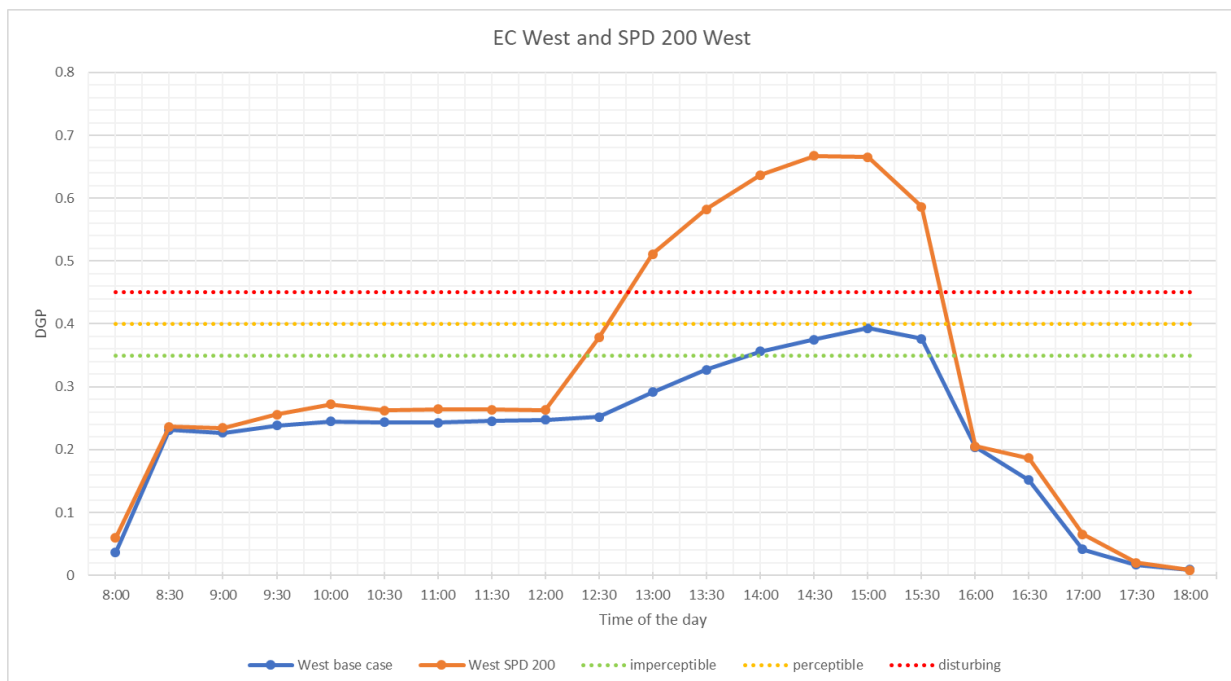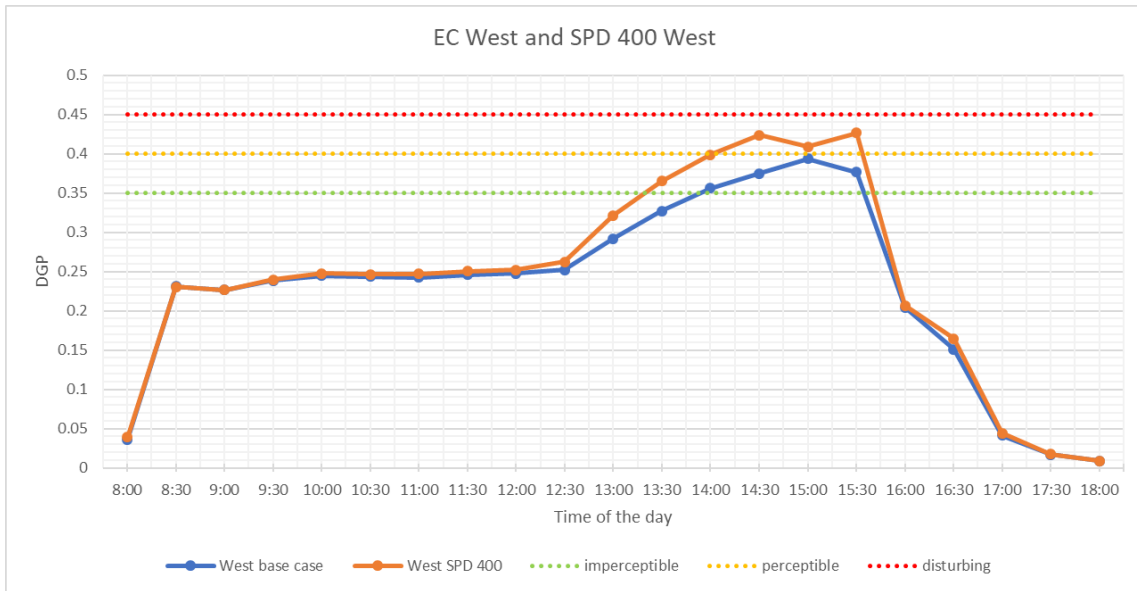


**Figure 3-20** DGP values on 21st of December for EC base case West and SPD 400  base case West



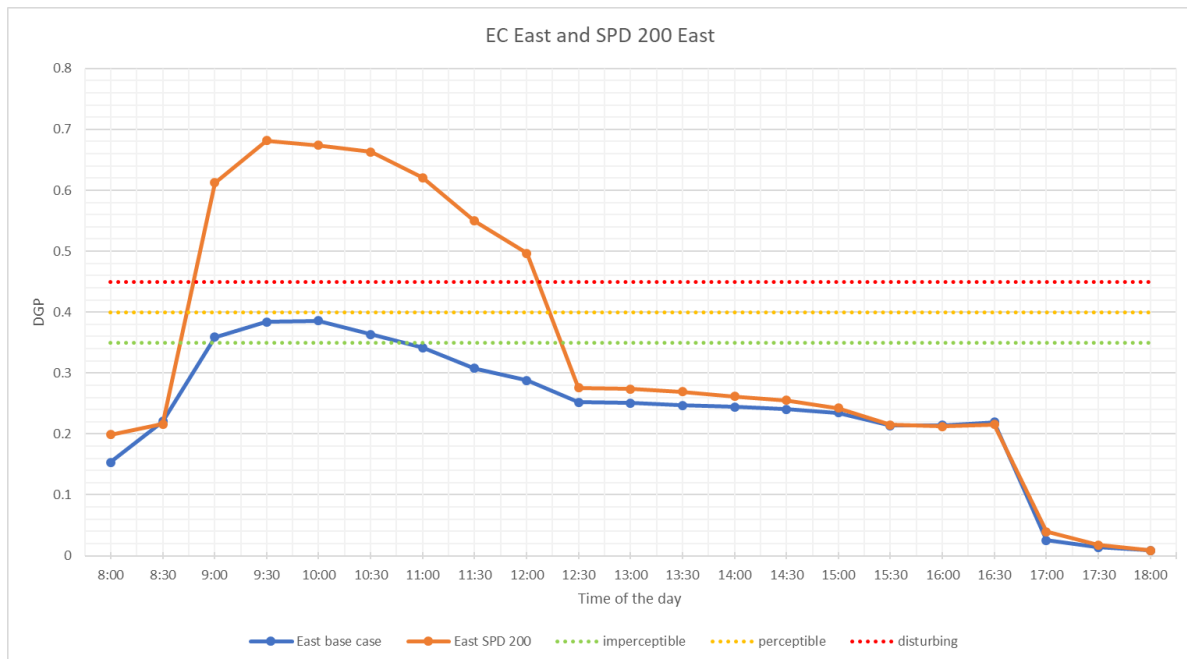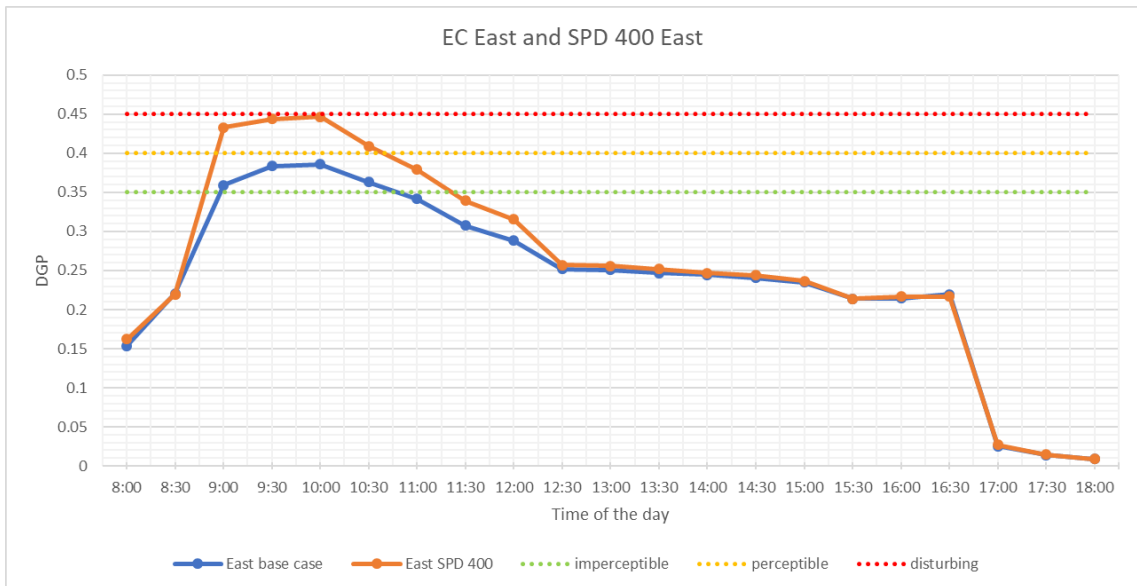**Figure 3-21** DGP values on 21st of December for EC base case East and SPD 400 base case East

### 3.1.8  SPD 500 base case West and East and SPD 550

Analyzed SPD with a thickness of 500 μm has a total visual transmission value of 1.7% and haze value of 65.5%. The simulation was performed considering the same orientations and occupant positions (West and East, 1.5 m away from the glazing). The results of point in time glare simulations are presented in **Figure 3-22** and **Figure 3-23**.
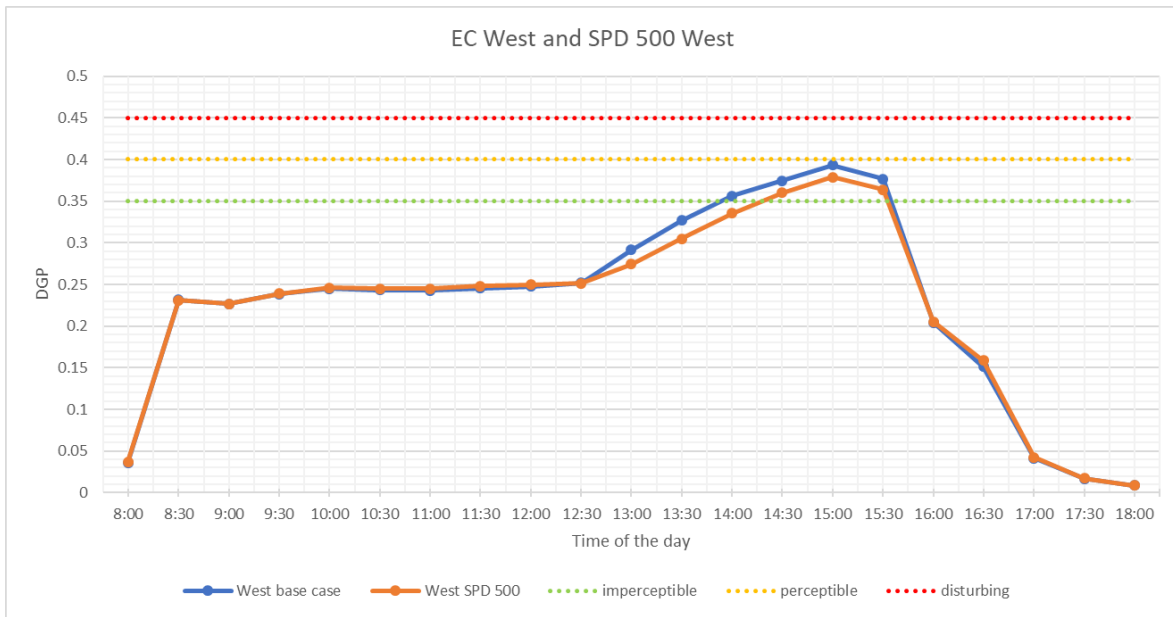


**Figure 3-22** DGP values for 21st of December for EC base case West and SPD 500 base case West
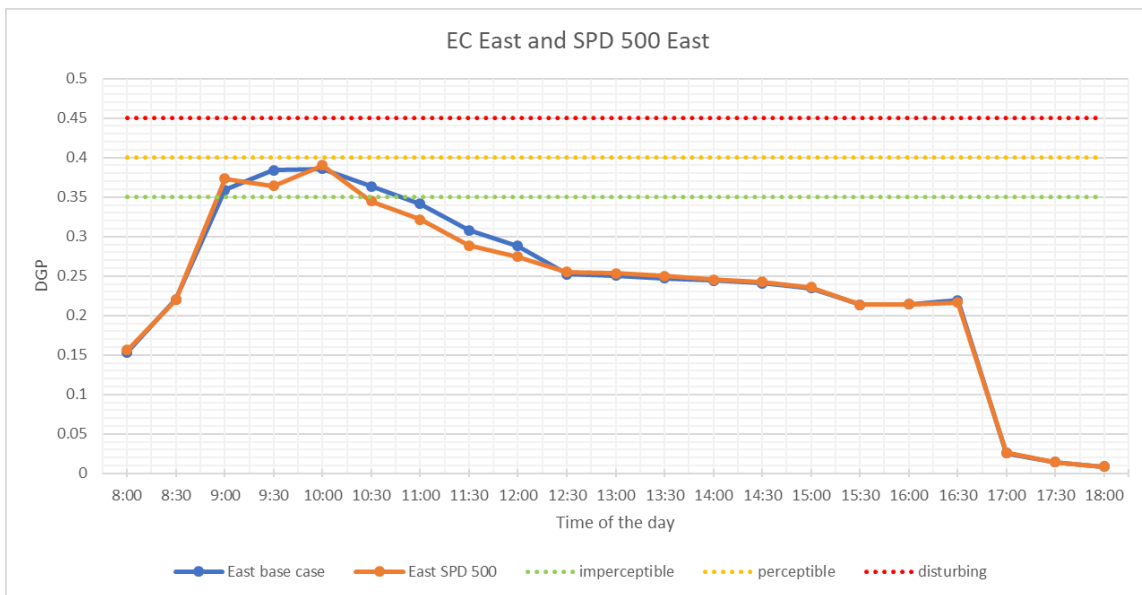


**Figure 3-23** DGP values for 21st of December for EC base case East and SPD 500 base case East

Obtained performance of SPD 500 case is relatively similar to the performance of electrochromic material. The DGP values during the time period when the sun is in the field of view of the occupant are on average 1-2% smaller for SPD. The reduction in DGP is obtained while the total transmittance of considered SPD material is 0.7% bigger in comparison with EC material.

Further reduction in the transmittance of SPD by increasing its thickness has produced the data which is unreliable. For example, while simulating SPD material with a thickness of 550 μm, which has a total transmittance value of 1.2%, diffused reflectance value of 1.6%, specular reflectance of 4.6% and haze value of 70.3%, it was observed that for East oriented occupant for the time interval from 8:30 a.m. to 10:30 a.m. the sun is not visible through the SPD material (**Figure 3-24**). Similar situation was observed for West oriented occupant for the time period from 3:00 p.m. to 4:00 p.m. (**Figure 3-25**).
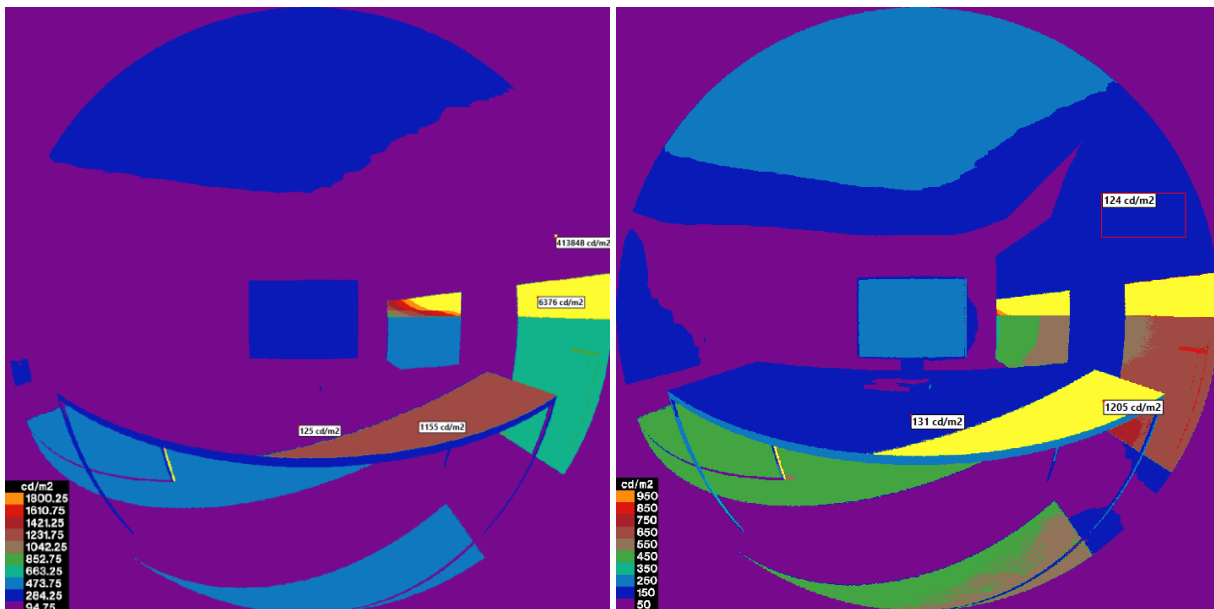


**Figure 3-24** Falsecolour image with luminance bands for EC base case East at 10 a.m. (left); SPD 550 case East at 10 a.m. (right)
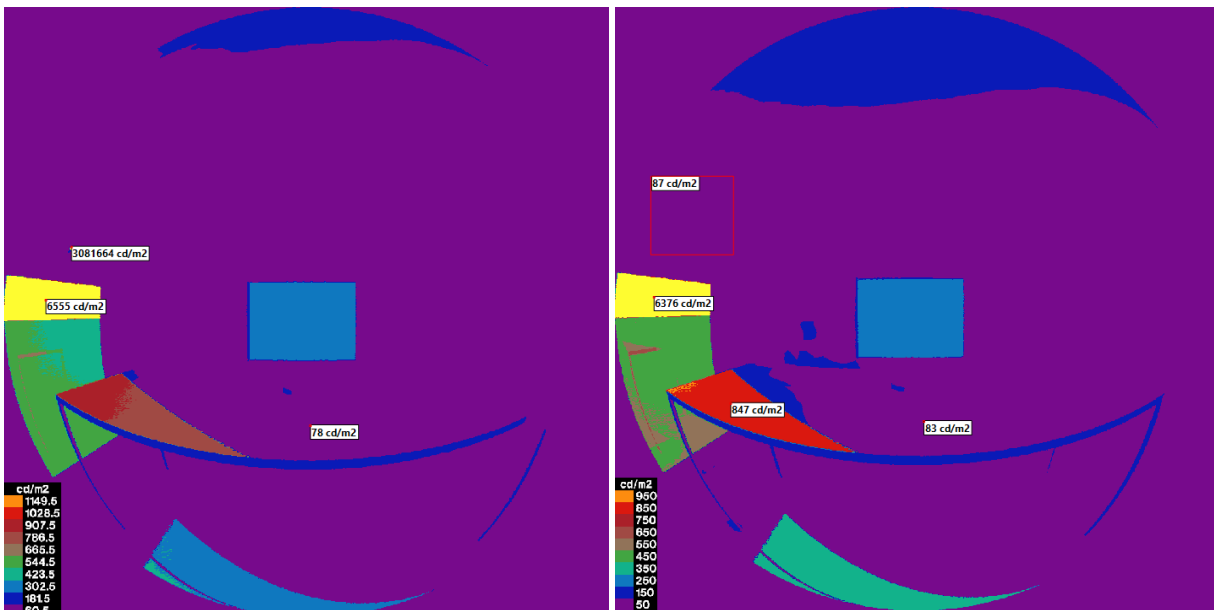
**Figure 3-25** Falsecolour image with luminance bands for EC Base case West at 3 p.m. (left); SPD 550 case West at 3 p.m. (right)

Since this phenomenon appears for both orientations of the occupant and is present for a particular time of the day, the possible explanation could be that the combination of extremely low direct transmittance (0.35%) and an attack angle of the direct sun rays for mentioned periods of time cannot be properly handled and calculated by evalglare software.

### 3.1.9  Summary of glare analysis results

Summarizing the results of point-in-time glare simulations we can note several key-findings. First of all, using the method, described in section 2.3 we were able to achieve reduction of daylight glare probability to acceptable levels (<0.4) for the occupant located 1.5 m. away from the center of the glazing for both East and West orientations. The results were obtained for the 21st of December, when the sun is in its lowest altitudes. This consideration enabling us to make an assumption that for the rest of the year the values of daylight glare probability would not exceed the values, found in this simulation cases.

Secondly, we can observe that both of the studied dynamic materials were able to control the glare from the direct sun present in the field of view of the occupant. SPD material has shown a better performance for the cases, when the material is 400-550 µm thick in comparison to EC when analyzing DGP distribution throughout the whole day. Improved performance was obtained by reducing the overall contrast levels in the scene by allowing more light to enter the room through the upper part of the glazing in a diffused way while still decreasing the direct component of transmitted visible light, thus reducing the luminance intensity of the main glare source-the sun disk.

When analyzing SPD material, a progressive approach with a gradual increase of thickness was used to find an optimal for given simulation settings (room geometry, user position, materials optical properties, etc.) values of direct and diffused transmittances of the material. The results have partially confirmed the findings of another researchers (35). Nevertheless, when analyzing the performance of SPD material with a 550 µm thickness, inconsistencies in results was observed.

The analysis of the case where the upper part was increased has shown that initially found area might be considered as an optimal one on the preliminary states of the shading strategy design. When being increased, the EC glazing in its darkest state creates overly darkened environment for considered user position, increasing the contrast levels between dark and bright objects.

Our further analysis was aimed to investigate overall light distribution behavior in considered test room with adopted size and material alternatives of the fenestration system.

## 3.2   Horizontal illuminance results

### 3.2.1  Reference case

The point-in-time illuminance on the work plane level varies due to the daily sun position changing, while the useful daylight illuminance on the work plane is within 100 lux to 2000 lux at the simulation time which is from 8 a.m. to 6 p.m. Hence, a legend from 100 lux to 2000 lux is set up. This legend setting is used in all subsequent illuminance graph in Chapter 2.8.

To evaluate the horizontal illuminance, the reference case is simulated firstly. The transmittance of the glazing of the test room was set to 65% Tvis. The point-in-time illuminance result is present in **Figure 3-26**. To quantitively evaluate the useful daylight illuminance, **Figure 3-27** is created to indicate the percentage of space where illuminance lies between 100 lux and 2000 lux. **Figure 3-28** and **Figure 3-29** indicate the percentage of space with illuminance over 2000 lux and the percentage of space with illuminance less than 100 lux, respectively.

As **Figure 3-28** indicates, illuminance on the work plane is always below 2000 lux at 8 a.m. Around 70% space is within UDI range and illuminance on 30% space is below 100 lux.

At 9 a.m., space within UDI range reduces a lot and large space is at visual discomfort risk, reaching 43% of the room space. Besides, the over lit area spreads from the window in the northwest direction into depth of the room during this time, even covering the area near back wall. This phenomenon can be explained by that sun is in the East orientation and large amount of daylight pass through the window due to the high $T_{vis}$ of the glass.

From 10 a.m. to 12 p.m., the useful daylight illuminance increases and spreading of over lit area is reduced comparing with the phenomenon at 9 a.m. However, illuminance increases on the work plane near the northern wall. The percentage of space where illuminance is over 2000 lux reaches 40% at 12 p.m. Almost half room space near window is at visual discomfort risk and the illuminance on the rest half space is almost higher than 1000 lux. This situation may be explained by that the sun rises and it is close to the middle of sun path during this time.

From 1 p.m. to 3 p.m., the UDI changes slightly, keeping around 54% to 57%. And the distribution of over lit area is different from the one in the morning, spreading in northeast direction into the room, causing half room space near window as well as center part of room at visual discomfort risk. UDI increases significantly from 3p.m. to 4 p.m. since the sun is low in the west orientation and most transmitted sunlight falls on East edge of the room.

Generally, the illuminance on very large room space exceeds 2000 lux from 9 a.m. to 3 p.m. which causes visual discomfort risk. In order to optimize the visual condition of the test room, electrochromic glass is adopted as dynamic glass to evaluate furtherly.

### 3.2.2   EC base case

For the EC base case, the height of the electrochromic glazing is 0.85 m and the transmittance of lower part glass is 0.65. The results of illuminance are present in **Figure 3-26**.

At 8 a.m., there is no room space where illuminance is over 2000 lux. Around 78% area illuminance is lower than 100 lux and 22% room space which is close to window is in the UDI range. As the graphs indicate, although the horizontal illuminance on the part of work planes is higher than 2000 lux from 9 a.m. to 4 p.m., EC base case performs better on illuminance evaluation compared with reference case, because of much less over lit area during the time.

 From **Figure 3-27**, the percentage of room space within UDI range increases significantly from 8 a.m. to 9 a.m. and then it reduces by 7.7% from 9 a.m. to 10 a.m. Besides, the percentage of the space with illuminance over 2000 lux is highest at 10 a.m. in the morning, when almost 19% room space is under visual discomfort risk. It is caused by low sun position, letting more daylight transmission into the depth of room. Up to 11 a.m., the percentage of space within UDI range increase to 84.7%, and the percentage remains similar from 11 a.m. to 2 p.m.

From 9 am to 12 am, over lit area spreads in northwest direction but doesn't exceed half of the room, considering daylight passes through window glass in northwestward. Only the space near window is at visual discomfort risk and most area is within UDI range.  As time passes, illuminance gradually increases in the middle of room because the sun rises, close to the middle of the solar trajectory.

Over lit area increases from 1 a.m. to 3 p.m. and the daylight diffuse into the room along Northeast due to the sun position changing from East to West. Meanwhile the space within UDI reduces from 85% to 80%. Over lit area is peak at 3 p.m. in the whole day and the percentage of space with illuminance higher than 2000 lux reaches 19.3%. It can be explained by that more daylight transmits through window due to solar altitude, causing large over lit area. As **Figure 3-26** indicates, the percentage of room space within UDI range increases a lot from 3 p.m. to 4 p.m. Meanwhile there is less space with illuminance over 2000 lux and the value reduces significantly from 4 p.m. to 5 p.m. Furthermore, illuminance on the whole work plane level is lower than 100 lux at 6 p.m. Hence, daylight on the work plane is insufficient and the room lighting condition should be contributed by artificial light.

### 3.2.3   EC increased size case

Analyzed EC increased size case, the height of the upper electrochromic glass enlarges by 50% compared with base case, which is 1.275 m. The transmittance of the lower glass keeps the same as 0.65.

From **Figure 3-28**, the horizontal illuminance on the work plane is lower than 2000 lux in the whole day, which means there is no visual discomfort risk produced by the direct sunlight. Enlarging the height of electrochromic glazing effectively reduces the risk in visual discomfort on the work plane compared with base case. As we see from **Figure 3-27**, the horizontal illuminance on the whole work plane is lower than 100 lux at 8 a.m. and from 5 p.m. to 6 p.m. Hence, the increased EC glass causes insufficient interior lighting condition during the early morning and late afternoon due to blocking much sun light. In order to satisfy the visual requirement, artificial lighting need to be provided. At 9 a.m., 62.7% room space is under UDI range and the illuminance on 33.7% room space which is far away from window is lower than 100 lux. From 10 a.m. to 3 p.m., the horizontal illuminance on the table close to the window is around 600 lux to 1000 lux, which keeps occupant in a comfort working condition. At 3 pm, the illuminance on the table which is close to window is within the UDI range, meanwhile the illuminance on the work plane far away from window is insufficient. Because of low sun position and large sized EC glass on tinted state, daylight can't transmit deeply inside of the room.

Enlarging the height of upper electrochromic glass reduces horizontal illuminance less than 2000 lux on the whole work planes, meanwhile the illuminance on the work plane is insufficient in the early morning and in the late afternoon. Especially, illuminance on the work plane away from window is less than 500 lux for a long time. Hence, we need to reduce the height of the enlarged electrochromic glass to supply enough daylight on the working space.

| Time | Reference case | EC Base case | EC increased size case |
| --- | --- | --- | --- |
| 8 a.m. | | | |



| | | lux |
| --- | --- | --- |
| | | 2000.00< |
| | | 1810.00 |
| | | 1620.00 |
| | | 1430.00 |
| | | 1240.00 |
| | | 1050.00 |
| | | 860.00 |
| | | 670.00 |
| | | 480.00 |
| | | 290.00 |
| | | <100.00 |

9 a.m.

10 a.m.



11 a.m.

12 p.m.



1 p.m.



2 p.m.

3 p.m.
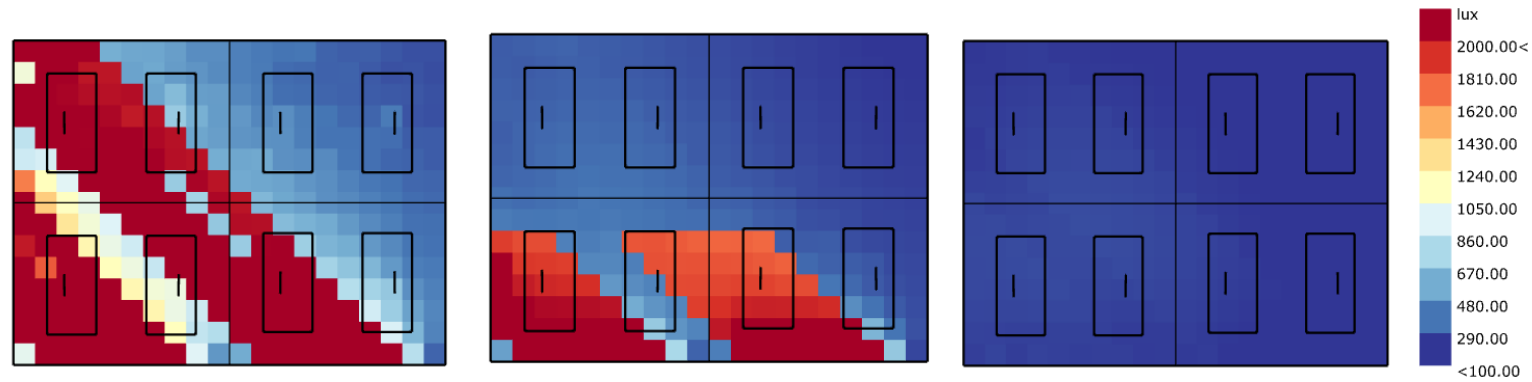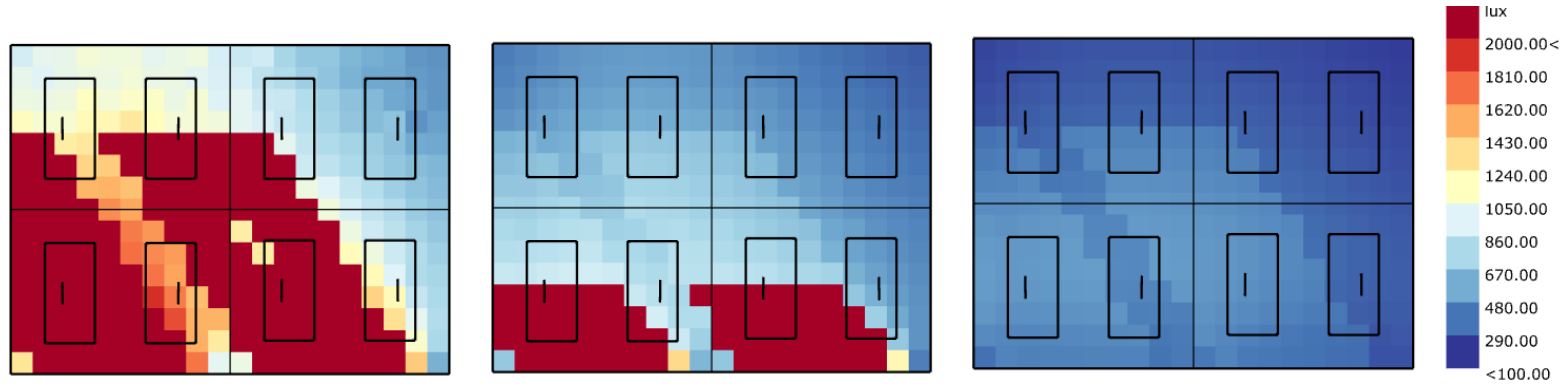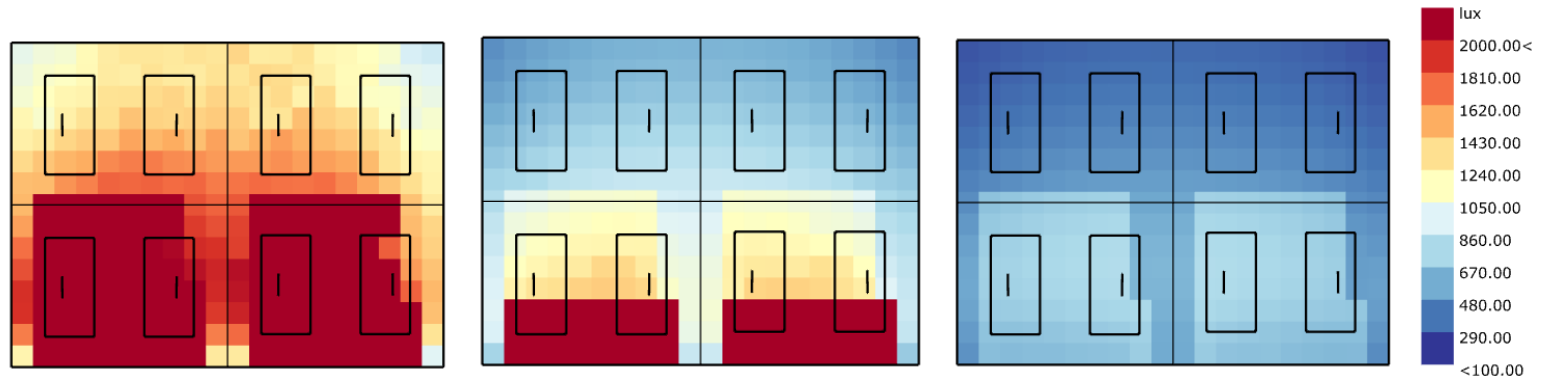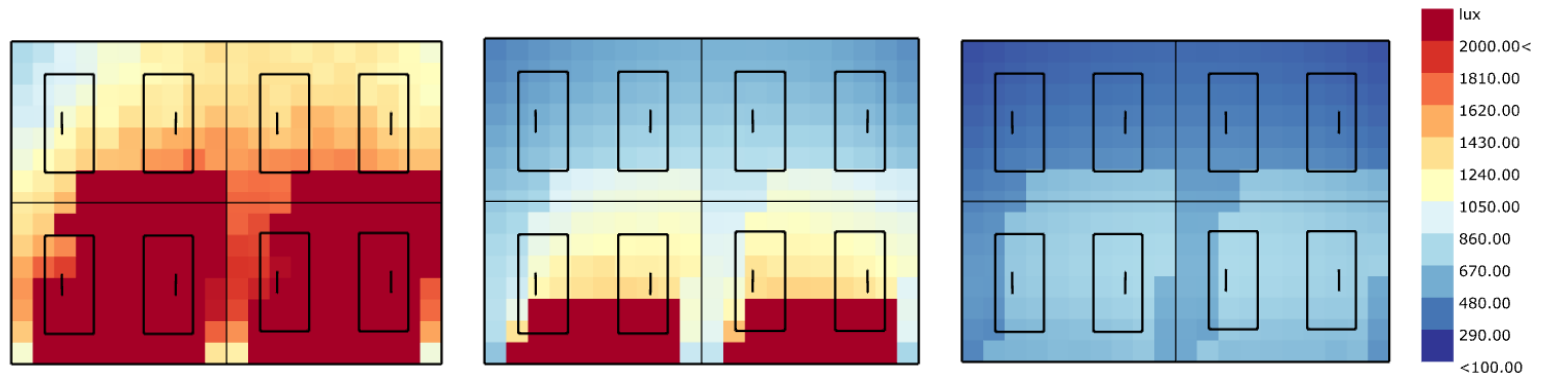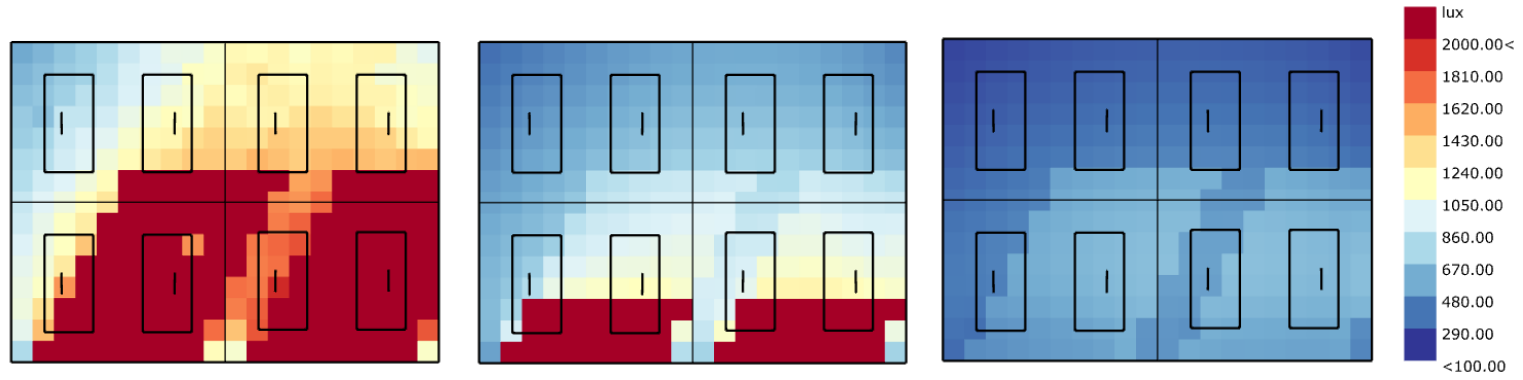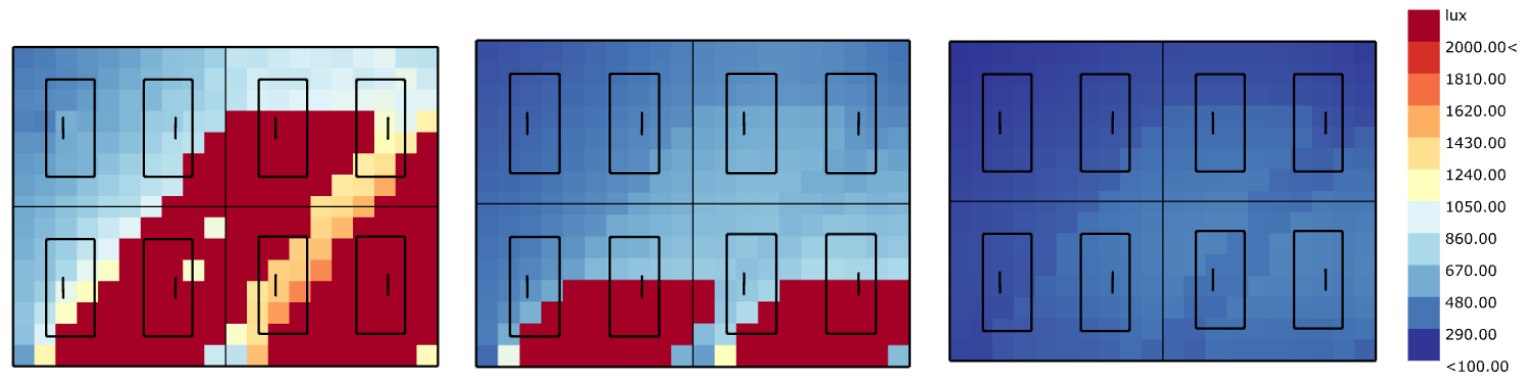


4 p.m.
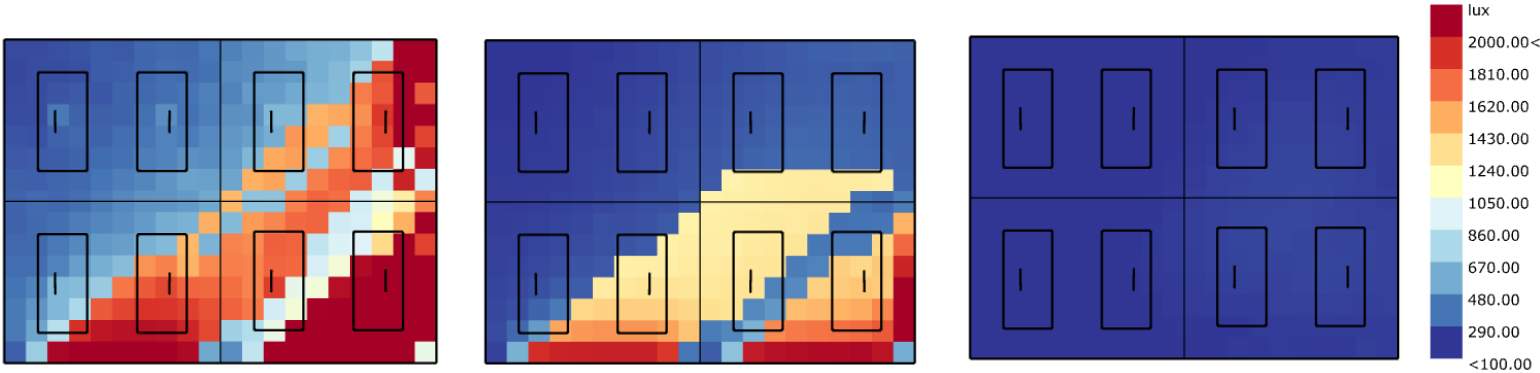
5 p.m.
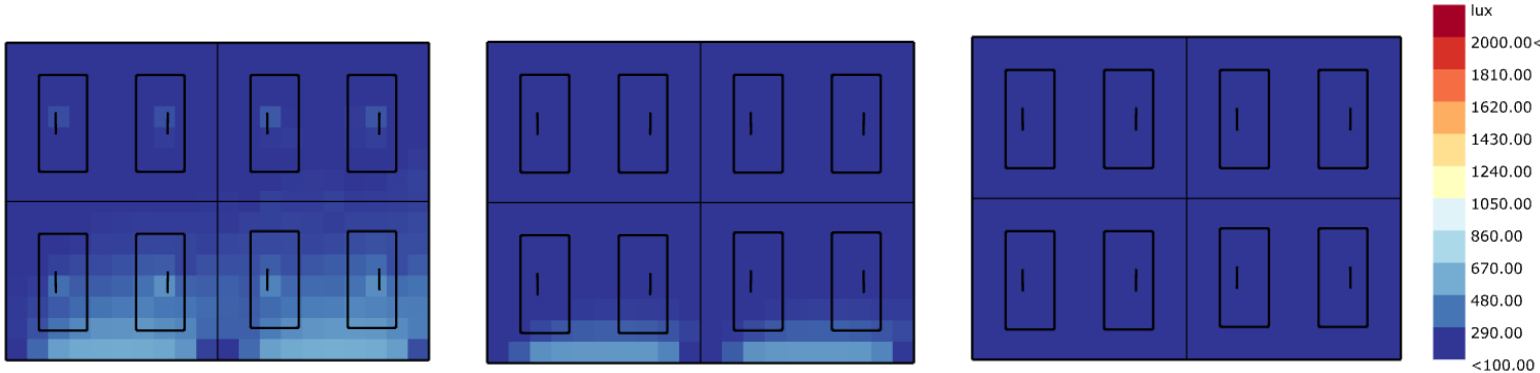


6 p.m.
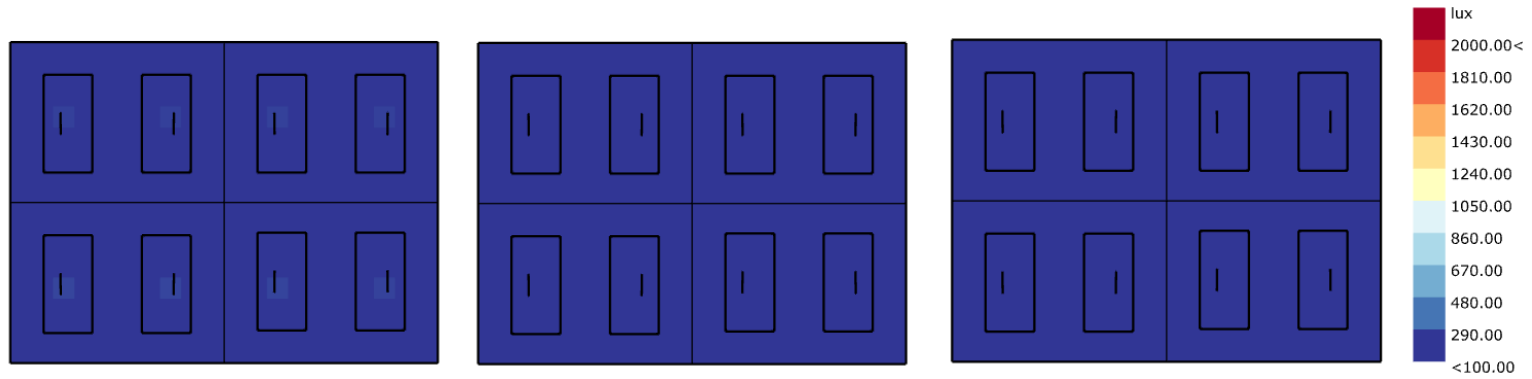
Figure 3-26 Point-in-time illuminance for reference case, EC base case and EC increased size case
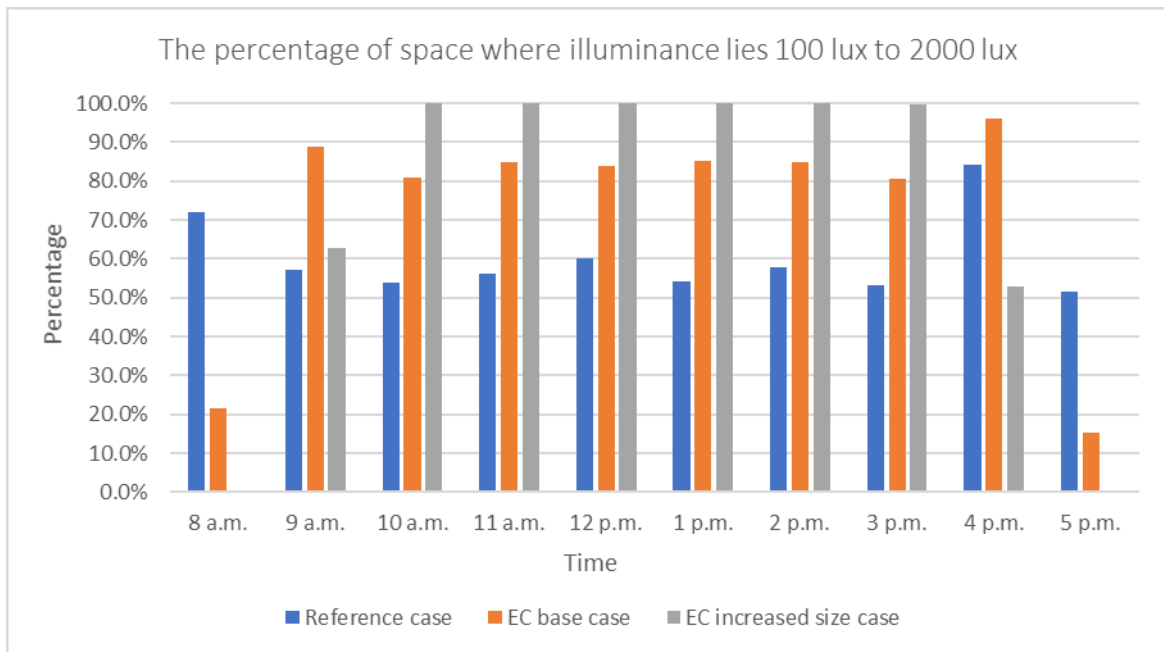
**Figure 3-27** The percentage of space with illuminance within UDI range for reference case, EC base case and EC increased size case
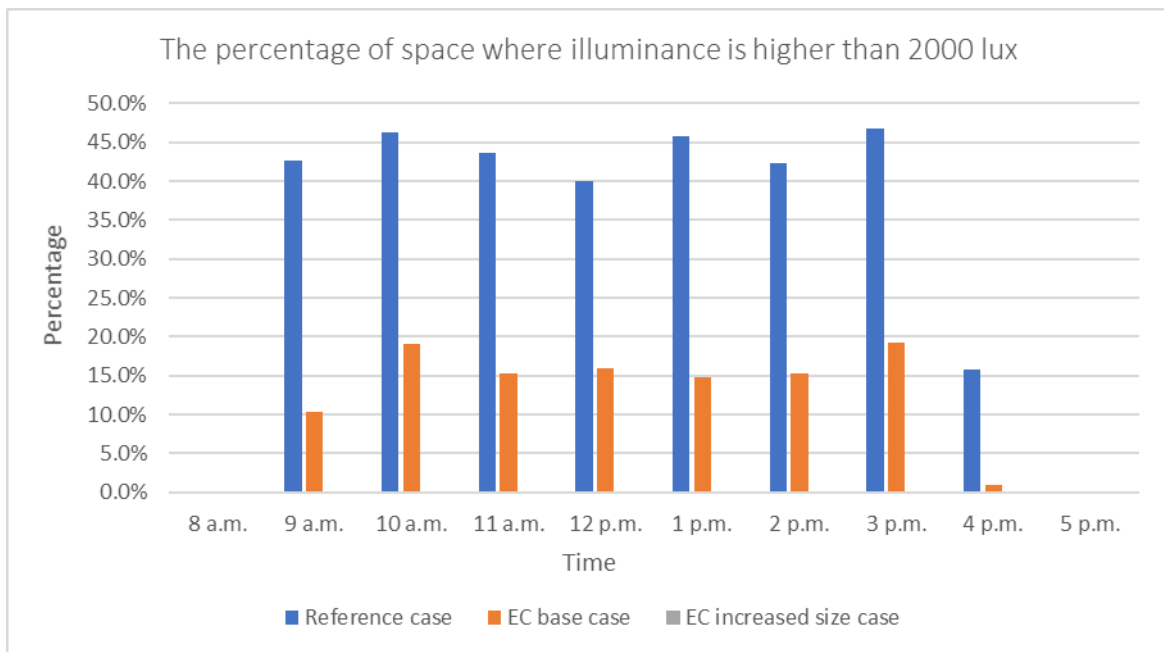


**Figure 3-28** The percentage of space where the illuminance is higher than 2000 lux for reference case, EC base case and EC increased size case
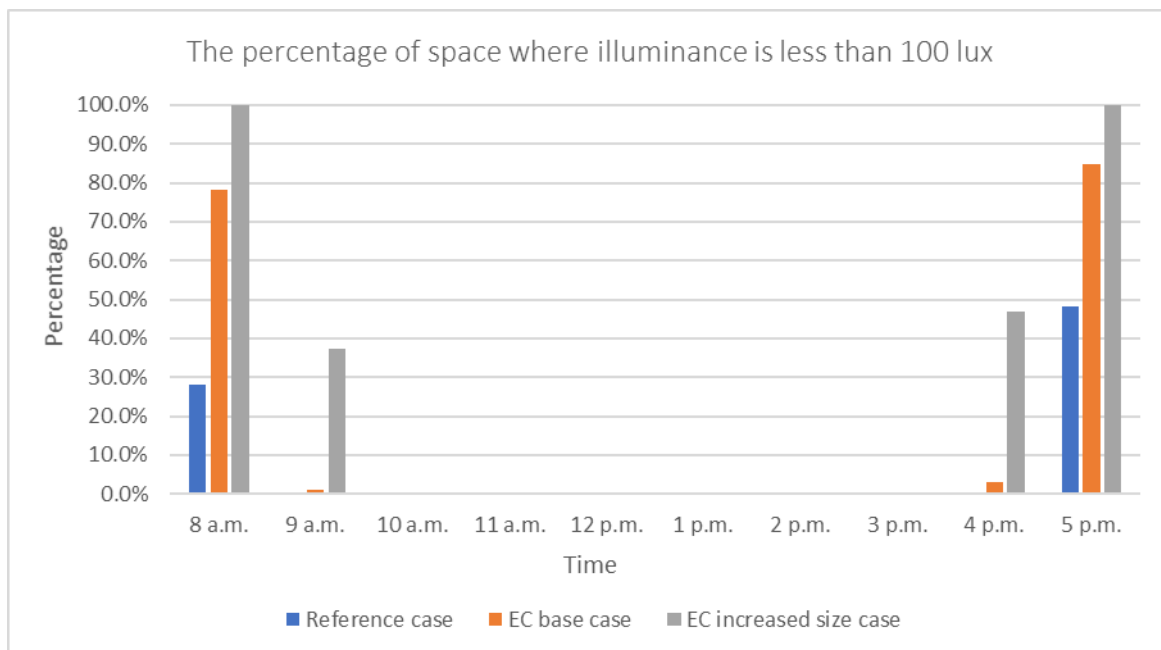
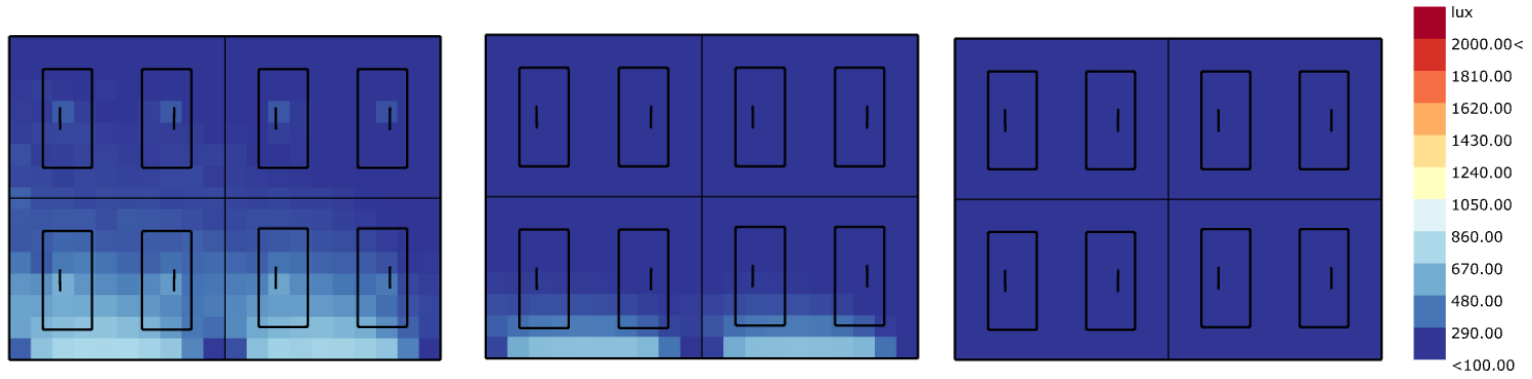**Figure 3-29** The percentage of space where the illuminance is less than 100 lux for reference case, EC base case

and EC increased size case

### 3.2.4  SPD 200µm base case

The effect of electrochromic glass on the horizontal illuminance is analyzed above, in terms of standard height and increased size. To evaluate the performance of trans material, SPD 200 µm layer is used on the dynamic glass. The total transmittance is 16% and the transmittance haze is 17%.

From **Figure 3-30**, the illuminance distribution of SPD 200 µm base case is significantly different with the result of EC base case. At 8 a.m., there is no space where illuminance is over 2000 lux in this case. Comparing with EC base case, more space within UDI range exists in SPD 200 µm base case, reaching around 35%. Accordingly, space with illuminance below 100 lux for SPD 200µm base case is less, which is benefit to visual condition. From 8 a.m. to 9 a.m., the useful daylight illuminance increases a lot and the space within UDI reaches 84% of the room. Meanwhile, illuminance on 16% space is over 2000 lux which is higher than the percentage of EC base case, because the high visual light transmittance of SPD material let more daylight inside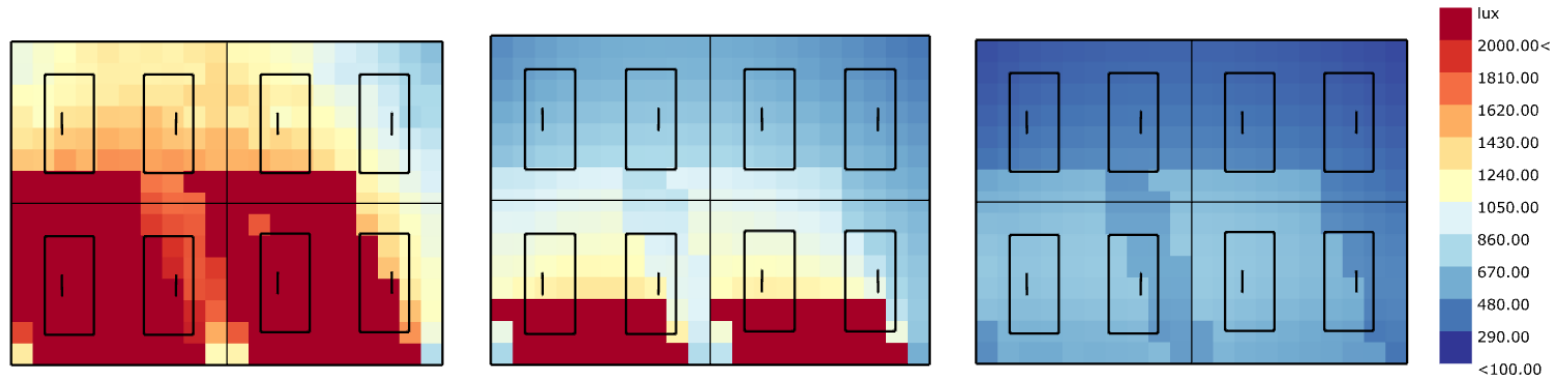 of room. Large area of work plane near window is under visual discomfort risk due to the low sun position during the time. As **Figure 3-33** indicates, illuminance is always higher than 100 lux from 10 a.m. to 3 p.m. From 9 a.m. to 10 a.m., useful illuminance reduces significantly and around 45 % room space is under visual discomfort risk at 10 a.m. which is much higher than the percentage of EC base case. This situation is caused by high visual light transmittance

of the SPD 200 μm layer, equaling to 16%. More daylight is transmitted through the window. As we can see from the graph, even the center of the room and part of table far away from window is under the risk, which is worst situation during the day. From 10 a.m. to 12 p.m., UDI increases slightly and illuminance over 2000 lux decreases accordingly. However, the space where illuminance is higher than 2000 lux is still large, most part of tables near window is under visual discomfort risk. Comparing with EC base case, the situation is much worse during the period. From 2 p.m. to 4 p.m., UDI increases significantly, and UDI is much close to the value of EC base case from 3 p.m. to 4 p.m. Room space lying UDI range is peak at 4 p.m., reaching 96% which is equal to the percentage for EC base case. The reason is low sun position where SPD material with high transmittance and diffusivity doesn't affect the interior illuminance.

In conclusion, SPD 200 μm base case cause more risk of visual discomfort compared with EC base case, because the total transmittance is much higher, and the diffuse property of the material also increase the percentage of risk.

### 3.2.5   SPD 400μm, 500μm and 550μm base case

To better evaluate the performance of SPD material, the thickness of SPD layer is increased. SPD material with 400μm, 500μm and 550μm thickness are implemented in the dynamic glass, respectively. Given 400μm SPD layer is used, the total transmittance of upper glass is 3% and transmittance haze is 53.8% when SPD is at "off" state.  The total transmittance of SPD layer with 500μm thickness is 1.7% and transmittance haze of the material is 65.5%. SPD with thickness of 550μm has a total visual transmission value of 1.2% and haze value of 70.3%.

**Figure 3-31**, **Figure 3-32** and **Figure 3-33** present the percentage of space with illuminance lying UDI range, exceeding 2000 lux and below 100 lux, respectively. From a quantitative point of view, the percentage of space where illuminance lies on three respective ranges is almost the same for three different SPD base cases, which indicates that SPD material with total transmittance from 1.2% to 3% doesn't influence interior horizontal illuminance significantly.

At 8 a.m., there is no space where illuminance exceeds 2000 lux and 76% space where illuminance is lower than 100 lux. Only 24% room space is within UDI which is a little bit higher than the percentage of EC base case, so the room needs artificial light to be compensation.

From 9 a.m. to 3 p.m., illuminance on the work plane level is always higher than 100 lux and tables close to the window are over lit since the illuminance there exceeds 2000 lux. Comparing three SPD simulation cases with EC base case, the percentage of room space within UDI range and over 2000 lux is completely the same although the total transmittance of SPD layer is little higher than the one of electrochromic glass. While, the diffusion of interior daylight is different viewed from point-in-time illuminance graphs present in **Figure 3-30**.

From 9 a.m. to 10 a.m., the centre of room for SPD 400μm is brighter than other cases, which means the illuminance is a bit higher for SPD 400μm base case and it is around 500 lux to 1080

lux. This phenomenon can be explained by that SPD material with relatively higher haze value diffuses more daylight into the depth of room and this performance is benefit to occupant sitting far away from window. Comparing the performance of daylight diffusion, we may conclude that the higher diffusivity of SPD material, the more daylight diffuses into the depths of the room.

From 10 a.m. to 11 p.m., the percentage of area where illuminance lies UDI range increases, and more daylight diffuses along northwest direction into the depth of room because the sun is in east orientation and low position of the sun let more daylight pass through the window. Illuminance in the room centre increases during this time. For SPD 400μm base case, the illuminance in the middle of room is higher than 1200 lux which supplies relative excess daylight on the work plane although the value is still within UDI range, if we evaluate horizontal illuminance according to more stringent and detailed criteria, in which the recommended light level for the normal office work is around 500 lux to 1000 lux (53). Meanwhile, SPD material with 550μm thickness is optimal among them since the room centre illuminance is below 1200 lux. The reason causing the situation is that high haze value and relative low diffusivity of SPD 550μm layer diffuses less daylight inside of the room.

The track of daylight distribution changes from northeast to northwest during 11 a.m. to 1 p.m., due to the variation of solar orientation. Meanwhile, room space within useful daylight illuminance remains the same, around 85%. At 12 p.m., over lit area spreads perpendicular to the window since the sun is in the middle of trajectory. Similar with previous time, illuminance in the middle of room is lowest but comfort for occupant working for SDP 550μm base case. Besides, illuminance distribution on the deep area of room is similar with each other.

As we can see from **Figure 3-31**, useful daylight illuminance reduces significantly from 2 p.m. to 3 p.m., and it can be explained by that more daylight transmits through window due to solar altitude, causing large over lit area. From 3 p.m. to 4 p.m., UDI increases and there is a little more space with UDI range for three SPD simulation cases comparing with EC base case. Especially at 4 p.m., the distribution of illuminance is almost the same for SPD material with different thickness as well as EC base case considering the sun position is low and more daylight enters the depth of room. Useful daylight illuminance reduces a lot at 5 p.m. for each simulation cases, each cases have 84% space below 100 lux. Hence the daylight is insufficient for the work plane level, requiring compensation from artificial lighting.

In general, the interior daylight performance of SPD material with 550μm thickness is better among these simulation cases, while the result of this case is not reliable because of some calculation methods that used in Radiance with trans material, which has been mentioned in Chapter 2.7.

| Time | SPD 200μm | SPD 400 μm | SPD 500 μm | SPD 550 μm |
|------|-----------|------------|------------|------------|

8 a.m.
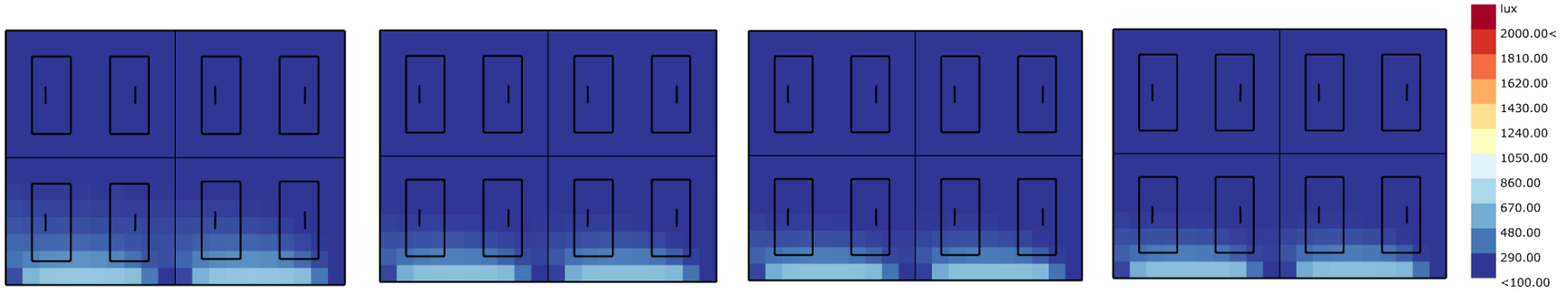


9 a.m.
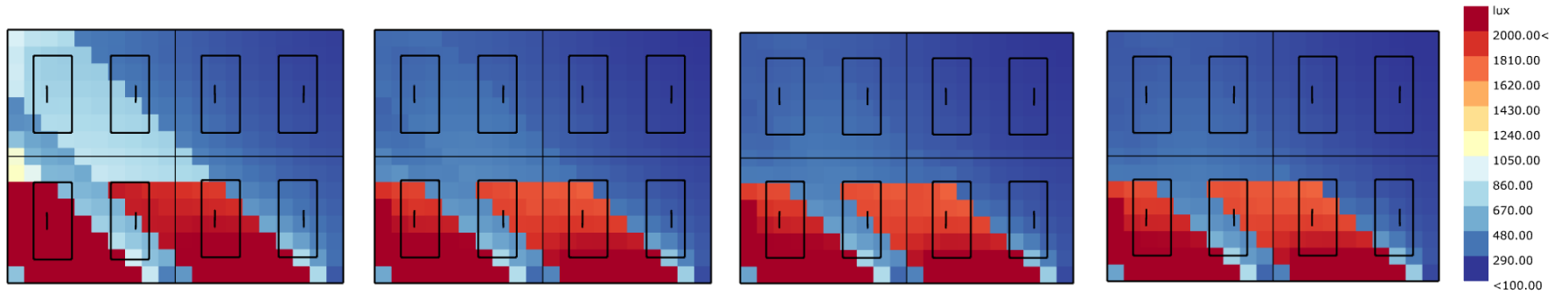


10 a.m.
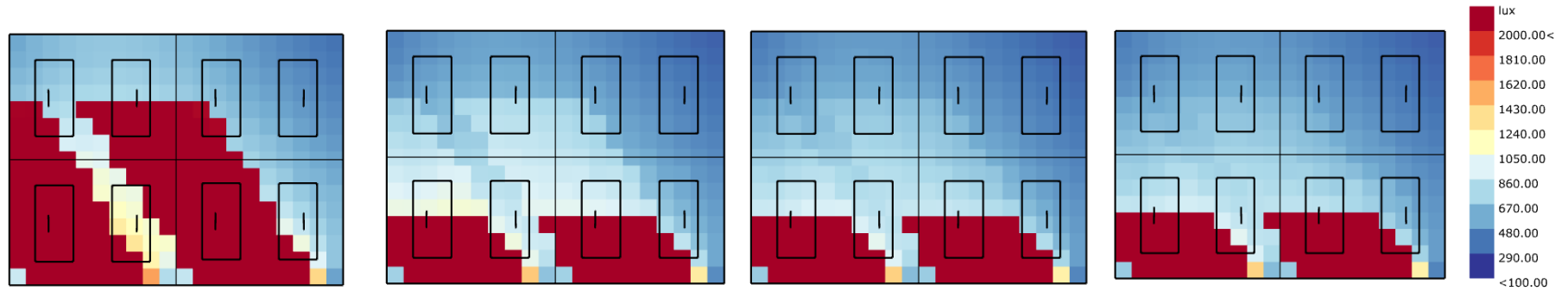
11 a.m.
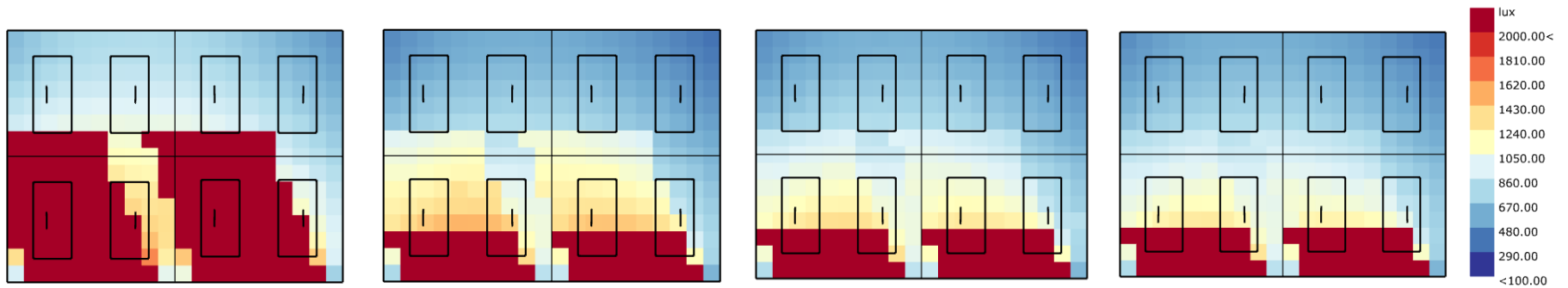


12 p.m.

1 p.m.



2 p.m.

3 p.m.



4 p.m.
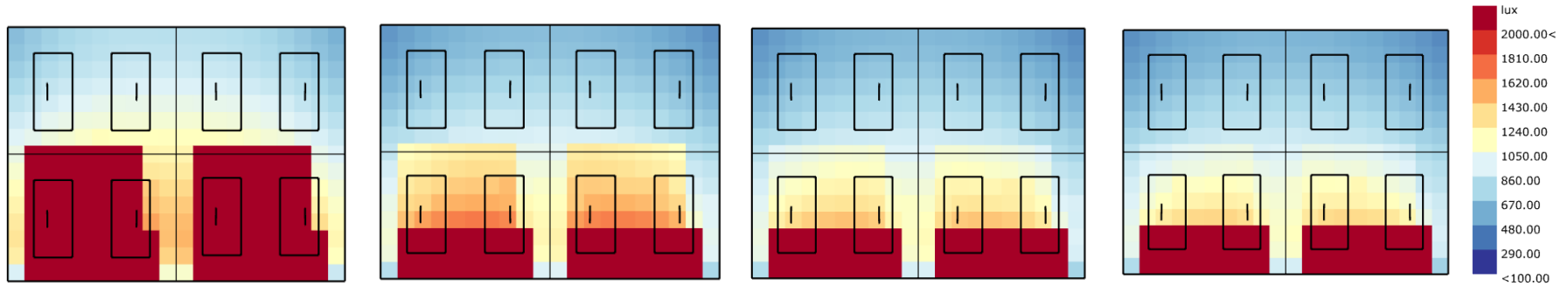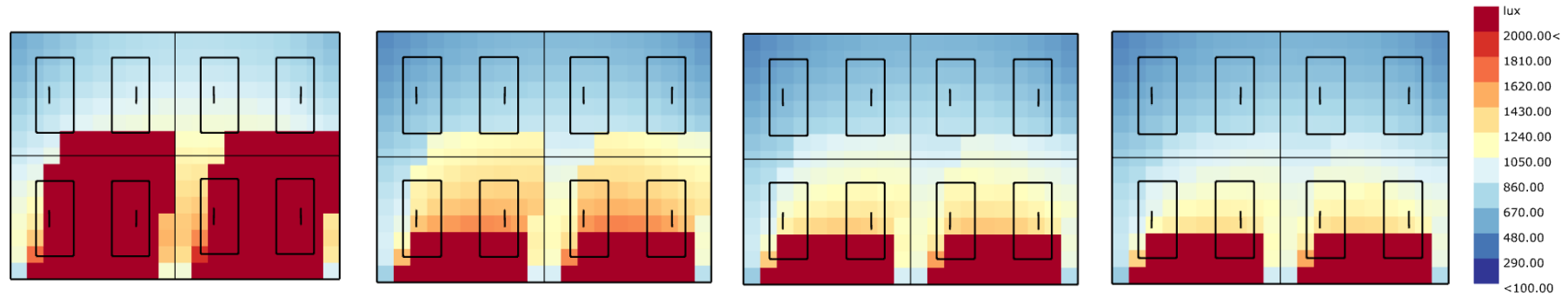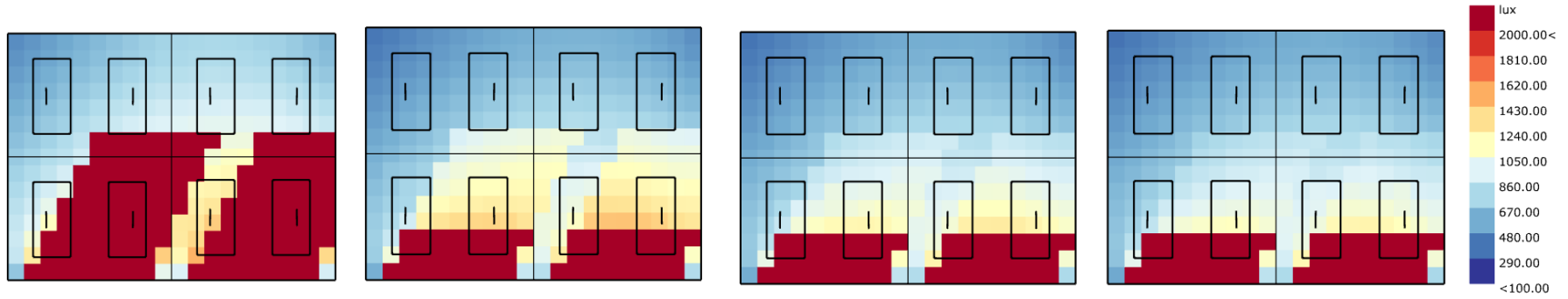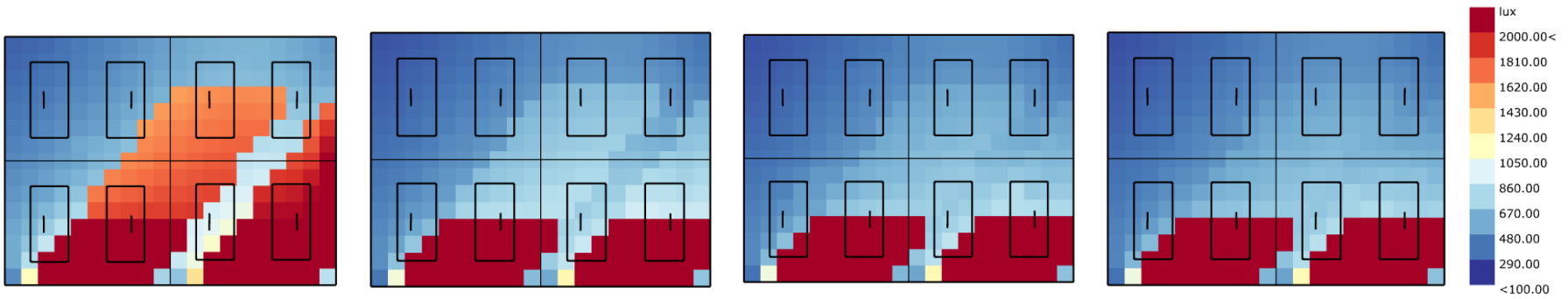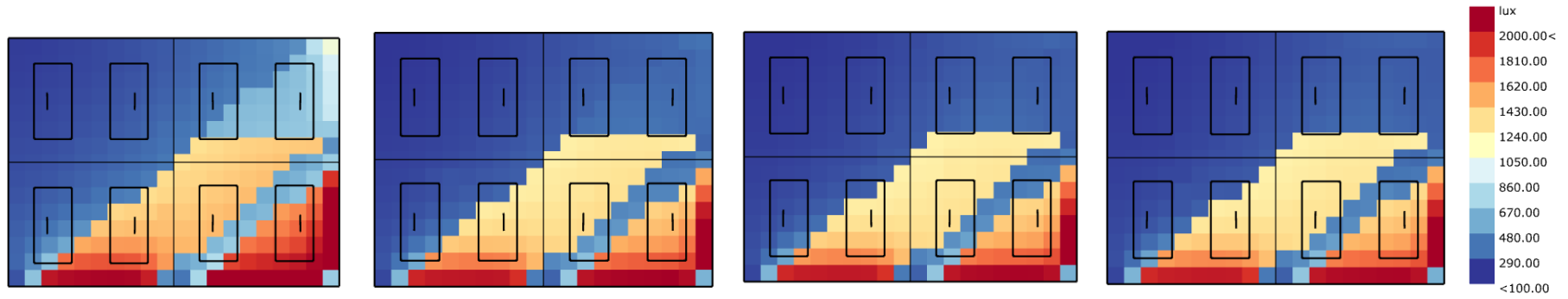
5 p.m.
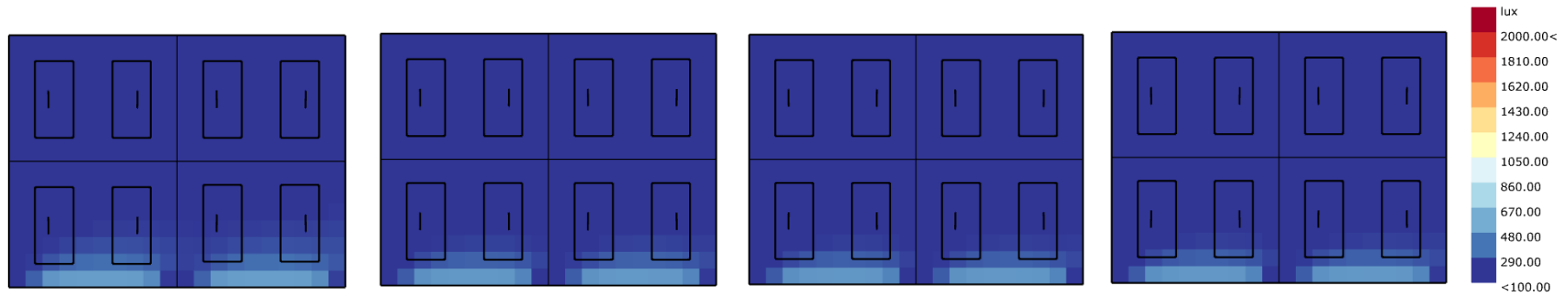


6 p.m.
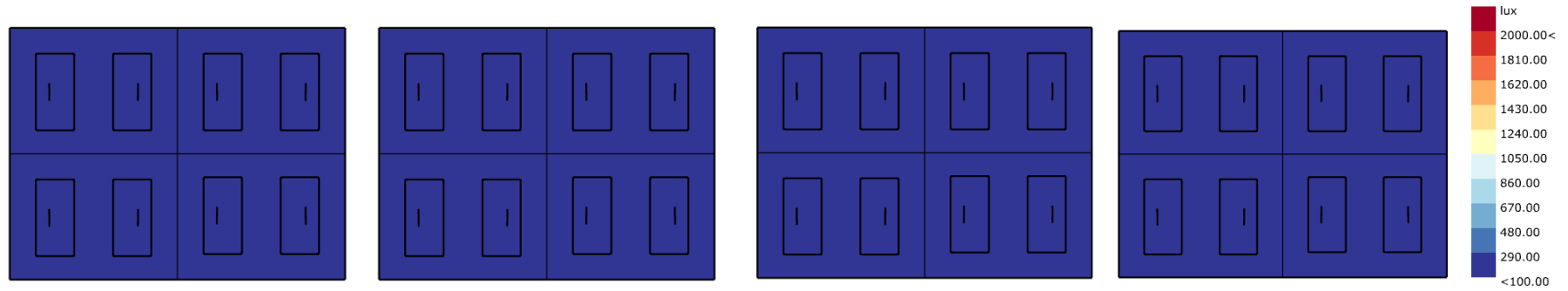
**Figure 3-30** Point-in-time illuminance for SPD material with 200μm, 400μm, 500μm, 550μm thickness, respectively.
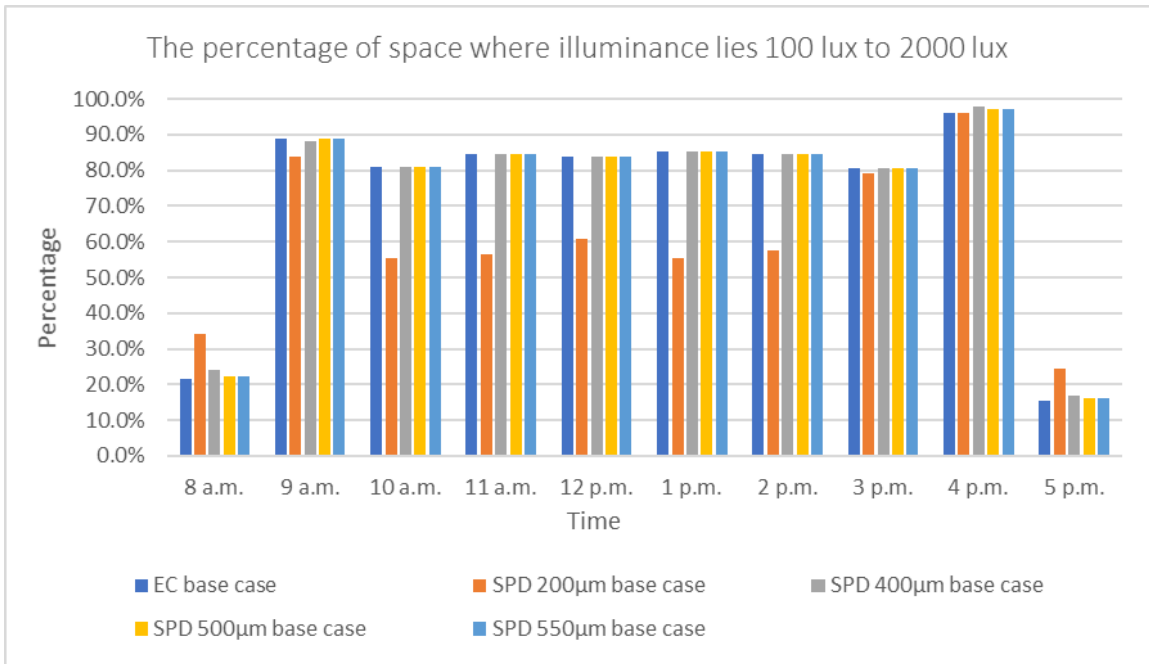
**Figure 3-31** The percentage of space with illuminance within UDI range for EC base case and SPD base case
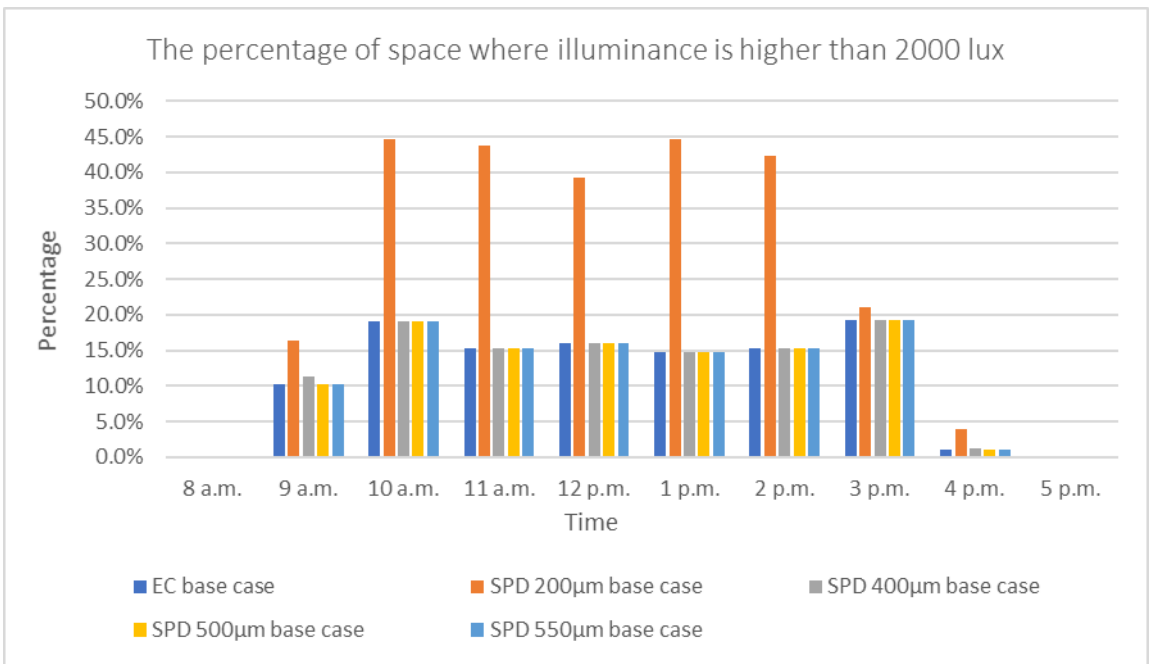


**Figure 3-32** The percentage of space where the illuminance is higher than 2000 lux for EC base case and SPD base case
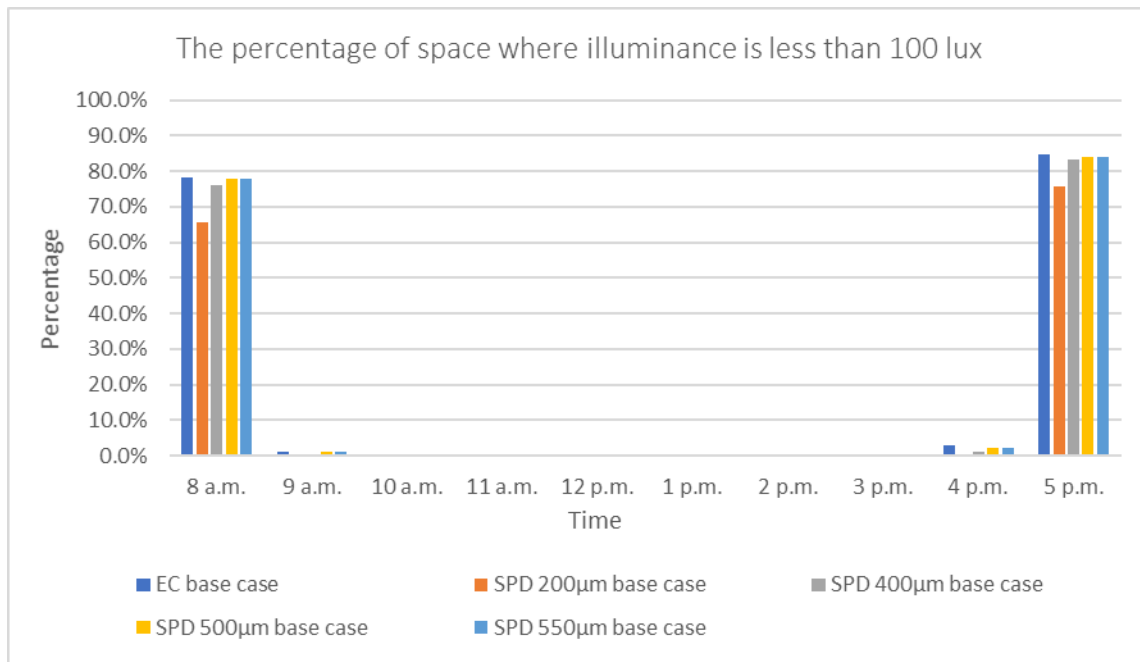
**Figure 3-33** The percentage of space where the illuminance is less than 100 lux for EC base case and SPD base case

### 3.2.6  **Summary of horizontal illuminance evaluation**

This chapter assesses interior daylight condition of test room by analysing horizontal illuminance on work plane level. We can summarize illuminance results from several aspects.

First, useful daylight illuminance is adopted as criteria to evaluate interior daylight distribution considering the illuminance on work plane varies both spatially and temporally. Percentage of room space is calculated to quantitively indicate the interior illuminance distribution. For each simulation cases, daylight is insufficient at 6 p.m. since the sun position is rather low and less sunlight transmit through the window. Hence, artificial lighting should be supplied. Horizontal illuminance varies greatly from 8 a.m. to 5 p.m. and the result of some simulation cases are much different.

Secondly, reference case performs worst for horizontal illuminance evaluation among simulation cases since large over lit area exists, even covering work plane near back wall. The result indicates that it is not feasible for no shading window covering by double low-e glass, which would cause visual discomfort risk for occupant working inside.

We can see that interior daylight condition is getting better when the dynamic material is applied on window glass. Electrochromic glass and SPD glass block much visible daylight transmission through window, reducing over lit area of the room. Comparing illuminance result, SPD layer with 20μm thickness is worst in interior daylight control, causing large space where illuminance exceeds 2000 lux. It can be explained by that high visual light transmittance of SPD material let more daylight pass through window causing more space over lit. For EC base case and other three thicker SPD material, the percentage of space within UDI range is almost the same although the total light transmittance is different. However, the daylight diffusion is different inside of the room. More daylight diffuses into the depth of room for SPD 400μm material due to the high diffuse transmittance. The illuminance in the middle of the room is higher than EC as well as other two SPD base cases and the value is still within the UDI. If we evaluate horizontal illuminance according to more stringent and detailed criteria, the recommended light level in the normal office work is around 500 lux to 1000 lux (53). For SPD 400μm case, much daylight diffusion causes illuminance exceeding 1000 lux in the middle of the room, which supply excess daylight on the work plane based on the stringent criteria (53). According to the recommended illuminance on the office work plane, SPD material with 550μm thickness performs better, providing proper daylight on the work plane during daytime.

By increasing the upper electrochromic glass by 50 %, we obtain more space where illuminance lies UDI range. There is no space with illuminance over 2000 lux and the whole room is within UDI range from 10 a.m. to 3 p.m., which creates a comfortable light environment. The result can be explained by that the increased size EC glass block much daylight inside of the room and reduce the risk of over light. The diffusion of the daylight is reduced compared with EC base case, much lowering the illuminance in the middle of room. While remaining horizontal illuminance with UDI range at most daytime, daylight is insufficient

in the early morning and late afternoon, which may cause energy consumption of artificial lighting.

## 3.3   Calculation of energy consumption and scheduling

Analyzing the results of performance of electrochromic glass in terms of controlling glare and its daylight performance we have seen that occupant-based method proposed in chapter 2.3 may find its use. The DGP values were kept within an acceptable range of $0 - 0.4$ and point-in-time UDI metric is within $100 - 2000$ lux for the most time of the day, from 9 a.m. to 4 p.m.

While obtaining comfortable visual conditions for an occupant one must also consider the energy performance of the adopted technology. The benefits of using hi-end technologies that are capable to provide control over the excessive solar radiation are inevitably associated with higher initial and, perhaps, operational costs. Nevertheless, those costs might be payed-off by reducing the costs connected to the maintenance of the shading system. Furthermore, the productivity of the office workers is reported to be higher when having the continuous view to the outside. The view to the outside is provided when the EC glazing is not in its darkest state. Those conditions might be found in a day with an overcast sky, for example.

To evaluate the approach more detailed, we were particularly interested in energy consumption that is associated with the use of electrochromic active glazing. The evaluation was done in comparison to a conventional shading strategy that is able to control the glare by the use of the automated roller blind.

The amount of energy used is dependent on the operation schedule of the electrochromic glazing and the roller blind. Findings in chapter 3.1 and other researches  (18) (19) suggest that the glare might be a suitable control parameter for controlling the operation of the shading system. Similarly to the graphs of DGP profile for two orientations for Milano, we have obtained the graphs for the cities of London and Athens. The area of the glazing that was used as a dynamic glass was found according to the chapter 2.3. The graphs of DGP profiles for London and Athens are presented in **Figure 3-34**, **Figure 3-35**. Based on the DGP profiles and considering the possible orientation of the occupants inside the test room we have created a schedule for the operation of the electrochromic glass. The schedule was created considering the fact that when all occupants are oriented in one direction, the electrochromic glass is turned in its darkest state only when the sun is in the field of view of the occupant. When the orientation is mixed, the schedule is arranged in a way that glare would be avoided for any orientation (east or west). The schedules are presented in **Table 3-1**. The time period of the year that was used for calculations was found according to the sun path diagram where the time with the sun being in the field of view of the occupant was found. For Milano it is

from 15 of October to 28 of February, for London it is from 22 of September to 22 of March, for Athens it is from 15 of November to 5 of February.
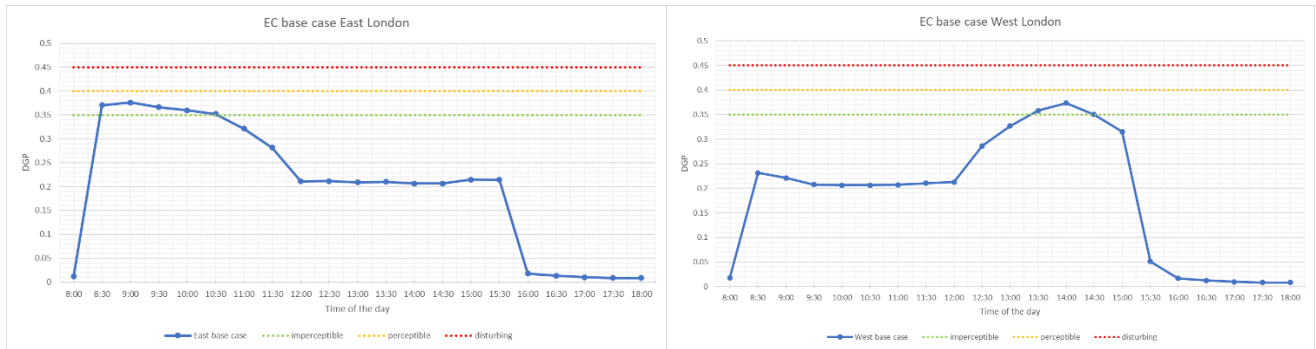


**Figure 3-34** DGP profiles for 21st December for EC base case for London
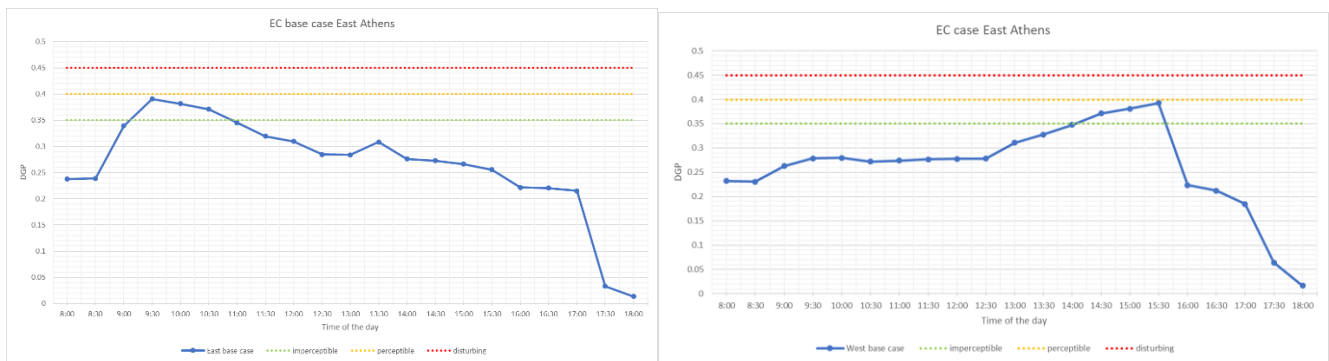


**Figure 3-35** DGP profiles for 21st December for EC base case for Athens

Table 3-1 Dynamic glazing operation schedule

| | Milano | | | London | | | Athens | | |
|---|---|---|---|---|---|---|---|---|---|
| | Facing East | Facing West | Facing East and West | Facing East | Facing West | Facing East and West | Facing East | Facing West | Facing East and West |
| 8 a.m. | ON | OFF | ON | ON | OFF | ON | ON | OFF | ON |
| 9 a.m. | ON | OFF | ON | ON | OFF | ON | ON | OFF | ON |
| 10 a.m. | ON | OFF | ON | ON | OFF | ON | ON | OFF | ON |
| 11 a.m. | ON | OFF | ON | ON | OFF | ON | ON | OFF | ON |
| 12 p.m. | ON | ON | ON | ON | ON | ON | ON | ON | ON |
| 1 p.m. | OFF | ON | ON | OFF | ON | ON | OFF | ON | ON |
| 2 p.m. | OFF | ON | ON | OFF | ON | ON | OFF | ON | ON |
| 3 p.m. | OFF | ON | ON | OFF | ON | ON | OFF | ON | ON |
| 4 p.m. | OFF | ON | ON | OFF | OFF | OFF | OFF | ON | ON |
| 5 p.m. | OFF | OFF | OFF | OFF | OFF | OFF | OFF | OFF | OFF |
| 6 p.m. | OFF | OFF | OFF | OFF | OFF | OFF | OFF | OFF | OFF |

After definition of the schedule and the analysis period we have found the number of sunny hours for all considered locations. Then by combining the schedule and the actual hours when the sky is clear in the given location we were able to obtain an average annual schedule used for calculating energy consumption. To define the number of sunny hours we have used EPW weather files obtained from EnergyPlus weather data (54). To define the clear sky conditions based on weather data file we have used the values of *global horizontal irradiance* and *diffused horizontal irradiance.* The criteria for determining sky clearness using solar irradiance data are always taken in the form of clearness index, $K_t$, and diffuse fraction, K (55); where,

$$K_t = \frac{GHI}{I_0}$$

Where, *GHI* is global horizontal irradiance [Wh/m²]; $I_0$ is the extraterrestrial solar irradiance [Wh/m²]. $I_0$ is defined as follows (56).

$$I_0 = 1367.7 * \left( 1 + 0.033 * \cos \left( \frac{2\pi}{365} * DOY \right) \right)$$

Where, *DOY* is the day of the year.

$$K = \frac{DHI}{GHI}$$

Where, *DHI* is diffuse horizontal irradiance [Wh/m²].

The values of $K_t \leqslant 0.15$ and $K \geqslant 0.98$ can represent a sky as overcast and these criteria are used for the present analysis. The number of sunny hours and number of hours when the shading is operating are presented in

Table 3-2 The number of sunny hours and shading working hours

|  | Period with the sun in the FOV | Orientation | Number of sunny hours in a year | Number of sunny hours in an analyzed period | Number of shading working hours |
|---|---|---|---|---|---|
| Milano | 15.10 - 28.02 | West | 1887 | 297 | 234 |
|  |  | East |  |  | 126 |
|  |  | Mixed |  |  | 297 |
| London | 22.09 - 22.03 | West | 1826 | 346 | 181 |
|  |  | East |  |  | 230 |
|  |  | Mixed |  |  | 340 |
| Athens | 15.11 - 05.02 | West | 2778 | 348 | 154 |
|  |  | East |  |  | 263 |
|  |  | Mixed |  |  | 348 |

The average power consumption for electrochromic glass and automated roller blind was found as follows:

$$E_{tot,EC} = E_m * A_{EC} + E_{swit} * A_{EC}$$

Where, $E_{tot,EC}$ is the total power consumption of electrochromic glass; $E_m$ is the power consumption of electrochromic glass when maintaining the glass on tinted state; $E_{swit}$ is the power consumption of electrochromic glass when switching the glass from clear state to tinted state; $A_{EC}$ is the area of EC glass.

$$E_m = H * P$$

Where, $H$ is the number of hours when EC glass is operating. $P$ is the power supply to maintain working of EC glass, which is 0.4 W/m², referring technical data of IQ Electrochromic Glass (26).

$$E_{swit} = N * P_{swit} * \frac{T_{on}}{60}$$

Where, $N$ is the number of days when EC is working. $P_{swit}$ is the power supple to switch the glass from clear state to tinted state, which is 2.5 W/m², referring technical data of IQ Electrochromic Glass (26); $T_{on}$ is equal to 5 min, which is transition time of glass from clear to tint (26).

Power consumption of automated roller blind was found assuming that the schedule of operation is the same as for the EC glass, but the blinds are operated twice a day: when the sun appears and leaves the field of view. The formula used for calculation goes as follows:

$$E_{roller} = \frac{h}{L_s} * \frac{t}{3600} * P_{roller} * N * 2$$

Where, $h$ is the height of roller blind covering window glass; $L_s$ is the circular length of shaft, equaling to 0.157 m (57); t is the time when shaft rotates one circle, which is 2 s/rad (57); $P_{roller}$ is the power supply for roller blind, equaling to 95 W; $N$ is the number of days when roller blind is working.

As a result, we have obtained average annual energy consumption for electrochromic glass and an automated roller blind. The results are presented in **Figure 3-36**. The amount of energy consumed by electrochromic glazing is generally 5-9 times larger than for automated roller blind. In Milano for West oriented occupants the difference in annual energy consumptions is 252 Wh, while for London, when the orientation of occupants is mixed, the difference is 871 Wh. As we can see, although the average annual energy consumption of electrochromic glass being operated in a way that the glare is avoided is several times greater than for automated roller blind, in absolute values the amount of consumed energy is small in comparison to other utilities that are used in the offices (HVAC, PC equipment, lighting, etc.).
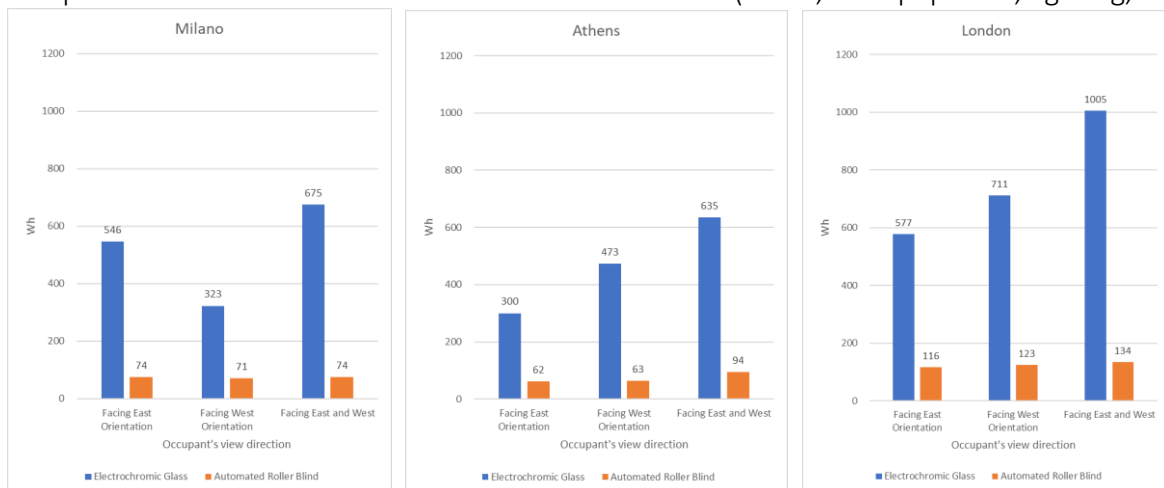


**Figure 3-36** The average annual power consumption of EC glass and roller blind in terms of occupant view direction for Milano, Athens, London

# Chapter 4  Discussion and recommendations

In our research the performance of dynamic glazing materials together with an occupant-based method of finding the area that is suggested to be covered by a dynamic material was evaluated. The evaluations of performance in terms of visual conditions were done considering a South exposed test room, located in Milano, with an occupant located 1.5 m. away from the glazing. Adopted orientations of the occupant were West and East. The assessed parameters were DGP, calculated discretely with a time interval of 30 minutes, from 8 a.m. to 6 p.m. and UDI, calculated by running point-in-time daylight illuminance simulations with a time interval of 1 hour. The date of simulation was chosen as 21st of December and the sky conditions were set to be clear. This date and sky conditions are chosen to evaluate the performance in, perhaps, the worst conditions that could be found during the year – the sun is its lowest annual altitudes and the intensity of sun luminance is the highest. Performance parameters were calculated for several cases: reference cases – where no shading control strategy was applied, base cases – where the height of the upper part was found using the adopted in chapter 2.3 method, and increased size cases – where the height of the upper part was enlarged. Base cases were compared to increased size cases to evaluate the change in performance due to the height change. Furthermore, increased height was considered to investigate if the size, found in a base case, might be further optimized. The reduction of the height was not considered since it would inevitably contradict to the question (b), stated in our research questions, because it would mean that for a particular period during the day the sun disk would be directly visible for an occupant. Electrochromic material and SPD material with different thickness were analyzed to find an optimal among them considering their different optical properties. The thicknesses considered for SPD material were 200μm, 400μm, 500 μm and 550μ. The selection of thickness was based on the fact that total light transmission together with the ratio of diffusely and directly transmitted light are thickness dependent.

The results of point-in-time glare simulations has shown that a glazing, partially covered by a dynamic material is able to reduce the daylight glare probability perceived at a given occupant position and orientation of the view to acceptable values (DGP < 0.4). Both electrochromic glazing and SPD glazing were able to fulfill this objective. Nevertheless, the values of DGP obtained by simulations were within a range of 0.25-0.4 meaning that the characteristic DGP range was *perceptible*, particularly for the hours when the sun was in the field of view. To assure the DGP not going beyond *disturbing* (DGP >0.4) threshold it was observed in our study that the transmittance of the dynamic glass should not exceed at least the value of $T_{vis}$ = 1.7% (SPD 500 μm), since the results obtained for SPD 400 μm with $T_{vis}$ = 3% point out that for the hours with the sun in the field of view, the DGP is reaching 0.45.

In our study, in addition to controlling the glare within acceptable range, horizontal illuminance above 2000 lux which is considered as over lit should be avoided. Comparing with reference case, both dynamic glazing material, EC glass and SPD, can reduce over lit area during the analyzed time period. Focusing on the percentage of space within UDI range, the value corresponding to EC glass and SPD material increase by 30% on average comparing with the one of reference case. In the early morning and late afternoon, the over lit area of reference case spreads from window to depth of the room, even reaching the area near northern wall. While over lit area reduces significantly in EC simulation cases and SPD simulation cases, maximum 1.5m away from the window in the early morning and late afternoon. More space within UDI range means dynamic glazing blocks most of the visible light passing through window, optimizing the interior daylight distribution. The over lit area existing can be explained by the fact that the sun is low and only upper window glass is used as a shading control strategy. Besides, over lit area spreads from window, along northwest in the morning and northeast in the afternoon due to the sun position during that time.

The comparison of the DGP results obtained for the case when the upper part was found parametrically and for the case when the height of the upper part was increased with respect to the base case have shown that the visual conditions in terms of glare are better for the base case configuration. When the height of the upper, tined to the darkest state, dynamic glazing is reducing the overall illuminance values at the eye-level of the occupant, thus increasing the contrast levels. This observation is supported by the fact that when the values of DGP for the base case are reaching their maximum values, the DGP for the increased case are surpass the corresponding values of the base case for both considered orientations. Even though, the amount and luminous intensity of the glare sources are reducing for the increased size case, the biggest role in contributing to the DGP value is held by the sun disk in the field of view. Because of that, even having the same glare source in both cases, in the increased size case the produced DGP value is higher. This leads us to a conclusion that when considering the DGP, the height of the upper glazing portion found by using the adopted parametric approach might be considered as optimal.

The analysis of the EC simulation case where the upper part is increased has shown that the space within UDI range increases comparing with EC base case, avoiding over lighting in the whole day. This phenomenon indicates blocking more visible daylight and improvement of interior useful illuminance can be achieved by enlarging the height of active glazing. Especially, all the room space is under UDI range from 10 a.m. to 3 p.m. and the illuminance in the middle of room is around 500 lux to 800 lux which is comfort for people working there. While much deep room space is underlit in the early morning and late afternoon, considering the illuminance on the work plane level is below 100 lux, which causing lighting compensation by artificial light. Although room space is within UDI range in the most time, the interior daylight distribution is not the best condition if we evaluate horizontal illuminance based on more stringent and detailed criteria (53), which recommends light level in the normal office work around 500 lux. The space in the depth of the room is below 500 lux which also might cause visual discomfort for the occupant working there. In general, interior useful daylight

illuminance is improved by increasing the height of EC glass, meanwhile, underlit area is caused in the depth of room.

When evaluating different material options for the dynamic glazing, the SPD material was expected to produce an improvement in visual conditions due to the fact that a portion of the light transmitted in a diffused manner would produce a reduction in contrast levels in the scene, scattering the light coming directly from the sun to occupant's eyes and allowing us to use more transparent state, improving the daylight distribution inside the test room while still maintaining the glare probability within an acceptable range. Nevertheless, the results of glare evaluations have shown that in order to control the glare from direct sun rays, the values of visual transmittance are suggested to be in a range of 1-2%. SPD material with a thickness of 200μm, $T_{vis}$ equal to 15% and $T_{diff}/T_{vis}$ equal to 17.5% appears to be unsuitable since the daylight glare probability is reaching 0.7 with the sun in the field of view. A progressive approach in testing different thicknesses of SPD with a gradual reduction of total transmittance and increase of haze has shown that the performance of SPD is at best equal to electrochromic material in terms of glare control. Possible relative to EC achievable increase of visual transmittance is 0.7% when using SPD 500 μm. The point-in-time glare simulations of SPD with the thickness 550 μm has reviled the difficulties in simulating near to zero transmittance of translucent materials using Radiance engine, since the obtained results were evidently not correct.

We were expecting the improvement of interior daylight distribution because the diffused light can increase the horizontal illuminance of the deep room space. And this improvement can be obtained by using SPD material properly. Analyzing the horizontal illuminance of SPD material with 200μm thickness is shown that over lit area increases significantly. Over lit area increases more than twice comparing with the one of EC base case from 10 a.m. to 2 p.m. Large space is over lit from window to the depth of room in the morning and late afternoon. This phenomenon can be explained by the fact that high visible light transmittance allows more daylight to enter room causing visual discomfort risk inside. For other three thicker SPD materials, room space within UDI range is almost the same as the one of EC base case and the reason is that they have similar light transmittance, around 1% to 3%, and the contribution of daylight diffusion is low although the diffuse transmittance and haze transmittance is higher for SPD material. SPD material with relative low transmittance doesn't affect over lit area but daylight distribution is different among SPD material with 400μm, 500μm and 550μm thickness. More daylight diffuses into the depth of room for SPD 400μm layer due to the relatively higher diffuse and total transmittance. The illuminance is higher than EC as well as other two SPD base cases along northwest in the morning and northeast in the afternoon, supplying more daylight in the depth of room. The difference of illuminance in the middle of room is the highest at 12 p.m. since the sun is in the middle of sun path and more daylight is transmitted and diffused inside room. The light diffusion degree is the lowest for SPD 550μm considering the diffuse transmittance is the lowest and the daylight distribution of SPD500μm is the same as the condition of EC. From this comparison, we can conclude that the thicker SPD layer, the less daylight is diffused (when the thickness is from 400μm to

550μm). As we mentioned previously, the recommended illuminance value is 500 lux for normal office work plane. For SPD material with 400μm, illuminance in the middle of the room is higher than 1000 lux from 11 a.m. to 2 p.m. which is not comfortable for the occupant working there.

The calculation of annual energy consumption for electrochromic glazing operated annually to control the glare was calculated for three locations, as well as the energy consumption of an automated roller blind operated by the same control criteria. Cumulative analysis of DGP values throughout the day for reference case and base cases has shown that a simplified schedule may be created based on the position of the sun in the field of view and the DGP value. The schedule was assuming two states of electrochromic device – ON and OFF, where in ON state the is the darkest tined state and OFF state is the clear state. Based on considered orientations we were able to consider three cases: all occupants oriented in East or West direction and mixed orientation of the occupants. The number of hours with a clear sky were selected for calculations, also considering adopted occupancy (8 a.m. – 6 p.m.) and the period of the year when the sun is in the FOV of the occupant. The information about the sky condition was obtained from EPW weather files, where the values of global horizontal irradiance and diffused horizontal irradiance were used to assess the sky conditions. The number of hours when the shading may be activated was 297 for Milano, 346 for London and 348 for Athens. The amount of energy required for operating electrochromic glazing was found considering the number of switching, number of hours when glazing had to be maintained in a tinned state and the time that it takes for electrochromic glazing for state transition. Energy need for automated roller blind was found considering the same schedule, the number of days when it had to be used, the power of the motor and the time for deploying and retracting. It was found that for each location with a test room being south exposed there is a particular orientation for the occupants when energy consumption may be reduced (West for Milano and East for London and Athens). Given that the considered number of sunny hours for all three locations on average was around 4% from the total amount of hours in a year and the power required for maintaining the state of the electrochromic glazing is 0.4 W/m$^2$, the annual power need for EC glazing, even being 5-9 times higher than for automated roller blind, was still not more than 1 kWh (London, mixed orientation) which might be considered relatively small. On the other hand, for SPD material maintaining transparent state requires energy consumption, meaning that having generally power need around 2 times bigger than for EC and overwhelming amount of time when the transparent state is desired, the use of such system might not be the most economical from energy consumption point of view.

## 4.1   Conclusion

In this research we have answered following research questions:

(a) Can the glare from the sun directly visible in the field of view of the occupant be controlled by using materials with dynamically adjustable optical properties?

Our analysis of simulation results has shown that daylight glare probability can be kept within an acceptable range when considering South exposure of the test room, several locations and occupant orientation to West and East. In those analyzed conditions with the sun being in the field of view of the occupant, both EC and SPD material when applied to the glazing portion were able to reduce the DGP from 1.0 to <0.4.

(b) What is the optimal area of the dynamic material that would guarantee a glare probability within acceptable range and how it can be found parametrically, based on the geographical location and a position of the occupant?

The method of finding an area of the glazing that must be covered by a dynamic material using a sun path diagram based on the position of the occupant has shown itself to be suitable for fulfilling the aim of controlling the glare with the sun being in the FOV. The area was found based on the location with an according sun path and the eye-level of the occupant and his location inside the test room. The comparison with an alternative increased size option has shown that increase in size of the upper part is not necessary not just from economical point of view, but furthermore it is worsening visual conditions for the occupant, increasing the contrast levels and reducing the amount of desirable natural daylight inside the room. In all considered in this study locations: Milano, London, Athens, using this approach the values of DGP were not exceeding disturbing range.

(c) What type of dynamic material is the most suitable for providing comfortable visual conditions in terms of glare evaluations and interior daylight distribution?

Among the tested alternatives of materials with different dynamic optical properties, electrochromic material with the ability of modulation its visual transmittance to achieve $T_{vis}$ = 1% has been considered as the most suitable. The results have shown that even with a visual transmittance of 3% the DGP is reaching disturbing range. Furthermore, it was found that the performance of SPD is little to no better in comparison to EC since the ability of SPD to diffusely transmit more daylight, while being expected to improve visual conditions, in fact found no use since the fraction of total light transmitted is to small when the material is in its darkest state to control the glare. Analyzing the UDI levels during the day it was observed that beneficial impact of diffusely transferred light is negligible. Taking into account energy consumption of SPD materials and their initial cost which are higher and the operation type where transparent state requires energy supply, electrochromic materials are preferable.

# Chapter 5    Bibliography

1. *Life-Cycle Thinking and the LEED Rating System: Global Perspective on Building Energy Use and Environmental Impacts.* **Sami G. Al-Ghamdi, Melissa M. Bilec.** s.l. : American Chemical Society, 2015.

2. *Daylight metrics and energy savings.* **J. Mardaljevic, L. Heschong, E. Lee.** 3, s.l. : Light. Res. Technol., 2009, Vol. 41.

3. *Experimental and simulation study on the performance of daylighting in an industrial building and its energy saving potential.* **Yuanyi Chen, Junjie Liu, Jingjing Pei, Xiaodong Cao, Qingyan Chen, Yi Jiang.** s.l. : Energy and Buildings, 2014, Vol. 73. ISSN 0378-7788.

4. *The role of window glazing on daylighting and energy saving in buildings.* **W.J. Hee, M.A. Alghoul, B. Bakhtyar, OmKalthum Elayeb, M.A. Shameri, M.S. Alrubaih, K. Sopian.** s.l. : Renewable and Sustainable Energy Reviews, 2015, Vol. 42. ISSN 1364-0321.

5. *A human-centric approach to assess daylight in buildings for nonvisual health potential, visual interest and gaze behavior .* **Maria L. Amundadottir, Siobhan Rockcastle, Mandana Sarey Khanie, Marilyne Andersen.** s.l. : Building and Environment, 2017, Vol. 113. ISSN 0360-1323.

6. *Combined effects of daylight transmitted through coloured glazing and indoor temperature on thermal responses and overall comfort.* **G. Chinazzo, J. Wienold, M. Andersen.** s.l. : Building and Environment, 2018, Vol. 144. ISSN 0360-1323.

7. *Blinded by the light: Occupant perceptions and visual comfort assessments of three dynamic daylight control systems and shading strategies.* **Julia K. Day, Benjamin Futrell, Robert Cox, Shelby N. Ruiz.** s.l. : Building and Environment, 2019, Vol. 154. ISSN 0360-1323.

8. *Impact of indoor environmental quality on occupant well-being and comfort: A review of the literature.* **Yousef Al horr, Mohammed Arif, Martha Katafygiotou, Ahmed Mazroei,**

**Amit Kaushik, Esam Elsarrag.** 1, s.l. : International Journal of Sustainable Built Environment, 2016, Vol. 5. ISSN 2212-6090.

9. *Dynamic daylight glare evaluation.* **Wienold, Jan.** Glasgow : Proceedings of the Eleventh International IBPSA Conference, 2009.

10. **Azza Nabil, John Mardaljevic.** *Useful daylight illuminances: A replacement for daylight factors.* s.l. : Energy and Buildings, 2006. ISSN 0378-7788.

11. *Occupant productivity and office indoor environment quality: A review of the literature.* **Yousef Al Horr, Mohammed Arif, Amit Kaushik, Ahmed Mazroei, Martha Katafygiotou, Esam Elsarrag.** s.l. : Building and Environment, 2016, Vol. 105. ISSN 0360-1323.

12. *Assessment of building façade performance in terms of daylighting and the associated energy consumption in architectural spaces: Vertical and horizontal shading devices for southern exposure facades.* **Hussain H. Alzoubi, Amneh H. Al-Zoubi.** 8, s.l. : Energy Conversion and Management, 2010, Vol. 51. ISSN 0196-8904.

13. *Visual Comfort Analysis of Innovative Interior and Exterior Shading Systems for Commercial Buildings using High Resolution Luminance Images.* **Konis, K., E. Lee, and R. D. Clear.** 3, s.l. : The Journal of the Illuminating Engineering Society , 2011, Vol. 7.

14. *The influence of shading control strategies on the visual comfort and energy demand of office buildings.* **Gyeong Yun, Kap Chun Yoon, Kang Soo Kim.** s.l. : Energy and Buildings, 2014, Vol. 84. ISSN 0378-7788.

15. **Eleanor S Lee, Stephen E Selkowitz, Glenn D Hughes, Robert D Clear, Gregory J Ward, John Mardaljevic, Judy Lai, Mehlika Inanici, Vorapat Inkarojrit.** *Daylighting the New York Times Headquarters Building: Final Report.* 2005. LBNL-57602.

16. *Comparative control strategies for roller shades with respect to daylighting and energy performance.* **Athanasios Tzempelikos, Hui Shen.** s.l. : Building and Environment, 2013, Vol. 67. ISSN 0360-1323.

17. *GlareShade: a visual comfort-based approach to occupant-centric shading systems.* **Alireza Hashemloo, Mehlika Inanici & Christopher Meek.** s.l. : Journal of Building Performance Simulation, 2016, Vol. 9. ISSN: 1940-1493.

18. *Daylight glare probability measurments and correlation with indoor illuminance in a full-scale office with dynamic shading controls.* **Iason Konstantzos, Athanasios Tzempelikos.** s.l. : International High Performance Buildings, 2014.

19. *The effect of luminance distribution patterns on occupant preferences in a daylit office environment.* **Kevin Van Den Wymelenberg, Mehlika Inanici, Peter Johnson.** 2, s.l. : The Journal of the Illuminating Engineering Society of North America, 2010, Vol. 7. ISSN: 1550-2724.

20. *Active dynamic windows for buildings: A review.* **Casini, Marco.** s.l. : Renewable Energy, 2018. ISSN 0960-1481.

21. **Saint-Gobain.** Performance & Acoustical data. *SageGlass Lightzone.* [Online] [Cited: 11 June 2019.] https://www.sageglass.com/sites/default/files/mkt-043_performance_and_acoustical_data_flyer.pdf.

22. —. SAGEGLASS® PRODUCT GUIDE. [Online] [Cited: 2 June 2019.] https://www.sageglass.com/sites/default/files/productguide_mkt_48.pdf.

23. *A comparative energy analysis of three electrochromic glazing technologies in commercial and residential buildings,.* **Nicholas DeForest, Arman Shehabi, Stephen Selkowitz, Delia J. Milliron,.** s.l. : Applied Energy,, 2017. ISSN 0306-2619,.

24. *Performance requirements for electrochromic smart window.* **Antonio Piccolo, Francesca Simone.** s.l. : Journal of Building Engineering, 2015, Vol. 3. ISSN 2352-7102.

25. **Halio Smart Glass. [Online] [Cited: 10 7 2019.] https://halioglass.eu/.**

26. **IQ electrochromic glass product. [Online] [Cited: 7 7 2019.] https://www.iqglassuk.com/storage/documents/IQ_Glass_-_Electro_Chromic_Glass_-_Product_Specification_Sheet_2017.pdf.**

27. Smart Film International. [Online] [Cited: 10 7 2019.] http://smartfilmsinternational.com/.

28. Heliotrope-The next generation of smart glass. [Online] Heliotrope. [Cited: 10 07 2019.] https://heliotropetech.com/.

29. *A comparative energy analysis of three electrochromic glazing technologies in commercial and residential buildings.* Nicholas DeForest, Arman Shehabi, Stephen Selkowitz, Delia J. Milliron. s.l. : Applied Energy, 2017, Vol. 192. ISSN 0306-2619.

30. *Conventional fixed shading devices in comparison to an electrochromic glazing system in hot, dry climate.* Aldawoud, Abdelsalam. s.l. : Energy and Buildings, 2013, Vol. 59.

31. *Energy savings due to building integration of innovative solid-state electrochromic devices.* Alessandro Cannavale, Francesco Martellotta, Pierluigi Cossari, Giuseppe Gigli, Ubaldo Ayr. s.l. : Applied Energy, 2018, Vol. 225. ISSN 0306-2619.

32. *Office buildings with electrochromic windows: A sensitivity analysis of design parameters on energy performance, and thermal and visual comfort.* Jean-Michel Dussault, Louis Gosselin. s.l. : Energy and Buildings, 2017, Vol. 153. ISSN 0378-7788.

33. *Electrochromic glazings: dynamic simulation of both daylight and thermal performance.* Bernard Paule, Eloise Sok, Samuel Pantet, Julien Boutiller. s.l. : Energy Procedia, 2017, Vol. 122. ISSN 1876-6102.

34. *Application issues for large-area electrochromic windows in commercial buildings.* E.S. Lee, D.L. DiBartolomeo. 4, s.l. : Solar Energy Materials and Solar Cells, 2002, Vol. 71. ISSN 0927-0248.

35. View Inc. research studies. *view.com.* [Online] 2019. [Cited: 2 June 2019.] https://view.com/assets/pdfs/view-light-transmission-visual-comfort-white-paper.pdf.

36. *Electrochromic glass vs. fritted glass: an analysis of glare control performance.* Ahoo Malekafzali Ardakan, Eloïse Sok, Jeff Niemasz,. s.l. : Energy Procedia, 2017, Vol. 122. ISSN 1876-6102.

37. *End user impacts of automated electrochromic windows in a pilot retrofit application.* E.S. Lee, E.S. Claybaugh, M. LaFrance. s.l. : Energy and Buildings, 2012, Vol. 47. ISSN 0378-7788.

38. *Simulation of the thickness dependence of the optical properties of suspended particle devices.* David Barrios, Ricardo Vergaz, Jose M. Sánchez-Pena, Braulio García-Cámara, Claes G. Granqvist, Gunnar A. Niklasson. s.l. : Solar Energy Materials and Solar Cells, 2015, Vol. 143. ISSN 0927-0248.

39. *Daylighting performance and glare calculation of a suspended particle device switchable glazing.* Aritra Ghosh, Brian Norton, Aidan Duffy. s.l. : Solar Energy, 2016, Vol. 132. ISSN 0038-092X.

40. *Effect of sky conditions on light transmission through a suspended particle device switchable glazing.* Aritra Ghosh, Brian Norton, Aidan Duffy. s.l. : Solar Energy Materials and Solar Cells, 2017, Vol. 160. ISSN 0927-0248.

41. *Toward a quantitative model for suspended particle devices: Optical scattering and absorption coefficients.* David Barrios, Ricardo Vergaz, Jose M. Sanchez-Pena, Claes G. Granqvist, Gunnar A. Niklasson. s.l. : Solar Energy Materials and Solar Cells, 2013, Vol. 111. ISSN 0927-0248.

42. Davidson, Scott. Grasshopper. Algorithmic modeling for Rhino. [Online] [Cited: 2 May 2019.] https://www.grasshopper3d.com/.

43. Niemasz, Jeff. DIVA for Rhino. Environmental analysis for buildings. [Online] Solemma. [Cited: 12 April 2019.] http://diva4rhino.com/.

44. Ladybug Tools LLC. [Online] [Cited: 3 April 2019.] https://www.ladybug.tools/.

45. ASHRAE Standard Project Committee 140. *ANSI/ASHRAE Addendum a to ANSI/ASHRAE Standard 140-2001.* 2004. ISSN 1041-2336.

46. Lawrence Berkeley National Laboratory. The RADIANCE 5.1 Synthetic Imaging System. [Online] [Cited: 23 April 2019.] https://floyd.lbl.gov/radiance/refer/ray.html#Materials.

47. *A Critical Investigation of Common Lighting Design Metrics for Predicting Human Visual Comfort in Offices with Daylight.* Kevin Van Den Wymelenberg, Mehlika Inanici. 3, s.l. : Leukos, 2014, Vol. 10.

48. *Degree of eye opening: A new discomfort glare indicator.* J.A. Yamin Garretón, R.G. Rodriguez, A. Ruiz, A.E. Pattini. s.l. : Building and Environment, 2015, Vol. 88. ISSN 0360-1323.

49. *Investigation of existing discomfort glare indices using human subject study data.* Jae Yong Suk, Marc Schiler, Karen Kensek. s.l. : Building and Environment, 2017, Vol. 113. ISSN 0360-1323.

50. *Daylight glare probability measurements and correlation with indoor illuminances in a fullScale office with dynamic shading controls.* Iason Konstantzos, Athanasios Tzempelikos. s.l. : 3rd International High Performance Buildings Conference at Purdue, July 14-17, 2-14.

51. *Daylight glare evaluation with the sun in the field of view through window shades.* Iason Konstantzos, Athanasios Tzempelikos. s.l. : Building and Environment, 2017, Vol. 113. ISSN 0360-1323.

52. wxfalsecolor. *tbleicher.* [Online] [Cited: 11 May 2019.] https://sites.google.com/site/tbleicher/radiance/wxfalsecolor.

53. Illuminance, Recommended Light Levels. [Online] [Cited: 05 07 2019.] https://www.noao.edu/education/QLTkit/ACTIVITY_Documents/Safety/LightLevels_outdoor+indoor.pdf.

54. Weather Data. *EnergyPlus.* [Online] [Cited: 2 6 2019.] https://energyplus.net/weather.

55. *Overcast sky conditions and luminance distribution in Hong Kong.* Danny H.W. Li, Chris C.S. Lau, Joseph C. Lam. 1, s.l. : Building and Environment, Vol. 39. ISSN 0360-1323.

**56. Reno, Matthew & Hansen, Clifford & Stein, Joshua.** *Global horizontal irradiance clear sky models : implementation and analysis.* 2014.

**57. Roller bilind technical catalogue. [Online] [Cited: 6 7 2019.]** https://www.shadowline.eu/wp-content/uploads/Shadowline-Technik-Rollo-ENG28012016.pdf.